Final Report

Title of project : *A study of the fundamental science underlying the transport of intense femtosecond laser pulses in the atmosphere*

Period covered : *Oct. 1, 1997 to Dec. 31, 1998.*

Principal investigator :

Prof. See Leang Chin
Centre d'Optique, Photonique et Laser &
Département de Physique
Université Laval
Cité Universitaire, Qc. G1K 7P4
Canada

Sponsor : *U S Army Research Office*
Research Triangle Park
N.C., U.S.A.

Proposal number : *38069-RT*

Grant number : *DAAG55-97-1-0404*

Submitted to : *Army Research Office*
Dr. Iqbal Amad
Research Triangle Park
N.C., U. S. A.

Acknowledgement : *This work was also jointly supported by grants from the Natural Sciences and Engineering Research Council of Canada, the Cener for Research on Defense Valcartier (CRDV) of the Department of National Defense of Canada and Le Fonds-FCAR of the Province of Quebec, Canada.*

REPORT DOCUMENTATION PAGE

Form Approved
OMB NO. 0704-0188

1. AGENCY USE ONLY *(Leave blank)*	2. REPORT DATE	3. REPORT TYPE AND DATES COVERED
		Final

4. TITLE AND SUBTITLE

A Study of the Fundamental Science Underlying the Transport of Intense Femtosecond Laser Pulses in the Atmosphere

5. FUNDING NUMBERS

DAAG55-97-1-0404

6. AUTHOR(S)

See Leang Chin

7. PERFORMING ORGANIZATION NAMES(S) AND ADDRESS(ES)

Laval University
Quebec, Canada

8. PERFORMING ORGANIZATION REPORT NUMBER

9. SPONSORING / MONITORING AGENCY NAME(S) AND ADDRESS(ES)

U.S. Army Research Office
P.O. Box 12211
Research Triangle Park, NC 27709-2211

10. SPONSORING / MONITORING AGENCY REPORT NUMBER

ARO 38069.1-RT

11. SUPPLEMENTARY NOTES

The views, opinions and/or findings contained in this report are those of the author(s) and should not be construed as an official Department of the Army position, policy or decision, unless so designated by other documentation.

12a. DISTRIBUTION / AVAILABILITY STATEMENT

Approved for public release; distribution unlimited.

12 b. DISTRIBUTION CODE

13. ABSTRACT *(Maximum 200 words)*

We have identified and confirmed that ultrafast intense Ti-sapphire laser pulses after propagating through an optical medium self-transform into chirped white light laser pulses as manifested by the generation of supercontinuum. During the propagation of such pulses in air, self-focussing and filamentation take place together with strong field interaction with molecules in its path. Some important physical processes were studied. In particular, we observed a new type of fluorescence from the air molecules characteristic of intense field ionization and fragmentation unexpected from normal wisdom of plasma emission. An analytical tunnel ionization model of air molecules that agree with our experimental results was developed. It could be used in any theoretical modelling of such propagation. New techniques were developed to study the dynamics of filamentation. They allowed us to observed directly for the first time the signature of re-focussing. The dependence of filamentation on various laser parameters such as the chirp, the divergence, etc. was also measured. Preliminary results agree with what we expect based on current knowledge of ultrafast nonlinear optics.

14. SUBJECT TERMS			15. NUMBER IF PAGES
			16. PRICE CODE
17. SECURITY CLASSIFICATION OR REPORT	18. SECURITY CLASSIFICATION OF THIS PAGE	19. SECURITY CLASSIFICATION OF ABSTRACT	20. LIMITATION OF ABSTRACT

Final Report

Title of project : *A study of the fundamental science underlying the transport of intense femtosecond laser pulses in the atmosphere*

Period covered : *Oct. 1, 1997 to Dec. 31, 1998.*

Principal investigator :

Prof. See Leang Chin
Centre d'Optique, Photonique et Laser &
Département de Physique
Université Laval
Cité Universitaire, Qc. G1K 7P4
Canada

Sponsor : *U S Army Research Office*
Research Triangle Park
N.C., U.S.A.

Proposal number : *38069-RT*

Grant number : *DAAG55-97-1-0404*

Submitted to : *Army Research Office*
Dr. Iqbal Amad
Research Triangle Park
N.C., U. S. A.

Acknowledgement : *This work was also jointly supported by grants from the Natural Sciences and Engineering Research Council of Canada, the Cener for Research on Defense Valcartier (CRDV) of the Department of National Defense of Canada and Le Fonds-FCAR of the Province of Quebec, Canada.*

Final Report

Title of project : *A study of the fundamental science underlying the transport of intense femtosecond laser pulses in the atmosphere*

Period covered : *Oct. 1, 1997 to Dec. 31, 1998.*

Principal investigator :

Prof. See Leang Chin
Centre d'Optique, Photonique et Laser &
Département de Physique
Université Laval
Cité Universitaire, Qc. G1K 7P4
Canada

Sponsor : *U S Army Research Office*
Research Triangle Park
N.C., U.S.A.

Proposal number : *38069-RT*

Grant number : *DAAG55-97-1-0404*

Submitted to : *Army Research Office*
Dr. Iqbal Amad
Research Triangle Park
N.C., U. S. A.

Acknowledgement : *This work was also jointly supported by grants from the Natural Sciences and Engineering Research Council of Canada, the Cener for Research on Defense Valcartier (CRDV) of the Department of National Defense of Canada and Le Fonds-FCAR of the Province of Quebec, Canada.*

Signature : See Leang Chin
(See Leang Chin)

Date : *20 January 1999.*

Table of Content

General information

Title of project : *A study of the fundamental science underlying the transport of intense femtosecond laser pulses in the atmosphere*

Period covered : *Oct. 1, 1997 to Dec. 31, 1998.*

Principal investigator :

Prof. See Leang Chin
Centre d'Optique, Photonique et Laser &
Département de Physique
Université Laval
Cité Universitaire, Qc. G1K 7P4, Canada.
Tel: (418)656-3418; fax: (418)656-2623; e-mail: slchin@phy.ulaval.ca

Sponsor : *U S Army Research Office*
Research Triangle Park
N.C., U.S.A.

Proposal number : *38069-RT;* **Grant number :** *DAAG55-97-1-0404*

Submitted to : *Army Research Office*
Research Triangle Park
N.C., U. S. A.
Dr. Iqbal Amad, director, International Affairs.

Personnels involved in the work:

S. Petit, post-doc (May 3, 1998 -)
A. Talebpour, post-doc. (May 1, 1998 -)
Mahmoud Abdel Fattah, Ph.D. graduate student (Oct. 4, 1998 -)
A. Proulx, M.Sc. graduate student (May 3, 1998 -)
J. Yang, M.Sc. graduate student (May 3, 1998 -)
A. Brodeur, Ph.D. graduate student, part-time (Oct. 1 –Nov. 30, 1997)
L. Strach, M.Sc. graduate student, part-time (Oct. 1 – Dec. 31, 1997)
A. Talebpour, Ph.D. graduate student, part-time (Oct. 1, 1997 – April 30, 1998)
C. Belzile, undergraduate student, part-time (Jan. 10 – April 30 and Sept. 5 –31 Dec., 1998)
F. Borne, undergraduate student, part-time (Jan. 1 – Aug. 31, 1998)
S. Lagacé, technician (Oct. 1, 1997 -)

Acknowledgement : *This work was also jointly supported by grants from the Natural Sciences and Engineering Research Council of Canada, the Cener for Research on Defense Valcartier (CRDV) of the Department of National Defense of Canada and Le Fonds-FCAR of the Province of Quebec, Canada.*

Objective of the project: To study experimentally the fundamental processes of self-focussing and filamentation of intense femtosecond Ti-sapphire laser pulses propagating in air and the fluorescence resulting from the interaction of such laser pulses with complex molecules.

Possible application: A new type of LIDAR to detect chemical and biological pollutants in the atmosphere.

Abstract

We have identified and confirmed that ultrafast intense Ti-sapphire laser pulses after propagating through an optical medium self-transform into chirped white light laser pulses as manifested by the generation of supercontinuum. During the propagation of such pulses in air, self-focussing and filamentation take place together with strong field interaction with molecules in its path. Some important physical processes were studied. In particular, we observed a new type of fluorescence from the air molecules characteristic of intense field ionization and fragmentation unexpected from normal wisdom of plasma emission. An analytical tunnel ionization model of air molecules that agree with our experimental results was developed. It could be used in any theoretical modelling of such propagation. New techniques were developed to study the dynamics of filamentation. They allowed us to observed directly for the first time the signature of re-focussing. The dependence of filamentation on various laser parameters such as the chirp, the divergence, etc. was also measured. Preliminary results agree with what we expect based on current knowledge of ultrafast nonlinear optics.

1. Introduction

The materials contained in this report were obtained thanks to the support of not only ARO under the grant number given above, but also the Department of National Defense of Canada, the Natural Sciences and Engineering Research Council of Canada and Le Fonds-FCAR of the Province of Quebec, Canada. Although ARO's support represents eventually about 30% of the total budget of the year, it came at a critical moment when the funding of the principal investigator's laboratory was inadequate. This permitted the principal investigator to bridge the gap and to establish a continuity till other supports joined in a few months later. The official period of ARO's support is between Oct. 1, 1997 and Sept. 30, 1998. However, there had been some administrative delay in the transfer of funds from the US to Canada as well as the delay in hiring post-docs and students. As such, it is the principal investigator's opinion that it is fair to include in this report the work done during the three months after the official expiration date of the ARO grant.

This report presents the results of the study of some of the fundamental sciences that occurs during the propagation of intense femtosecond Ti-sapphire laser pulses in air. The phenomenon is summarized in what follows. When a femtosecond intense laser pulse propagates in air, it will self-focus into a tightly confined filament over many tens to hundreds of meters or more. Intense white light (supercontinuum) and rainbow-type of conical emission are generated in the forward direction. Very high localized intensity can be obtained 'naturally' at long distances. This consititutes a novel technique for the transport of intense laser pulses to long distances in the atmosphere as contrast to the transport of any other type of long (nanosecond) laser pulses which will always diverge due to diffraction. The principal

application we had in mind was a novel type of LIDAR for the detection of chemical and biological pollutants through monitoring the fluorescence finger prints of these molecules. Thus, our principal task was to study the details of propagation as well as the fluorescence arising from the fragmention of the molecules of interest.

Before the beginning of the project, the detail of the physical mechanism of the propagation of such pulses was a subject of debate [1-7] while we in Laval University have already contributed to the understanding of some of the primary physical processes in single filamentation[4,6]. The latter can be explained by the moving focus model limited by multiphoton ionization (MPI; in this report, MPI is considered as a general term that includes tunnel ionization). Different slices of the front part of the pulse self-focus at different positions giving rise to a continuous streak of self-foci; hence the perception of a filament. Supercontinuum generation and conical emission is a consequence of temporal-spatial self-phase-modulaltion (SPM) of the trailing part of the pulse by the self-induced plasma in the self-foci[5,6].

Our project was to study in more detail the physics underlying the propagation of the most powerful terawatt laser pulses and the limit of such kind of propagation. These include the knowledge of the intensity distribution in the dynamically changing laser pulse especially after self-focussing begins. We made use of our state-of-the-art femtosecond Ti-sapphire laser system to carry out the experiment. The project was separated into the following sub-projects: a) the technique of controlling the length of the filaments and the position at which filamentation starts by changing various laser parameters, namely, the chirp, pulse length, beam divergence and beam shape, b) multiple filamentation, c) the physics of the interaction of these pulses with atoms and molecules in the context of the above mentioned phenomena, d) the fluorescence resulting from the ionization and fragmentation of some sample molecules and e) measurement of such fluorescence in the laboratory environment using the LIDAR technique.

This ambitious project, of course, cannot be terminated in the span of one year. However, much progress was achieved. In particular, we have arrived at some important conclusions. (1) We have identified and confirmed that the supercontinuum is indeed a chirped white light laser pulse. The latter is part of the main pump pulse whose amplitude and phase has been severely modified during its interaction with the self-created plasma resulting in a strong anti-Stokes frequency broadening, hence white light laser pulse. (2) We have established experimentally an analytical formula for the MPI of air molecules (oxygen and nitrogen). Prior to our finding, no satisfactory theoretical formula was available in the intensity range where such ionizations take place. This can be used quantitatively by theoreticians who are modelling the propagation of intense femtosecond Ti-sapphire laser pulses in air. (3) The fluorescence of the products of ionization and fragmentation of air molecules is quite different from what nanosecond laser pulse induced plasma in air gives. Using the femtosecond laser pulse, the continuum characteristic of a plasma is too low to be detectable in our system while line emissions from some unexpected molecular ionic states dominate. (4) We confirmed the theoretically predicted phenomenon of multiple re-focussing during the propagation of the pulse through a geometrical focus. The theoretically predicted distortion of the laser pulse resulting in an intensity distribution with circular ring structures was also recorded directly on glass plates. Other results on the dependence of filamentation on the chirp, the divergence and the beam shape of the laser pulse have been observed.

In the course of the past year, two workshops have been organized by the principal investigator thanks to the support of ARO and DREV (Defense Research Establishment Valcartier, Canada). They were both focused on the problem of the propagation of intense femtosecond laser pulses in the atmosphere. One was a bilateral workshop (April 7-9, 1998) between Canada and the US with invited participants

coming from DREV, ARO, MICOM and the principal investigator's laboratory. The other was an international workshop (June 19-20, 1998) with invited participants from ARO, MICOM, US Air Force, Sandia National Lab., some US Universities (Michigan, Arizona, Cornell), DREV, France (Polytechnique), Germany (Jena), Russia (Moscow), Egypt (Cairo), National Research Council of Canada and two Canadian Universities (Laval, INRS). These activities have been filed in other reports submitted to ARO and will not be repeated in the text.

In what follows, some of the results which were given in the interim report and which were not changed since then are included for completeness.

2. Experiments

2-1. General

The modern ultrafast intense laser laboratory houses the million-dollar state-of-the-art **terawatt Ti-sapphire laser facility** giving out three beams simultaneously with the following characteristics (best performance):
Beam 1: 1 terawatt,10Hz, 200fs
Beam 2: 10 GW, 1 kHz, 120fs
Beam 3: 10 GW, 10Hz, 120fs;

These beams are very stable from the operational point of view. Once aligned, no day-to-day re-alignment is necessary for weeks and months. Fig. 1 shows the optical layout of the laser system. In the present work, mainly the terawatt beam was used. The energy of the beam was reduced significantly during all experiments because self-focussing starts at a much lower power. This is also precisely where the fundamental technical challenge is; i.e. how to inject at will a lot of energy into the filament at a long distance in the atmosphere.

2-2 Filamentation : dependence on laser parameters

2-2.a. Dependence on the chirp of the pulse

The femtosecond laser pulse is generated by the technique of chirped pulse amplification followed by pulse compression through a pair of parallel identical gratings. It is expected that changing the chirp in the pulse would change the self-focussing distance. We thus studied this aspect first.

When a femtosecond laser pulse double-passes through a parallel grating pair, a negative group velocity dispersion (GVD) is induced in the pulse; i.e. a negative chirp is introduced in the pulse. The group delay dispersion (GDD) after a double pass is given by [8]:

$$\left.\frac{d^2\phi}{d\omega^2}\right|_{\text{double-pass}} = -\frac{D\lambda^3/a^2}{\pi c^2\left[1-\left(\sin\alpha-\frac{\lambda}{a}\right)^2\right]^{3/2}} \qquad (1)$$

where $\phi = kz$, and the GVD parameter is given by $\frac{d^2k}{d\omega^2}$. Here, k is the wave number; ω, the angular frequency; D, the spacing between the identical grating pair; a, the grove spacing of the gratings; α, the

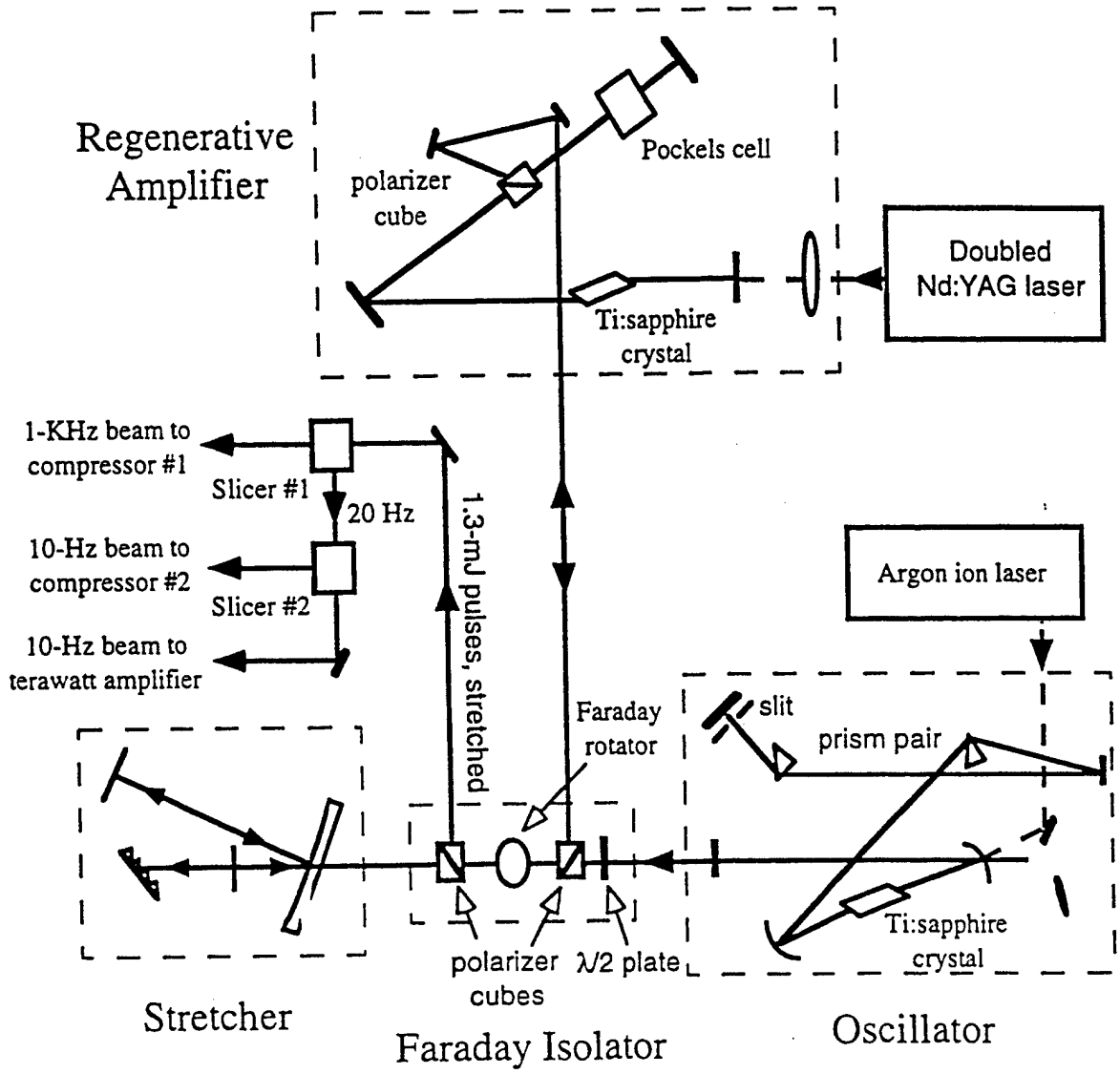

Fig. 1a. Optical layout of the oscillator and regenerative amplifier in the 3-beam femtosecond Ti-sapphire laser system.

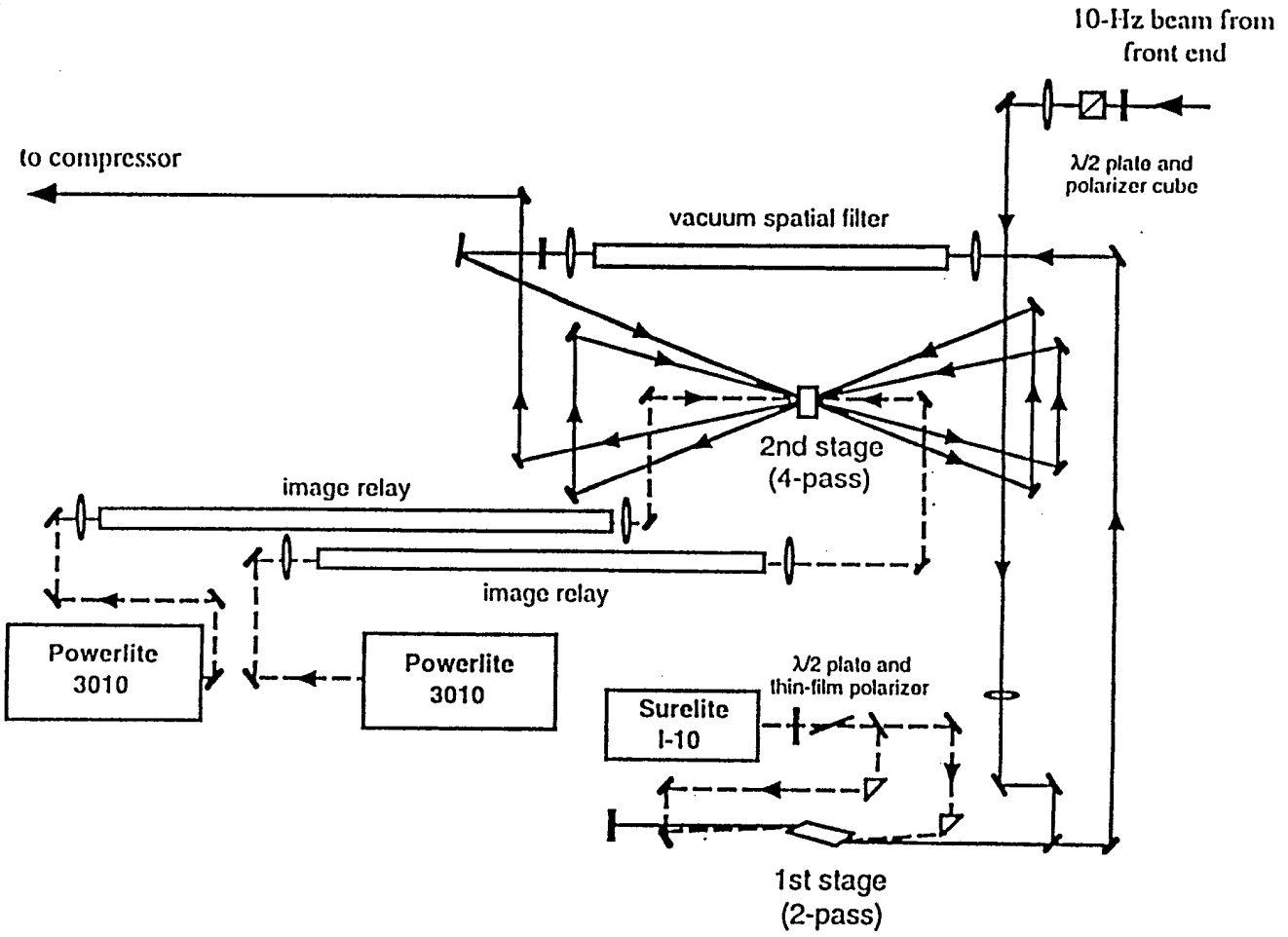

Fig. 1b. The two-stage amplifier system in the 3-beam femtosecond Ti-sapphire laser system.

angle of incidence to the first grating; λ, the wavelength and c, the speed of light in vacuum. The GDD in eq.1 is always negative.

The stretched and amplified long laser pulse (about 200ps) emitted from the amplifier chain before going into the compressor is positively chirped. Thus, it is expected that the laser pulse at the output of the compressor will have its chirp compensated. If the compensation is complete, the pulse becomes transform limited (shortest); if not, it will be chirped either positively (up-chirp) or negatively (down-chirp) depending on whether it is under-compensated (D too small, see eq.1) or over-compensated (D too large). Both types of chirped pulses are longer than the transform limited pulse. It is expected that by changing the distance D between the grating pair, one would be able to vary the beginning of the filament.

The dependence of the beginning of the filament as a function of the distance between the grating pair in the compressor (i.e. as a function of the chirp) was thus measured, initially in the 200m long corridor outside the laboratory and later on inside the laboratory. The beginning of the filament is defined qualitatively as the smallest burned spot on an ir-sensitive papers. The burned spot is in the form of a central small dot (of the order of one mm or less) surrounded by a larger pattern (a few mm in diameter which is roughly the diameter of the beam at the output of the compressor, 6mm at $1/e^2$). Fig. 2 gives the result of such a measurement.

It shows that at a constant pulse energy, up-chirped pulses (towards the right of the figure) and down-chirped pulses behave symmetrically; i.e. the distance from the output of the compressor to the beginning of the filament increases with the chirp in the same way regardless of the sign of the chirp. This could be explained by the fact that the lengthening of a femtosecond pulse by the chirp depends only on the square of the chirp; i.e. on the square of the GDD. For example, a normalized Gaussian wave packet that expresses the electric field E of a pulse is given by:

$$E(z,t) = \int_{-\infty}^{\infty} \exp[-i(\omega-\omega_0)^2/\Gamma^2]\exp[i(kz-\omega t)]d\omega \qquad (2)$$

where z is in the propagation direction; Γ, the width of the Gaussian component centered at ω_0 ; k and ω, the wave number and the frequency respectively and t , the time.

After integration, in the approximation that only linear chirp is considered, the intensity is given by:

$$I \sim |E|^2 \sim \exp\left[-\frac{(t-\alpha)^2}{2\left(1/\Gamma^2+\beta^2\Gamma^2/4\right)}\right] \qquad (3)$$

where $\alpha = \left.\frac{d\phi}{d\omega}\right|_{\omega=\omega_0}$, $\beta = \left.\frac{d^2\phi}{d\omega^2}\right|_{\omega=\omega_0}$. The width at the 1/e point is

$$t_p = 2\sqrt{2}\Gamma\sqrt{\frac{1}{\Gamma^4}+\frac{\beta^2}{4}} \qquad (4)$$

showing the dependence of the pulse width on β^2; hence on the square of the GDD parameter.

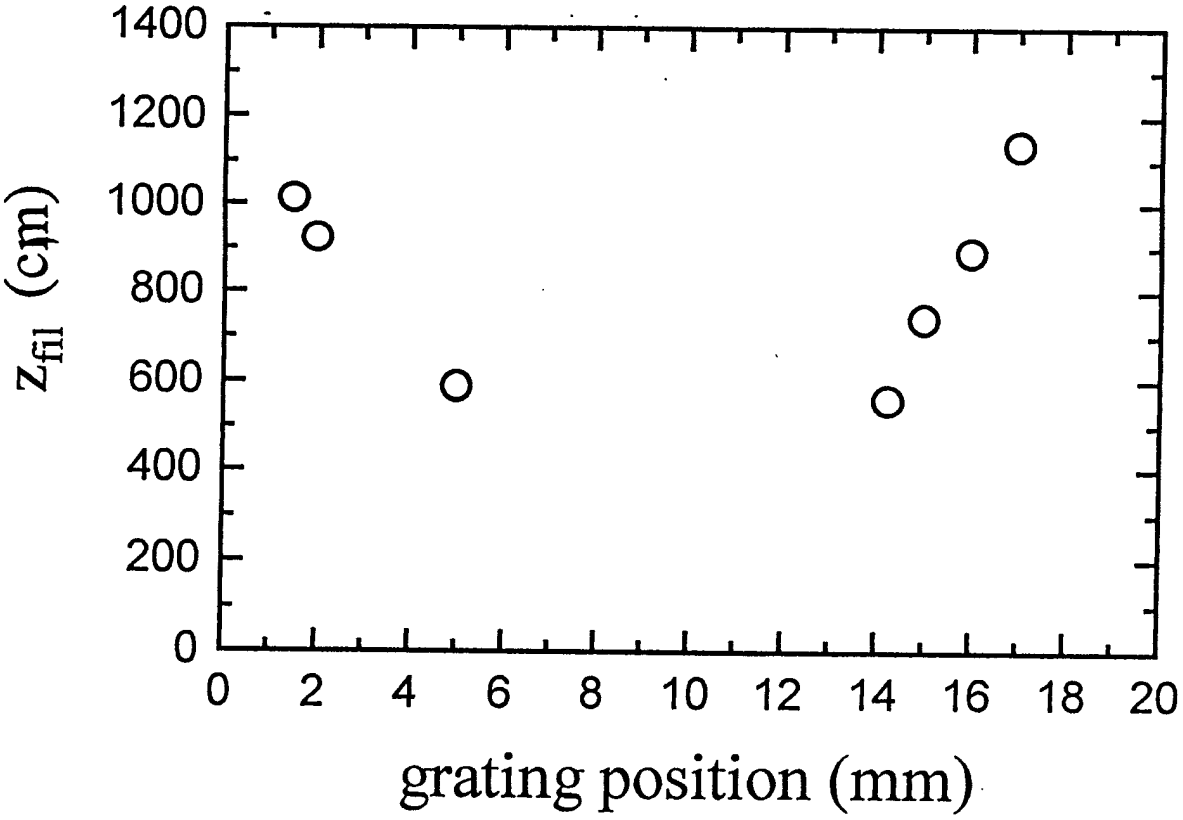

Fig. 2. Dependence of the beginning of the filament as a function of the spacing between the parallel grating pair in the compressor. Larger spacing is towards the left. Z_{fil} is the distance from the output of the compressor to the beginning of the filament. Input beam diameter ($1/e^2$): 6mm;. pulse energy: 6.2mJ; optimum pulse duration: 250fs.

Such lengthening of the pulse results in the lowering of the peak power when the pulse energy was kept constant; this leads to a longer self-focussing length z_f as can be seen in the following formula derived in self-focussing theory when a Guassian pulse is assumed [9].

$$z_f = \frac{0.367ka^2}{\{[(P/P_{crit})^{1/2} - 0.852]^2 - 0.0219\}^{1/2}} \qquad (5)$$

where P_{crit} is the critical power; P, the peak power of the pulse; k, the wave number; and a, the radius of the beam at the 1/e power level. Eq. 5 shows that as P decreases, z_f increases.

This is a re-affirmation of the dependence of self-focussing on the power (eq.5) but not on the instantaneous field amplitude and the phase of the field. This is true only under the slowly varying envelope approximation. For a 200fs pulse, such an approximation is still valid since the period of the field's oscillation at 800nm is about 2.7fs, still much shorter than the pulse duration.

The change of the positions of the beginning of the filament varied only from about 4 m to 12 m as shown in Fig. 2 although we expected much longer distances. It was found out after the experiments that the amplifier had not been re-aligned exactly back to its original state after changing some damaged optics. Instead, the new alignment was such that the beam was slightly convergent. Thus, the pulses self-focussed slightly earlier inside the laboratory before getting out into the corridor. Consequently, the mirror in the corridor was damaged and thus there was no way to measure the end of the filament. We were forced to do only a limited experiment inside the laboratory by meauring the position of the beginning of self-focussing.

Inspite of this, an important **conclusion** can be drawn from the above result. Self-focussing does not depend on the sign of the chirp but only on the absolute value of the chirp. The beginning of the filament can be varied by varying the absolute value of the chirp of the pulse.

2-2.b. Effect of divergence

During another series of experiments in the corridor, we found that double filamentation started to occur when the pulse energy was increased beyond 10mJ. This was expected. However, at such an energy, when the divergence of the pulse was increased, double filamentation disappeared leaving behind only one filament at the axis of the beam. At the same time, the position of the beginning of the filament moved further away from the compressor while the conical emission at a distance of about 120m from the output of the compressor became more intense and better resolved in color. Further increase in pulse energy caused the appearance of double filaments again while further increase in the divergence returned to single filament at the axis of the beam with stronger and better resolved conical emssion while the beginning of the filament moved further away. This situation repeated until we ran of of space in the adjustment of the telescope that changed the divergence of the beam before the compressor. The pulse energy was still low, only about 20mJ.

This result seems to indicate that there is a possibility to put more enengy into the pulse and still maintain one single filament simply by increasing the divergence of the beam. This could mean that more energy could be injected into the filament. Although it was not clear yet why the conical emission became more intense and better resolved in color, we present a tentative explanation as to why increasing the divergence of the beam gives rise to single filamentation along the beam axis.

Multiple filamentation originates from local (spatial))intensity fluctuation in the laser pulse's wave front. When the divergence increases, local intensity fluctuation at the wave front becomes weaker because the local wave surface is stretched into a larger more divergent surface. The local power is then not sufficient for self-focussing at the original localities. The central part of the spherical wave front is less affected by such an increase in the divergence as compared to the peripheral positions. (See Fig.3.) Hence, only the central part of the wave front would self-focus earlier draining the pulse energy into it. The consequence is the dominance of the central axial filament and the beam is now limited to a single filament.

We **conclude** that there is a possibility to transport high energy pulses to a long distance with only one filament by increasing the divergence of the pulse. Inspite of this, it is necessary to repeat this experiment with a better controlled divergence and higher energies so as to be able to move the beginning of the filament hundreds of meters from the compressor while injecting as much energy into the filament as possible.

2-2.c. Effect of beam shape

We thus prepared another series of experiments aiming at measuring the dependence of the filamentation on the laser pulse's divergence. This required modification of the telescope in front of the compressor as well as the replacement of some optics. Re-alignment of the laser chain was thus necessary before carrying out the following experiment.

A 1m focal length lens focussed the pulse into a vacuum system. At the exit, a lens of 25cm focal length was used to reduce the beam size by a factor of about 4. This second lens at the output of the vacuum system was mounted on a micrometer translation stage so that the laser pulse's divergence could be varied. The experiments carried out afterwards in the corridor outside the laboratory was inconclusive. We could not obtain a filament even if the energy per pulse was increased up to about 30mJ.

What we discovered was that the pulse's cross sectional shape was oval after propagating for a distance of about 30m whereas at the output of the compressor, it still looked round with a roundness of about 0.8 according to the measurement using a CCD camera. The beam tended to self-focus in one dimension but never reaching a strong spot . It is a bit similar to the astigmatism of a lens.

The laser beam was thus checked thoroughly. We found out that one of the gratings in the compressor has deteriorated too much and the bad beam quality could have been due to this grating. After changing this expensive piece of grating, together with a series of checks, we found out the following. It was very probable that some spatial chirp in the pulse was at the origin of the problem. This is discussed in section 2-2.d .

We **conclude** that in order to have an efficient self-focussing, the beam shape has to be as round as possible throughout the whole propagation length; i.e. cylindrically symmetric.

2-2.d. Effect of spatial chirp

In the course of carrying out the experiments in the previous section, we realized that the filament was not created along the central axis of the of the propagating pulse. The filament was off center of the pulse. We believed that this could be due to a kind of spatial chirp. After some lengthy search, the origin of this spatial chirp was discovered. It was due to the non-ideal beam shape again. We note that

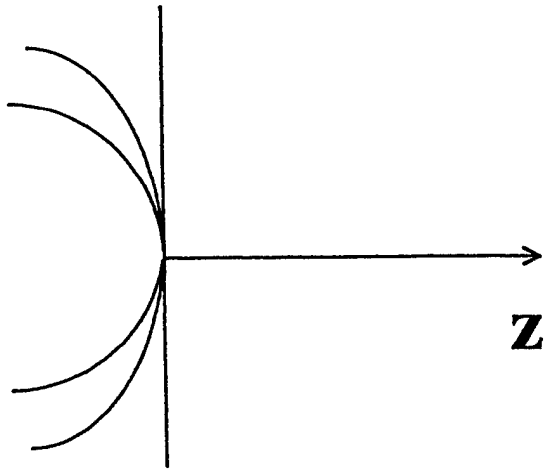

Fig.3. Wave fronts of various divergences illustrating the smaller change at the central region.

during the previous experiment, the pinhole in the vacuum telescope was removed because the laser kept damaging it every so often. The non-ideal beam shape causes the diffracted spectral patterns from the pair of gratings in the compressor to only partially overlapping with each other after a double pass. This partial overlap of the spectrum means that the local pulse duration across the cross section of the pulse is not uniform. Shorter pulse length means higher power. The shortest pulse length at a non-axial position might first build up self-focussing resulting in an off centered filament.

After inserting the pinhole back into the vacuum telescope, the pusle shape became much rounder with a roundness of about 0.9. The filamentation was improved; i.e. the filament was now nearer the axis, but not yet at the center. By increasing the divergence of the pulse, the filament became centered. This is a reconfirmation of the observation in section (2-3).

We **conclude** that a spatial chirp could generate an off-centered filament.

2-3. Improvement on the laser

The experimental results obtained in section 2-2 showed that a little defaults in the beam quality would produce distortions in the filament formation. This showed that the initial pulse characteristics are crucial to the success of the experiments. We thus improved step by step the quality of the beams along the whole chain as indicated in Fig. 4. First of all, the argon ion pump laser of the oscillator was replaced by a solid-state-diodes-pumped vanadium laser (Coherent's Verdi). Long time stability of the oscillator was improved. Secondly, we worked to improved the beam shape quality. For that, in order to inject a beam as perfect as possible in the amplifier stages, we introduced a new spatial filter between the regenerative amplifier and the high-power amplifiers. This spatial filter is a confocal telescope with two lenses (75 mm and 50 cm focal lengths) and a 220 μm diamond pinhole placed at the focal plane in a vacuum tube. Micro-damages inside the two-pass pre-amplifier crystal was suspected to be the source of beam shape distortion in the high power beam and a loss of power that we observed at the pre- amplifer stage. We changed the crystal. To avoid further damages, we increased the size of the injected beam in the preamplifier. Roundness better than 0.95 was measured before the second stage of amplification. Finally we obtained more than 170 mJ (at about 70% of the pumping capacity) before the compressor with a beam shape roughly Gaussian and a roundness of about 0.9 (Fig.5). The compressor too was completely re-aligned because a slight mis-alignment would induce spatial and temporal chirp and beam shape distortion. We performed third-order cross-correlation and FROG experiments to characterize and adjusted the final duration and the chirp of the pulses. We are now working with 220 fs slightly chirped pulses with a nearly Gaussian spatial shape.

In the corridor, we performed an experiment to study the influence of the initial divergence of the beam (Fig. 6). After the compressor we installed a confocal telescope formed with two 1 m focal length lenses. The surfaces of the lenses are coated for anti-reflection at 800 nm. The last lens is mounted on a translation stage to change the divergence of the beam. To avoid self-focusing and white-light generation in air in the telescope, we installed a plexiglass tube with two anti-reflection-coated glass windows and pumped by a turbo-molecular vacuum system. Because the pumping was through a small valve, the pressure inside the tube cannot be less than 1 Torr. Unfortunately, this was not low enough and we still observed a small filament inside the tube. This was enough to affect the shape of the long filament during the propagation. (For a better understanding, see next section and appendix 1.) Qualitatively, we observed that the more the beam is divergent the longer is the distance of the beginning of filamentation from the output of the compressor. But because of the small filament in the vacuum tube, we couldn't do any quantitative experiment. We are currently building a metallic vacuum

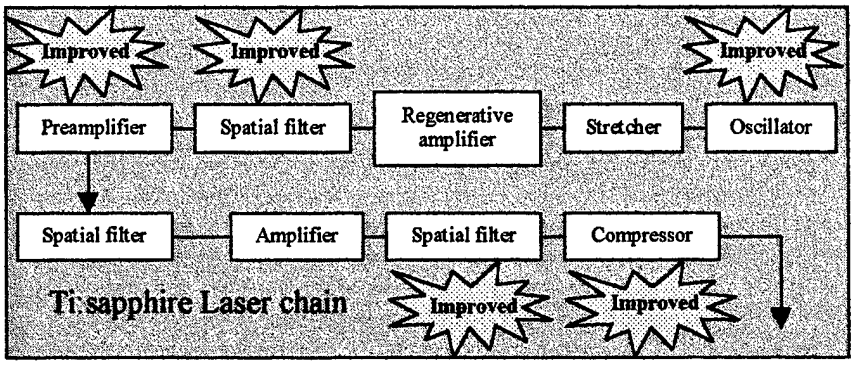

Fig. 4 *Improvements in the laser chain.*

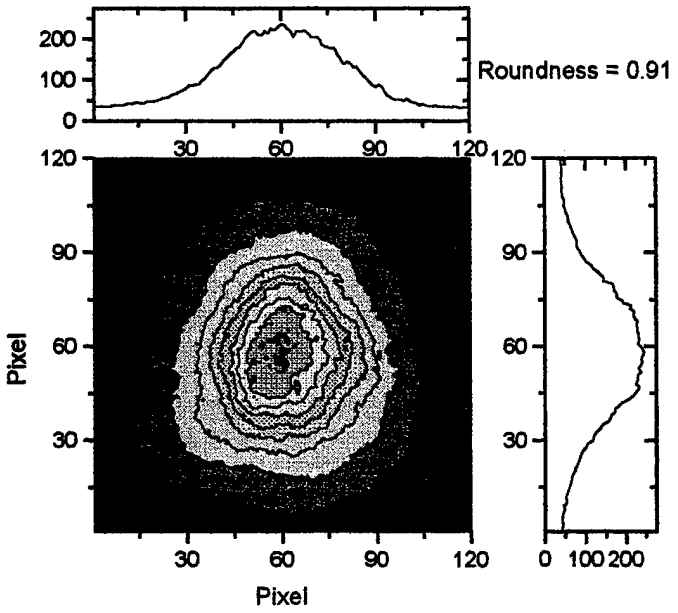

Fig. 5 *Beam shape before compressor*

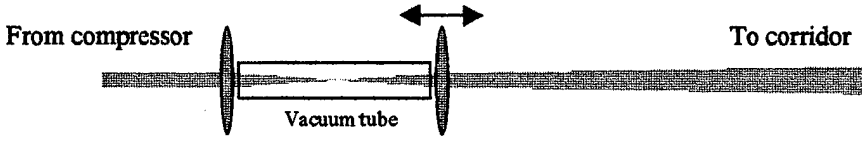

Fig. 6 *Divergence experiment's setup*

tube that will be pumped by the turbo-molecular pump through a larger openning in order to get the vacuum down to 10^{-3}-10^{-4} Torr.

2-4. White light laser

The supercontinuum generation in transparent optical media was first observed with picosecond laser pulses and nowadays are routinely obtained with the developpment of femtosecond laser sources. The mechanism of this process was widely studied and it is generally accepted that the basic reason is self-phase-modulation in the self-created plasma resulting in a large anti-Stokes broadening. This source ranging from the near IR to the UV is widely applied in laser physics as a tunable source in spectroscopy or as a seed for futher amplification in dye amplifiers or optical parametric amplifiers, etc. Because this source is generated by a coherent laser source and involves instantaneous nonlinear effects, it is tacitly accepted that the supercontinuum is also a coherent source. In this work, we showed that in terms of coherence length, the supercontinuum should be called a white-light laser.

The coherence length was measured using the technique of spectral interferometry with a Michelson interferometer followed by a spectrometer (Fig. 7). The spectrometer splitted the spectral components of the two delayed pulses coming from the Michelson interferometer into pairs of identical wavetrains limited by the spectral resolution of the apparatus. As long as the pairs of wavetrains overlap, interference appeared in the spectral domain (i.e. spectral modulation). The coherence length of a spectral component limited by the resolution of the spectrometer is defined as the delay range over which one observes spectral modulation. We compared the coherence lengths of of the spectral components of two types of white-light sources: the supercontinuum and a thermal incandescent lamp.

A Ti:Sapphire oscillator followed by a 1 kHz regenerative amplifier was used to generate 170 fs pulses centered at λ_0 = 800 nm with an energy less than 1 mJ. White light supercontinuum was generated by focusing the pulses into various liquids contained in a cell with fused-silica windows centered in a telescope (Fig. 7). Liquid water, CCl_4 and methanol were tested and the laser input intensity was adjusted by variable neutral density filters in order to be in a single filament regime. The telescope was adjusted in such a way that the output beam was collimated. The thermal source was a quark lamp and the output beam was collimated before entering in the Michelson interferometer. In both cases, the collimated beams illuminated directly the entrance slit of the spectrometer and the comparison of both types of sources was performed under identical experimental conditions.

The results are shown in Fig.8, where the ratio between the coherence lengths of the supercontinua and the incoherent source has been plotted versus the wavelength. One can see that this ratio is independent of the material where the supercontinuum is generated, which confirm that the generation of supercontinuum is a universal phenomenon. Moreover, in the range between 500 nm and 800 nm, all the ratios are appreciably equal to the corresponding ratio of the Ti:Sapphire laser pulse. On the wings of the spectra, this ratio decreases quickly. This might be due to the decrease by more than one order of magnitude of the supercontinuum intensity in these spectral regions so that the contribution from the incoherent plasma recombination light in the white-light filament becomes important. Otherwise, we expect that the relative coherence length to be the same as the other values. We therefore conclude that the relative coherence lengths of all the frequency components of the supercontinuum are essentially equal to that of the pump Ti-sapphire laser pulse. From the point of view of coherence length, the components of the supercontinuum should thus be called coherent laser pulses and together, they constitute a chirped white light laser pulse. A detailed analysis of the propagation of powerful femtosecond laser pulses leading to the formation of such chirped white light laser pulses is given in the invited paper written by the principal investigator and his co-authors. It will be published in the

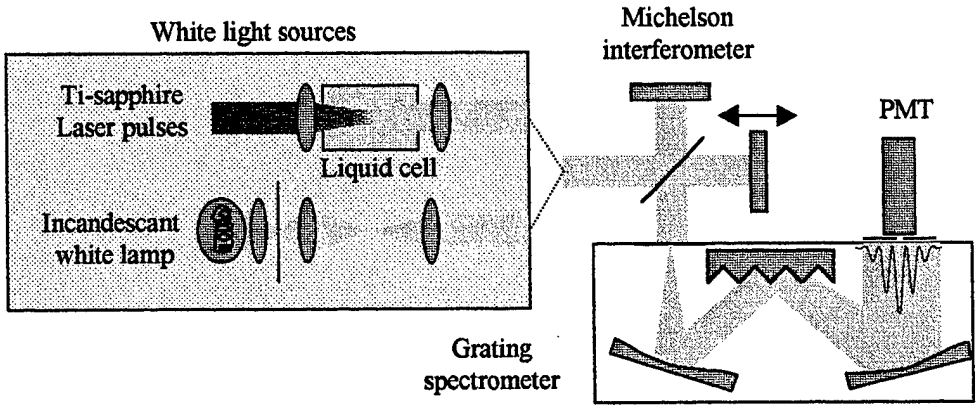

Fig. 7 *White-light coherence experimental setup*

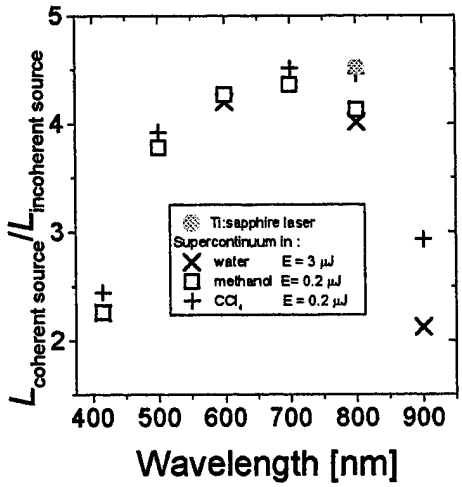

Fig. 8 *Ratio of the coherence length of a thermal white lamp and the white-light supercontinuum source. generated in various liquids [water, CCl_4, methanol).*

Journal of Nonlinear Optical Physics and Materials. The preprint is given in appendix 1. Appendix 2 shows the preprint of a paper on the justification of white light laser to be published in the Japanese Journal of Appied Physics (February 1999).

2-5. Re-focussing measured by a two-wire detector

Meanwhile we develop a new technique to measure the dynamic development of the filament. The detector consists of two parallel wires with a high voltage across it. The experimental set-up is presented in Fig. 9. Each wire has a length l=1 cm and they are separated by a distance d=1 cm. During the experiment, the voltage difference between the wires is kept constant (V=3 kV). The signal, S(t), is detected using a 500 MHz oscilloscope. Figure 10 shows some typical signals as the detector moves toward and away from the geometrical focal point of the lens. For our analysis, we measured the strongest peak-to-peak value of this signal. The structure of the signals are the same. They represents the damped oscillation of the whole electronic circuit excited by an impulsive signal. The strongest signal was obtained when the the two wires were parallel to the filament. If we put the two wires perpendicular to the filament we obtained the same signature as with the wires parallel; the difference being that the peak height of the signal was roughly a factor of 5 lower. Figure 11 shows the variation of the signal (maximum peak-to-peak) as a function of the voltage across the two wires.

We believe that the physical origin of the signal is related to the effect of electrostriction (generation of a 'DC' field) in the plasma column of the filament when the inversion symmetry of the gas was broken by charge separation in the region of high intensity or high ponderomotive potential plus the external static field. The induced 'DC' field in fact is an electrical pulse proportional to the intensity since the second order nonlinear polarization of electrostriction is proportional to the intensity. This electric pulse is as short as or shorter than the laser pulse duration (terahertz pulse). This fast pulse would induce a strong impulsive magnetic signal which in turn induces an electric current pulse in the circuit of the two-wire detector. Because the electric and magnetic pulses are very fast (about 100 fs), the electrical circuit cannot follow them faithfully and hence gives rise to an impulsive response (damped oscillation) characteristic of the response time of the circuit used. That's why the structure of the signals are the same. However, the peak value of the signal is proportional to the peak value of the electric and magnetic impulses; hence to the gross laser intensity in the filament. We are currently studying the detail of the technique.

Fig. 12 shows typical signals of the two-wire detector as a function of its position along the propagation axis at different laser energies. The filament was in between and parallel to the two wires. The peak of a curve indicates a high intensity zone, hence a self-focal region. The one before the geometrical focus moves towards the lens (away from the geometrical focus) as predicted by the moving focus model[9]. The appearance of other peaks after the geometrical focus is a direct manifestation of re-focussing[3-7]. In particular, we have reasons to believe that a third maxima on the curve at 30mJ (at around the position of 20 cm) might be due to another re-focussing of the laser beam. This is the first experimental evidence of multiple re-focussing predicted by the theoretical study of the Arizona group in a similar situation of a focussing geometry[3].

2.6. Fluence Profile of filament Recorded on Glass Plates

It is well known that for sufficiently strong laser pulses focused on a material's surface, ablation occurs. This damage could therefore be used to characterize the spatial fluence profile of the laser pulses as they propagate in air. The experiment was performed using 300 fs pulses focused by a 1.5 m

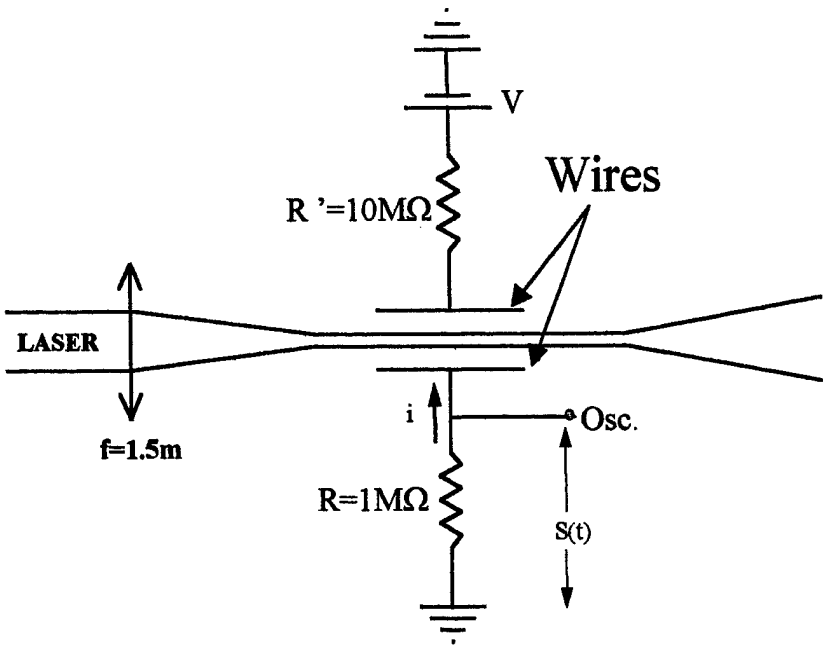

Fig. 9: The detector's circuitry

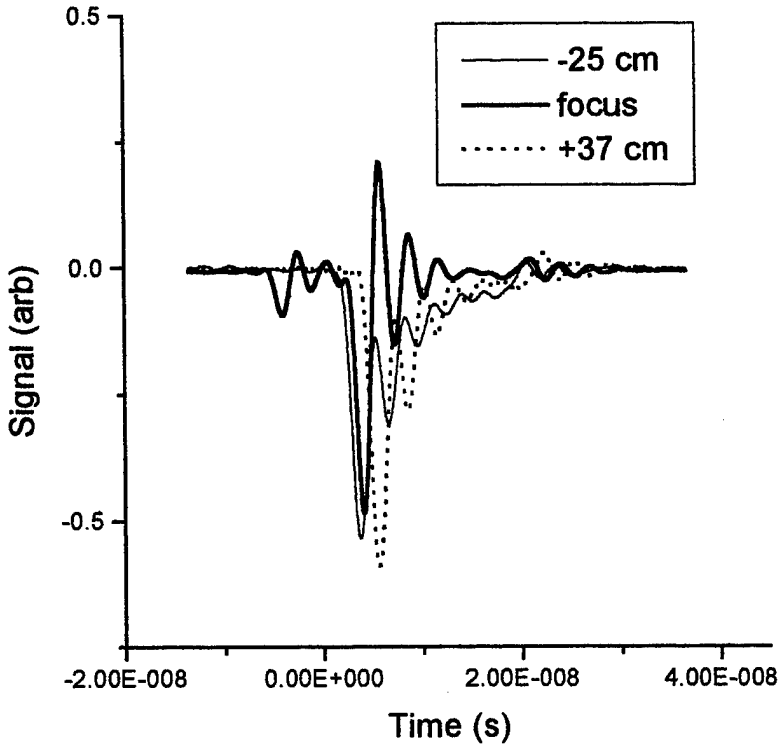

Fig. 10: The signal obtained by the detector

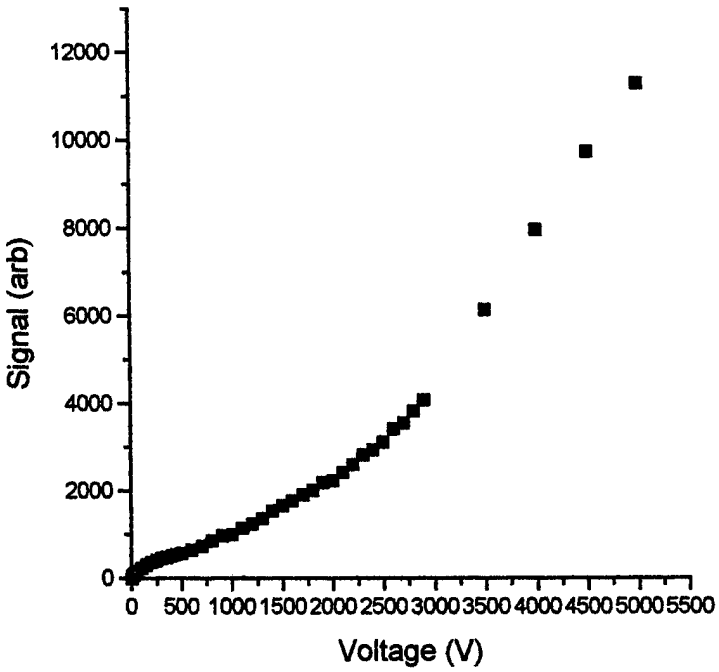

Fig.11: Peak-to-peak value of the signal as a function of the applied voltage.

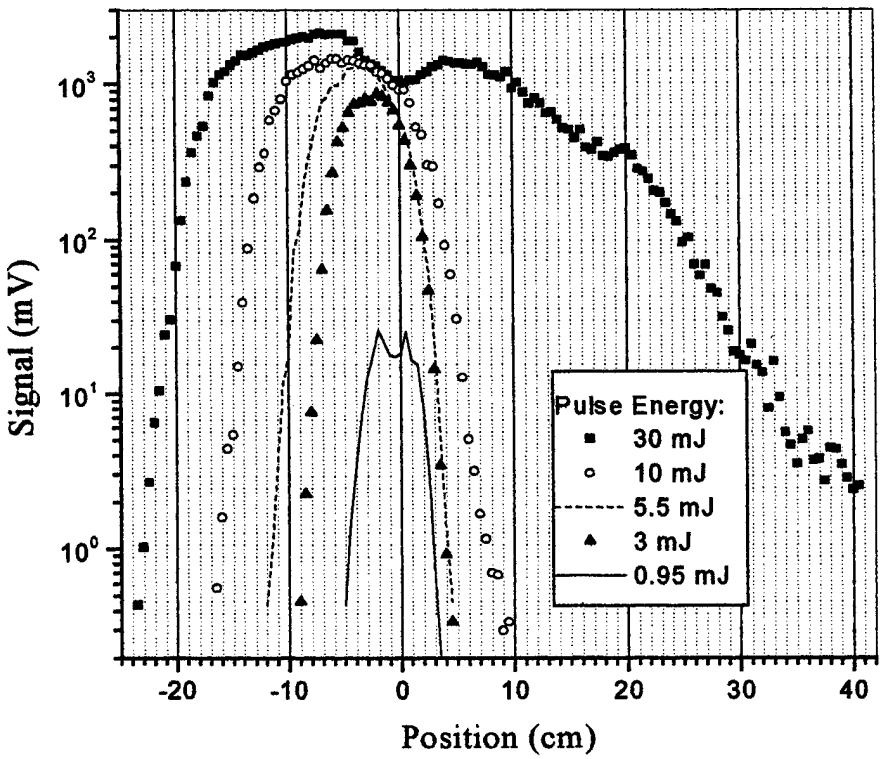

Fig.12: Typical results from the wire detector. The x-axis refers to the position of the detector w.r.t. the position of the focal point of the 1.5 m lens.

focal length lens. The laser beam had a diameter of roughly 1 cm. The experimental set up is shown in Fig.13.

In order to have a good representation of the evolution of the pulse shape, the samples are taken at different positions before and after the geometrical focus by increments of 0.5 cm. Afterward, a scan of the damages on the samples is done by a DekTak IIA profilometer. This apparatus allow us to get a direct measurement of the ablation profile on the sample by measuring the variations of the ablation depth across the damage. Since this ablation profile is in fact a measure of the fluence of the laser pulse, analyzing this profile can be helpful to acquire a better understanding of the filamentation process because it provides a step-by-step evolution of the filament

Fig.14a shows a typical damage spot at a position of 5mm from the geometrical focus and Fig. 14b shows its corresponding depth profile across a diameter. In Fig.14a, the damage consists of a central spot surrounded by a rather homogeneous circular ring and then by a complex outer region. By inspection of the DekTak scan (Fig.14b), we see that this homogeneous ring corresponds to the two shoulders separating the deep central hole from the two secondary craters. Because this is a one dimensional scan on a circularly symmetric damage, it follows that the two secondary craters represents in fact an ablated ring.This scan explains why the shoulders looks homogeneous on the picture: on the DekTak scan, they are at the same height as the surface of the non-ablated region of the sample. i.e.: the intensity of the laser pulse in this region was too low to create a damage. The sensitivity of the DekTak is not sufficient to detect fine circular craters; but these are evident on the picture as fine circular rings(Fig.14a).

Now, let's look at the information we can get about the pulse shape by inspection of the damages. First, the central crater of the damage is attributable to the intense filament developing at the center of the laser pulse as it propagates. Then, there is the ablated ring surrounding it. We believe that this ablated ring is due to intensity rings developed through the diffraction of the trailing part of the pulse by the plasma column created by the leading part of the pulse. In fact, Kosareva et al.[4-6] developed a theoretical model in which the front end of the laser pulse develops into an intense filament which ionizes the air. The plasma column diffracts the back-end of the pulse and this diffraction gives rise to circular rings of intensity structure which when interacting with the glass surface will create ablated rings as we observed on the damaged glass sample. In the case of non-focussed pulse propagation [1,2, 4-6], such rings would generate a ring structure of positive nonlinear Kerr index which would re-focus the pulse; hence, our first observation of re-focussing[4]. To our knowledge, this is the first direct experimental observation of the presence of such circular structures in the filament predicted by the theoretical models.

Starting at about 10mm from the geometrical focus and further, no such rings was observed except a central crater whose diameter reduces as the plate was moved away from the geometrical focus. This is understandable because the intensity of the focussed pulse away from the focus is lower.

2-7. Fluorescence

We have measured the fluorescence from air. The laser pulse was focussed into air by various long focal length lenses (from 1m to 7m). A filament with a length from about 10cm to about 50cm respectively was formed spanning the geometrical region. A pale bluish-white light can be seen in this filament region by the naked dark-adapted eyes. Part of this filament was imaged from the side onto the slit of a 0.5m spectrometer. Specta from air and from pure N_2 are the same while no spectrum can be detected in O_2 in the spectral range limited by our system. An example of the spectra from N_2 is shown

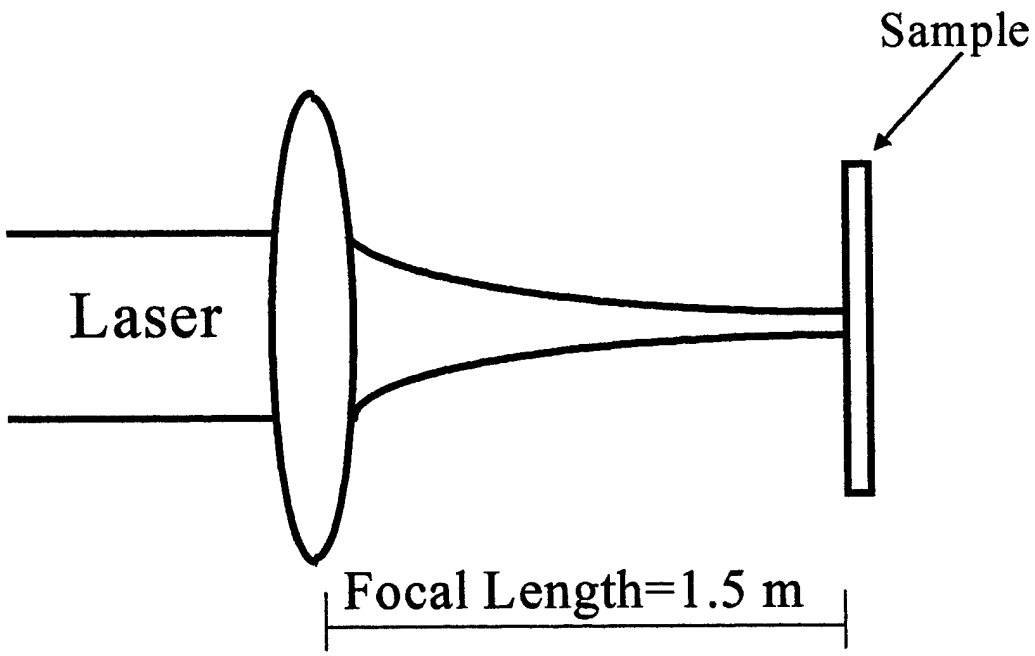

Fig.13: The experimental set-up

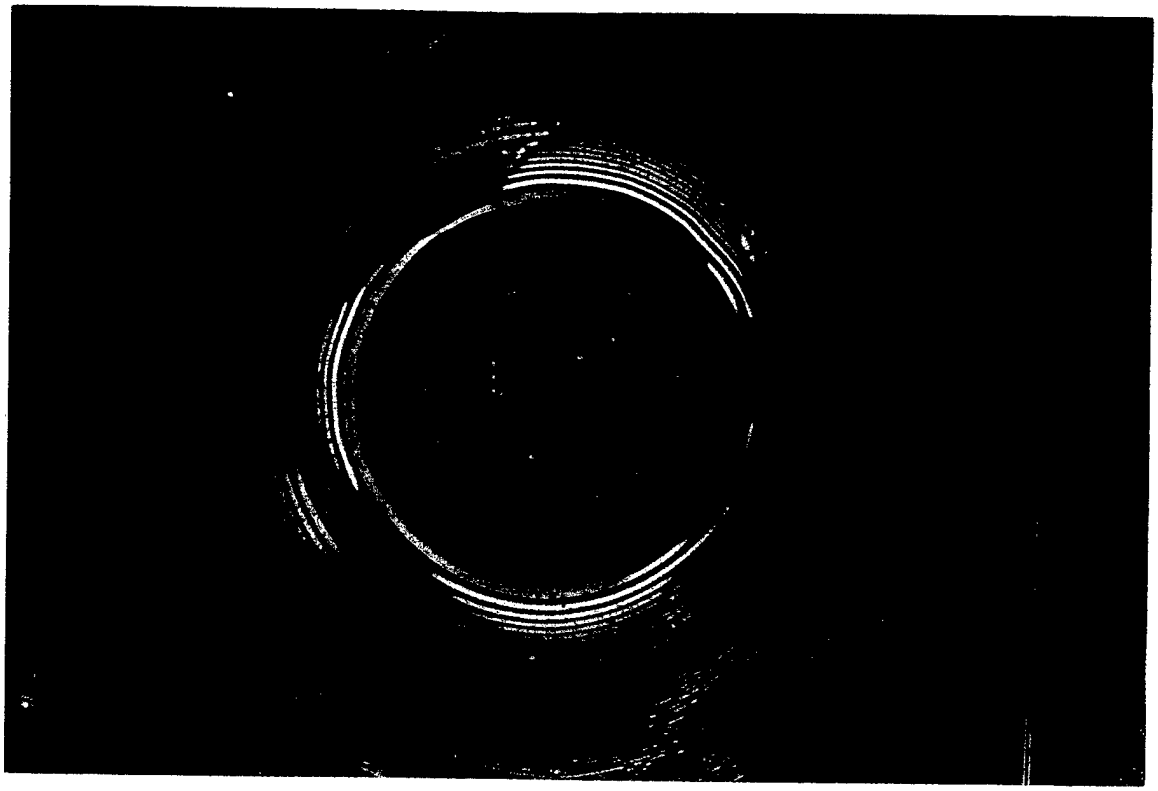

Fig.14 a: Photograph of the damage at the surface of the sample.
(Taken with a phase-contrast microscope)

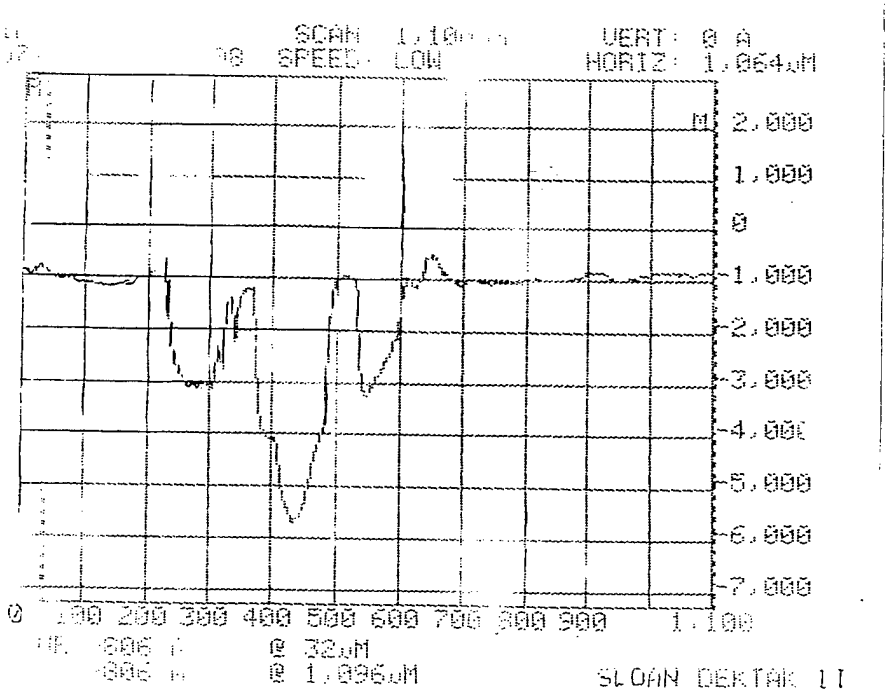

Fig.14 b: The DekTak scan of the damage presented on fig.14 a.
(The scan is made from left to right)

in Fig. 15. It consists of many sharp lines. This is compared to the spectra of ns laser induced breakdown in air using uv and red lasers (Fig. 16 and 17). The last two spectra are very similar whereas they are drastically different from the spectrum from the filament (Fig.15).

The spectra in Fig.15 were obtained from around the geometrical focal region at a pressure of 5 Torrs of N_2 when a 1m lens was used. The laser intensity was estimated to be $6x10^{14}$ W/cm^2 (the estimation of the intensity is based on the measured laser parameters; pulse duration, pulse energy and the spot size at focal region). From 470 nm up to 800 nm there is no signal, therefore this part is not presented in the figure. Below 300 nm and beyond 800 nm the detection efficiency of our spectrometer is very low. Thus we did not measure the spectrum in these regions.

The observed violet degraded lines are assigned to two band systems; the second positive system of N_2 ($C^3\Pi_u - B^3\Pi_g$ transition) and the first negative system of N_2^+ ($B^2\Sigma_u^+ - X^2\Sigma_g^+$ transition) respectively. The former could have come from the trapping of electrons in highly excited states[10]. The latter could be the result of electron re-scattering. Appendix 3 gives the preprint in which the first negative system of N_2 fluorescence is analysed in more detail.

This is an example of the consequence of ultrafast intense laser interaction with molecules. Because of the very short time scale involved, almost all interactions are electronic in nature and the consequences such as enhanced ionization followed by Coulomb explosion[11-14], re-scattering, etc. are very different to the so-called normal wisdom. Currently, we are studying the fluorescence from fragmenting hydrocarbons in the same spectral region. Preliminary results are as unexpected as those from air molecules.

2.8. Re-focussing measured by fluorescence

The fluorescence from air can be used as a measure of re-focussing. The total fluorescence measured from the side of the filament as described in the previous section was plotted as a function of the position with respect to the geometrical focus. The results are almost identical to those obtained by the two-wire detector. Fig. 18 shows a comparison between the results obtained by the two-wire detector and the fluorescence detector. In this experiment, we used a spherical mirror with a focal length of roughly 6.7 m. Both detectors give pretty much the same results; the difference being that the photomultiplier seems to be more sensitive. Detailed analysis of the experiment is given as a preprint in Appendix 4.

2.9. Ionization of N_2 and O_2

During the propagation of ultrafast intense laser pulses in the atmosphere, self-focussing is counteracted by the de-focussing effect of the self-generated plasma which results in the moving focus picture. The plasma is generated through MPI and not via cascade ionization because of the femtosecond time scale. Therefore, any meaningful simulation of the propagation needs a predictive model for the rate of MPI of the atmospheric gases. Such MPI is in the regime of tunnel ionization at which the Keldysh parameter γ is of the order of one. So far as we know, no suitable theory can fit our experimental results on the ionization of N_2 and O_2. In the light of our own theoretical analysis of the tunnel ionization (TI) of atoms and D_2 molecule in this regime[15,16], we have been able to offer a semi-emperical analytical model capable of correctly predicting the rate of TI of O_2 and N_2. This finding is very important for all models which attempt to simulate the propagation of femtosecond laser pulses in air. We present in Appendix 5 a preprint that gives a complete analysis of this model.

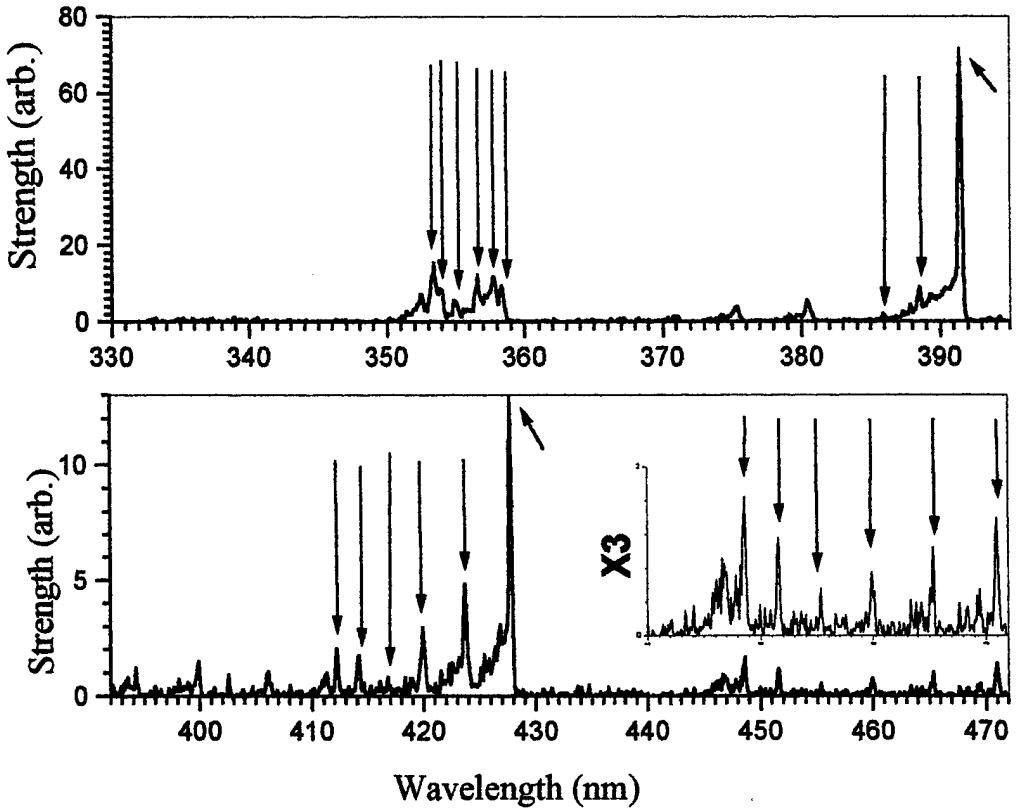

Fig.15: Spectrum of N_2 at a pressure of 5 Torr. The lines marked by arrows are assigned to the first negative band of N_2^+. In the inset of the lower graph, the signal in the range between 440 to 472 nm is multiplied by three to enhance the visibility of the peaks.

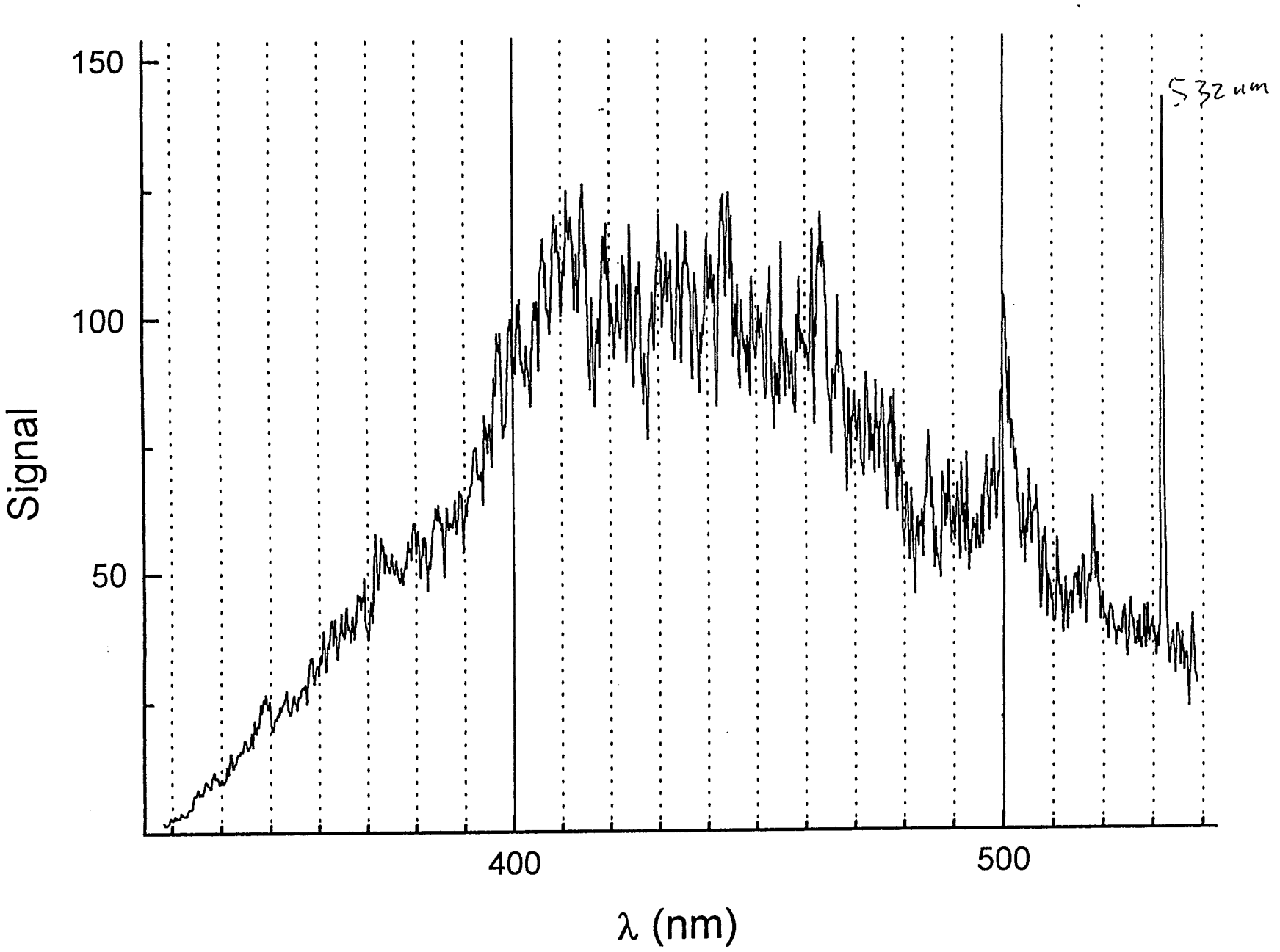

Fig.16.Spectrum from the spark created in air by a focussed second harmonic of a 5ns Q-switched YAG-laser pulse.

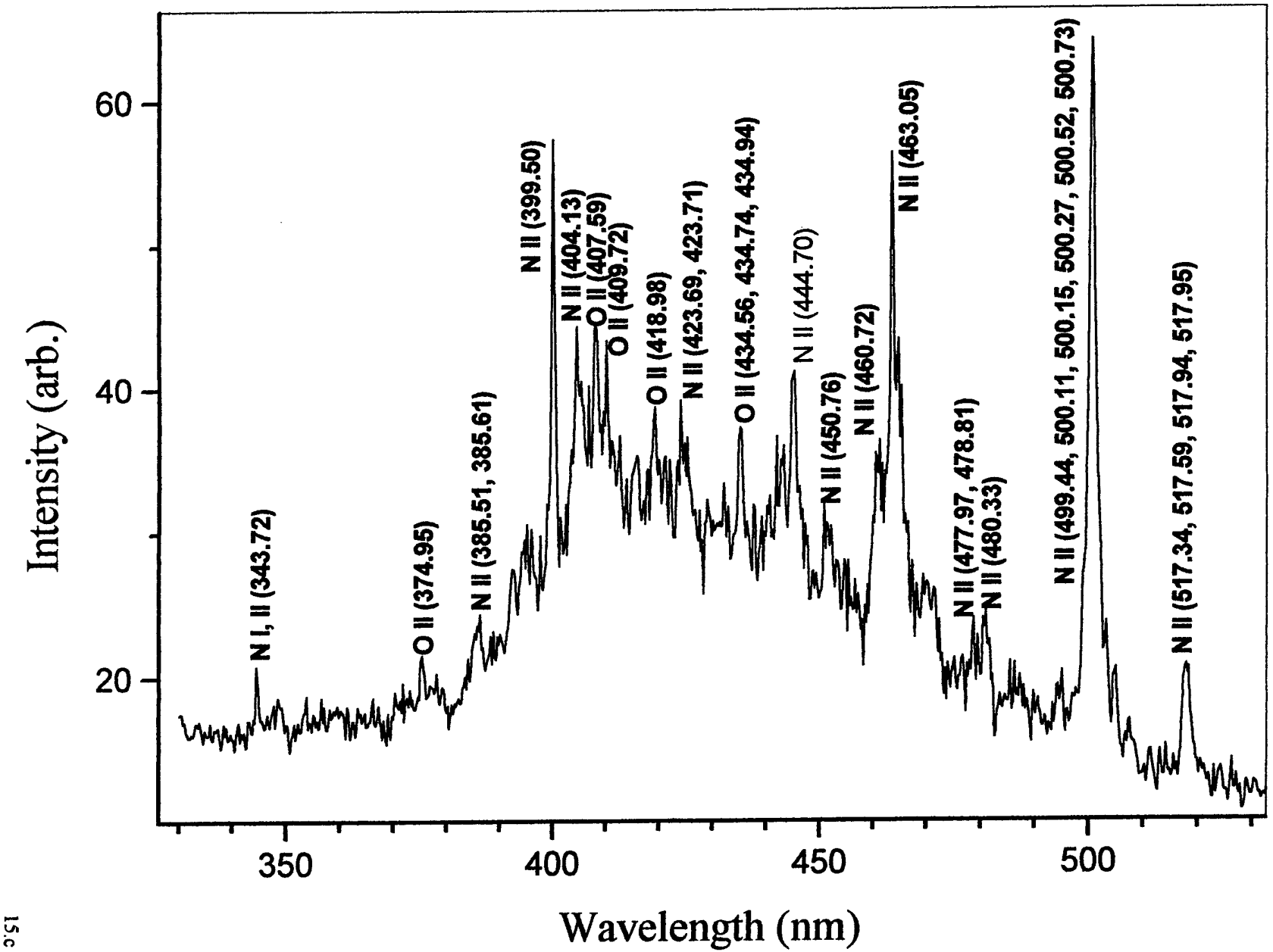

Fig. 17. Spectrum of the spark created in air using a focused 150 ps Ti-Sapphire (uncompressed) laser of 80 mJ pulse energy using a 25 cm focal length lens.

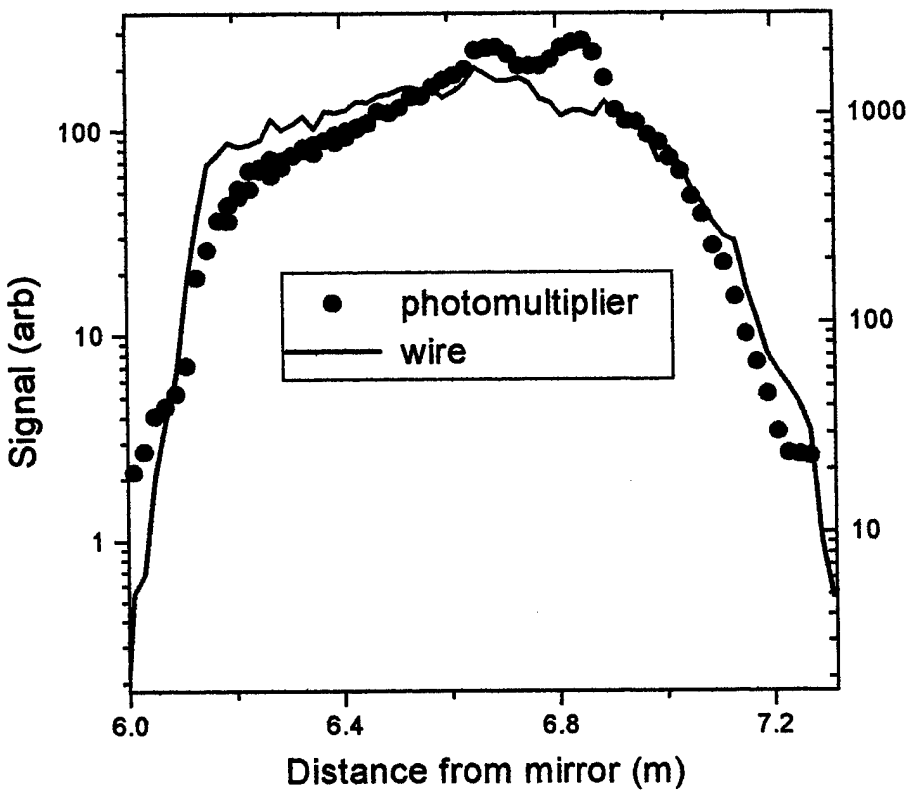

Fig. 18: Comparison between the signals from the wire detector and the photo-detector as a function of position with respect to the geometrical focus (one curve have been scaled in order to overlap the other)

3. Conclusion

We have made significant progress in the study of the propagation of intense femtosecond Ti-sapphire laser pulses in the atmosphere. We show that the universal consequence of the propagation of such pulses through any optical medium is the self-transformation into chirped white light laser pulses through self-focussing and SPM in the self-generated plasma. We have also made progress in the detail measurement of some of the phenomena during propagation based on new techniques. These are self re-focussing, special fluorescence from air, modelling of tunnel ionization of N_2 and O_2 and fluence patterns in the filament. The following gives some preliminary statements on the dependence of propagation on some laser parameters.

a. The position of self-focussing (beginning of filamentation) of intense femtosecond Ti-sapphire laser pulses depends only on the absolute value of the chirp created by a parallel grating pair.
b. Filamentation is very sensitive to the beam shape. Cylindrically symmetric pulse shape is desirable in order to have efficient fialmentation.
c. Spatial chirp of the pulse gives rise to off centered filament.
d. By increaing the divergence of the pulse, one could not only increase the position of the filament but also provoke single filamentation along the axis with higher energy in the pulse. This latter aspect points towards a way to transport high energy pulses to a long distance in the atmosphere with only one filament.

4. Collaboration from the Quantum Optics theory group in MICOM and the LIDAR group in DREV

It was understood from the beginning of this project that the quantum optics theory group in MICOM (USA) led by Dr. Charles M Bowden and the LIDAR group in DREV (Canada) led by Dr. Gilles Roy will collaborate closely with the principal investigator. The MICOM goup is to work on the modelling of the propagation while the DREV is to supply the LIDAR hardware as well as participate in the fluorescence measurement once the molecular signature is determined by the principal investigator. DREV will also provide the service of their machine shop to manufacture large pieces of experimental hardware whenever the principal investigator has a need.

So far, we have kept in touch with one another. Dr. Bowden and his new post-doc have come and visited us in November, 1998 while Dr. J-M Thériault from the LIDAR group of DREV has come to our laboratory to participate in the measurement of the fluorescence in the infrared using their FTIR spectrometer also in November, 1998. These works are beyond the scope of the current report and will not be discussed here.

5. References

1. A Braun, G Korn, X Liu, D Du, J Squire and G Mourou, Opt. Lett. 20, 73 (1995).
2. E T J Nibbering, P F Curley, G Grillon, B S Prade, M A Franco, F Salin and A Mysyrowicz, Opt. Lett. 21, 62 (1996). X M Zhao, P Rambo and J-C Diels, in *Quantum Electronics and Lasers*, Vol. 16 of the 1995 Technical Digest Series (OSA), p.178.
3. M. Mlejnek, E. M. Wright and J. V. Moloney, Opt. Lett. 23, 382(1998).

4. A Brodeur, C Y Chien, F A Ilkov, S L Chin, O G Kosareva and V P Kandidov, Opt. Lett. 22, 304 (1997).
5. O G Kosareva, V P Kandidov, A Brodeur, C Y Chien and S L Chin, Opt. Lett. 22, 1332 (1997).
6. O G Kosareva, V P Kandidov, A Brodeur and S L Chin, J. Nonlinear Opt. Phys. & Mat., 6, 485(1997).
7. H R Lange, G Grillon, J-F Ripoche, M A Franco, B Lamouroux, B S Prade, A Mysyrowicz, E T Nibbering and A Chiron, Opt. Lett., 23, 120 (1998).
8. E B Treacy, IEEE J Quantum Electron., QE-5, 454(1969).
9. J H Marburger, Prog. Quantum Electron., 4, 35 (1975).
10. A Talebpour, Y Liang and S L Chin, 'Population trapping in CO molecules' J Phys B:At Mol Opt Phys, 29, 3435-3442(1996). A Talebpour,C Y Chien &S L Chin, 'Population trapping in rare gases',*ibid*, 29, 5727(1996).
11. S L Chin, A Talebpour, T D G Walsh, S Larochelle, F A Ilkov and C Y Chien, 'The routes towards enhanced ionization', in 'Multiphoton Processes', Institute of Physics Conference Series # 154, (paper presented at the 7th International Conference on Multiphoton Processes, Garmisch-Partenkirchen, Germany, 1996); eds. P Lambropoulos and H Walther, p. 266-275, 1997; IOP Publishing Ltd, London.
12. A Talebpour, S Larochelle and S L Chin, ' Dissociative ionization of NO in an intense laser field:a route towards enhanced ionization' J Phys B:At Mol Opt Phys,30, 1927-1938 (1997).
13. A Talebpour, C Y Chien and S L Chin, 'The effect of dissociative recombination in multiphoton ionization of O_2', J Phys B:At Mol Opt Phys, 29, L677-L680 (1996).
14. T D G Walsh, F A Ilkov and S L Chin, 'The dynamical behaviour of H_2 and D_2 in a strong femtosecond, titanium:sapphire laser field', J Phys B:At Mol Opt Phys, 30, 2167-2175(1997).
15. S F J Larochelle, A Talebpour and S L Chin, 'Coulomb effect in multiphoton ionization of rare gas atoms', J Phys B: At Mol Opt Phys, 31, 1-10(1998).
16.A Talebpour, S Larochelle and S L Chin, 'Suppressed tunnel ionization of D_2 molecule in an intense Ti-sapphire laser pulse', J Phys B: At Mol Opt Phys, 31, L49-L58 (1998).

6. List of appendices

Appendix 1:

Preprint of the Invited paper to the Journal of Nonlinear Optical physics and Materials, 1999.

'Filamentation and supercontinuum generation during the propagation of powerful ultrashort laser pulses in optical media'

S. L. Chin, A. Brodeur, S. Petit, O. G. Kosareva and V. P. Kandidov

Appendix 2 : Preprint of the first paper on white light laser to be published in the Japanese Journal of Applied Physics, February 1999.

'The white light supercontinuum is indeed an ultrafast white light laser'

S. L. Chin, S. Petit, F. Borne and K. Miyazaki

Appendix 3: Preprint of the paper on the fluorescence from N_2 interacting with intense femtosecond Ti-sapphire laser pulses, submitted to the Journal of Physics B: Atomic, Molecular and Optical Physics, 1999.

' Photo-emission spectra of N_2 interacting with a femtosecond Ti-sapphire laser pulse'

A. Talebpour, A. Bandrauk and S. L. Chin.

Appendix 4: Preprint of the paper on the observation of re-focussing using the fluorescence technique, to be submitted to a journal in 1999.

'Re-focusing during the propagation of a focused femtosecond Ti-sapphire laser pulse in air'

A. Talebpour, S. Petit and S. L. Chin.

Appendix 5. Preprint of a paper on an empirical model on tunnel ionization of air molecules submitted to the Journal of Physics B: Atomic, Molecular and Optical Physics, 1999.

'Semi-empirical model for the rate of tunnel ionization of N_2 and O_2 molecules in an intense Ti-sapphire laser pulse'

A. Talebpour, J. Yang and S. L. Chin.

Appendix 1

Filamentation and supercontinuum generation during the propagation of powerful ultrashort laser pulses in optical media

S. L. Chin[1,3,*], A. Brodeur[1,#], S. Petit[1], O. G. Kosareva[2] and V. P. Kandidov[2]

1. Center for Optics, Photonics and Lasers &
Department of Physics
Laval University
Quebec City, Quebec, G1K 7P4
Canada.

2. International Laser Center
Department of Physics
Moscow State University
Moscow 119899, Russia.

3. on leave between Nov. 1 and Dec 31, 1998 at
Institute of Electro-Optical Engineering
College of Electrical Engineering
National Taiwan University
Taipei, Taiwan, Republic of China.

* e-mail: slchin@phy.ulaval.ca
# Present address:
Division of Engineering and Applied Sciences
Harvard University
Gordon McKay Laboratory
9 Oxford Street, Cambridge, MA 02138, USA.

Abstract

The fundamental physical mechanism responsible for the self-focussing , filamentation, supercontinuum generation and conical emission of a powerful ultrashort laser pulse in a transparent optical medium is reviewed. The propagation can be described by the model of moving focus modified by the de-focussing effect of the self-induced plasma through multiphoton interaction with the medium. Spatial and temporal self-phase modulation in both the neutral Kerr medium and the plasma transform the pulse into a chirped (elongated) and strongly deformed pulse both temporally and spatially. The manifestation of the deformation is supercontinuum generation and conical emission. A new phenomenon of refocussing was observed. It is due to the diffraction of the trailing part of the pulse by the plasma that results in a ring structure of positive index changes surrounding the plasma column. This ring structure re-focuses the pulse partially. The measured coherence lengths of the various frequencies components of the supercontinuum are independent of the optical media used and are essentially equal to that of the pump laser pulse when compared to an incoherent white light source. We thus justify that such a deformed pulse with a very broad spectrum could be called a chirped white light laser pulse.

1. Introduction

The phenomena of self-focussing, filamentation, white light continuum (or supercontinuum) generation and conical emission that occur during the propagation of a short intense laser pulse in an optical medium have been known for more than two decades. In the 70's, when ultrashort pulses were in the picosecond regime, these phenomena were not as pronounced as they are today with femtosecond pulses. Then, the phenomena occurred only in condensed matter and external focusing was necessary to achieve sufficient intensities. In this case, Bloembergen successfully proposed the model of moving focus in which the positive nonlinear Kerr index in the self-focus is cancelled by the negative index change due to the generation of a plasma. This resulted in the perception of a filament[1]. A more detailed introduction of this historical account is given by Kosareva et al [2].

It was the observation of the emission of a strong supercontinuum in gases by Corkum et al [3] using intense femtosecond dye laser pulses that aroused a new round of interest in the propagation of intense ultrafast laser pulses. A few years later, the work of the Michigan group[4] and that of the French Polytechnique group[5] demonstrated the generation of a very long filament (of the order of 10 m) when propagating 100-fs Ti-sapphire laser pulses in air without using a focussing lens [6] . The two groups[4,5] proposed a physical process based on the idea of a leaky guided mode. Our experimental and theoretical study of the same problem later showed that the basic physical process of the phenomena was better described by the moving focus model [2, 7, 8].

In this review, we shall give a physical picture (model) of the propagation/interaction processes based on the fundamental physics underlying these phenomena in both air (gas) and condensed matter. We shall justify through our new experimental findings that the supercontinuum is indeed a white light laser and that the laser pulse and the supercontinuum are non-separable; in fact, they are just one single pulse which has been re-shaped both temporally and spatially during the propagation/interaction although group velocity dispersion elongates the pulse temporally. We shall finally explain in a qualitative way why only ultrashort pulses could give rise to such phenomena and why using very short focal length lens might sometimes prohibit the observation of such phenomena even if the pulse is short.

2. Qualitative model

We start with the propagation in air and summarize the phenomena first. When an intense femtosecond laser pulse propagates in air, it self-focuses and the streak of moving foci gives the perception of a long filament. Theoretically speaking, this filament could be many km in length. In the forward direction, an intense white light (supercontinuum) is observed. Colorful conical emission is observed in the forward direction. The shorter the wavelength is, the larger the cone angle is. Inside the filament, molecules are ionized in the intense laser field. These are universal phenomena that also occur in other transparent optical media. We shall first describe the fundamental physics qualitatively.

A powerful 100 fs laser pulse is just a sheet of light 30 microns thick; yet the electromagnetic field in the sheet is so high that nonlinear processes take place during its propagation. The

results of our experimentation and theoretical calculation provide us with the following picture. We assume that the power distribution along the pulse in the propagation direction (i.e. in the time domain) is Gaussian and that the beam profile is Gaussian. In the slowly-varying envelope approximation and in a dispersionless medium the pulse can be viewed as a longitudinal stack of thin slices. Each slice obeys the cw theory of Gaussian beams.Ideally speaking, the most powerful slice at the center of the pulse will self-focus first (i.e. at the shortest distance from the output of the laser). The self-focal diameter achieved by a slice is then limited by the de-focussing effect of the plasma generated in the self-focus. Because of the very short pulse duration, the dominant ionization process is multiphoton ionization/tunnel ionization (MPI/TI). Cascade ionization can be neglected due to the long collision times between free electrons and atoms. The slices immediately ahead of and behind the central slice self-focus at two later positions, and so on. Medium ionization can alter the moving-focus picture by defocusing slices at the back of the pulse. (Note: If we assume that the pulse passes from the vacuum into the optical medium as is approximately the case when propagating the pulse into a condensed medium, these two slices will self-focus at the same position in the medium because all the slices start to self-focus only at the interface. However, as we shall show below, the consequence will be similar in the two cases once plasma generation interferes with the propagation.)

The moving-focus model can be visualized in Fig. 1b. Here, the pulse can be thought of as a "football" flying through air. In this loose analogy, the contour of the football represents the power profile of the pulse. The larger the diameter is, the higher the power is. The central slice of the football, which is the most powerful, forms a self-focus first. The adjacent slices form self-foci later. This analogy is only good in a lossless medium. Once ionization occurs at the self-focus of the most powerful central slice, the trailing part of the pulse will interact with the relatively long lived (order of nanosecond or longer) plasma. (This consequence is also true in the case when the pulse propagates from the vacuum into the optical medium.) The local electron density gradient is very steep in both the propagation (temporal) direction and the transverse direction because of the sudden steep rise in intensity in the self-focus and the highly nonlinear MPI/TI processes. Such steep gradients induces strong phase changes in the pulse ; i.e. self-phase modulation (SPM) both temporally and spatially. The power profile of the trailing part of the pulse is thus strongly disturbed. The leading part of the pulse encounters a neutral Kerr medium and hence will undergo only self-focussing which is ultimately stopped by the defocussing effect of the self-generated plasma.

The consequence of the ionization can be visualized in Fig. 1c. With this additional interaction with the plasma, the symmetrical "football" turns into an "octopus". We note that the contour of the football and that of the octopus-looking pulse represent their power profiles both temporally (in the propagation direction) and spatially (in the transverse direction). The complicated distribution of the pulse reflects the complicated temporal/spatial phase of the pulse's electromagnetic field; i.e. the temporal/spatial Fourier transform of the pulse will give rise to broad frequency sweep both spatially and temporally; i.e. supercontinuum and conical emissions together with the main laser frequency. The pulse is elongated (chirped) during its propagation in the optical medium because of group velocity dispersion of the various color components. Our eyes cannot detect the "football" or the "octopus" looking pulse; but it can detect the color of the pulse. Hence, one sees the white light and the conical emission as if they were separated from the main pulse; but in fact, they come from the single octopus looking but elongated

(chirped) pulse.

We first analyze the frequency sweep due to SPM that gives rise to supercontinuum and conical emission. The frequency shift, $\Delta\omega$, due to a change in the index of refraction, Δn, during the propagation of a (plane) wave in a nonlinear optical medium is given by $\Delta\omega=-(\omega/c)z(\partial/\partial t)\Delta n$ where c is the speed of light in vacuum and z is the propagation distance in the nonlinear medium. In a Kerr medium, to the first approximation, $\Delta n = n_2 I$ where I is the intensity of the laser. Hence, $\Delta\omega \sim -(\partial/\partial t)I(t)$. Only the leading part of the pulse encounters a neutral Kerr medium. Hence, one expects to see only a Stokes (red) shift because $(\partial/\partial t)I(t) > 0$ at the leading part of the pulse. But in practice, the trailing part of the pulse also sees some neutrals, in particular, in the peripheral region of the filament. Blue shift should also occur.

In a plasma, $(n_0 + \Delta n_p)^2 = 1 - \omega_p^2/\omega^2$ where the subscript p denotes plasma; the plasma frequency $\omega_p = [(4\pi e^2/m)N_e(t)]^{1/2}$ (where e and m are the electron charge and mass in cgs units, respectively and $N_e(t)$ is the MPI/TI generated time dependent density in cm^{-3}; i.e. $N_e(t)$ depends on the intensity of the laser.) In air, for $N_e(t)$ not too high, $\omega_p < \omega$. This is always the case in the self-focus where the intensity is clamped down to between 10^{13}-10^{14}W/cm^2 at which single ionization dominates[9]. The maximum electron density in this case is reached when MPI/TI is saturated; i.e. of the order of the gas density; i.e. 10^{19} /cm^3. (Note that a density of the order of 10^{18} /cm^3 is already sufficient to stabilize the filament[1].) This gives $\nu_p = \omega_p/2\pi \sim 3\text{x } 10^{12}$ Hz which is smaller than the optical frequency. Hence, $\Delta n_p \sim -\omega_p^2/2\omega^2$ ($n_0 \sim 1$ in gases) and $\Delta\omega$ is positive; i.e. an anti-Stokes (blue) shift. $\Delta\omega \sim (\partial/\partial t)N_e(t) \sim (\partial/\partial z)N_e(z)$ since $z = ct$. The value of this gradient in the temporal domain (longitudinal direction) is large because the intensity is high. The trailing slices of the pulse encounter a long plasma column in the filament. Each of these slices, while self-focussing into the plasma, sees only the "sudden" rising electron density in front of it; i.e.$(\partial/\partial z)N_e(z) > 0$. The electron density decreases slowly towards the end of the filament. The Stokes shift is thus small. Hence, one expects to measure essentially a blue (anti-Stokes) shift. This shift is large as has been justified by Bloembergen[1] because, as mentioned above, the electron density gradient is large. More recent experiments by François et al [10] using 1ps dye laser pulses focussed into a high pressure CO_2 gas also showed that the supercontinuum was due to SPM in the plasma generated in the self-focus. Since the electron density gradient sweeps from a low to a high value, it gives rise to a positive continuous frequency sweep. Because the laser frequency is in the near ir, the blue shifted frequency is naturally swept through the visible region, hence the white light (supercontinuum).

In the course of self-focusing of the pulse front a large gradient of the electron density arises not only in the longitudinal direction (temporal domain) but also in the transverse direction. This radial gradient causes spatial SPM and leads to the axially symmetric broadening of the angular (spatial) spectrum of the pulse. The increase Δk_r (k_r is the radial wave number) in the width of the angular spectrum due to the plasma is proportional to the absolute value of the radial derivative of the electron density: $\Delta k_r \sim \left|(\partial/\partial r)N_e(r)\right|$. The angular broadening comes from the same leading part of the pulse which gives rise to spectral blueshifting described above. This part of radiation simultaneously experiences frequency shift $\Delta\omega$ and angular shift $\theta = \theta_0 + \Delta k_r/k_z$, where $\Delta k_r << k_z$ and θ_0 is the initial small divergence of the input Gaussian beam. Fig. 2 shows the relations between the various wave vectors related to the divergence angle of the conical

emission. In the plasma the nonlinear contribution to the refractive index is negative, and the radiation diverges. The stronger is the plasma-induced nonlinear interaction the larger is the divergence and spectral blueshifting. As a consequence, shorter wavelengths predominantly propagate at larger angles. This effect is the origin of the conical emission. Unlike the case of the plasma nonlinearity, in the conditions of a Kerr medium the nonlinear contribution to the refractive index is positive. Stokes-shifted radiation converges towards the axis and its intensity maximum propagates at zero angle. This is why we should not expect rings in the Stokes side of the spectrum, where Kerr-induced nonlinear interaction dominates.

At any position along the filament conical emission mainly comes from a group of self-focusing slices in the pulse front, the intensity of which has attained the ionization threshold. In this part of the pulse the derivatives $(\partial/\partial r)N_e(r)$ and $(\partial/\partial t)N_e(t)$ change little with propagation because they are determined by the ionization rate. As soon as the ionization threshold is reached, the electron density rapidly increases. This rapid growth starts at the intensity of about $3\times10^{14}W/cm^2$ and is similar at any position along the filament. As a result, the cone angle of each color should be essentially independent of the position of the self-focus along the filament.

3. Experimental and theoretical justification[2,7,8]

In what follows, we shall justify the above qualitative picture through more rigorous experimentations and numerical simulations. The main features of the picture are: moving focus or the football model (see Fig.1) that degenerates into an elongated octopus looking pulse the spatio-temporal Fourier transform (SPM)of which results in the large spectral broadening both temporally and spatially; i.e. supercontinuum generation and conical emission. Our experiments and numerical simulation also reveal a new unexpected phenomenon, namely, re-focussing of the pulse.

3a. Experiments

The experiment was performed using a Ti-sapphire chirped-pulse-amplification laser system consisting of a Kerr mode-locked oscillator, a stretcher, a regenerative amplifier followed by two stages of multipass amplification in two Ti-sapphire amplifiers. The central wavelength was 800nm, pulse duration, 230fs and $\Delta\nu\Delta t = 0.59$. The beam radius at the output of the grating compressors was $a = 3.5 \pm 0.2$ mm ($1/e^2$ level of intensity). The beam was sent into a long hallway by means of several transport mirrors and propagated freely to the end of the hallway for a total distance of 111m.The energy of the pulse was controlled by a half-wave plate and a polarizer located before the amplifiers. The standard deviation of the pulse energy was about 5% of the average value.

The first qualitative experimental justification of the moving focus model is the following. If one puts a piece of burn paper (Kodak linograph direct print paper) in the path of the filament, the moving focus (or football) model would predict a central stronger burn spot surrounded by a larger but weaker burn pattern. This is indeed observed as shown by the burn pattern in Fig. 3 which is typical at any position after the formation of a filament.

Once during our experiment the last transport mirror was damaged by the filament. The damage

on the mirror was a small "hole" (coating burned away) whose size was the same as that of the central stronger burn pattern on a burn paper (Fig.3). Despite this hole, we observed no change in the filament. This observation is consistent with the moving-focus model, because if the central spot (self-focus) is eliminated at a certain position along the propagation path, the rest of the pulse will still self-focus down stream and still give rise to filamentation. The eliminated spot represents one slice of the pulse and the other slices still self-focus as usual.

A more quantitative way to justify the moving focus model is to put a pinhole at various positions z along the propagation axis(Fig. 4). The size of the pinhole is such that only the self-focussed part of the pulse (i.e. filament) can pass through. We would expect that the transmission of the pulse through the pinhole as a function of position would show a low transmission before the beginning of self-focussing. Once self-focussing starts, the transmission would increase quickly, peak at a position where the central slice at the peak power of the pulse self-focuses and then decrease towards the end of the filament.

In the slowly varying envelope approximation and neglecting dispersion, the self-focal distance z_f of a slice of the pulse is approximated to be that given by the self-focussing theory of a Gaussian cw beam[11] when its power P exceeds the critical power $P_{crit} = 3.77\lambda^2/8\pi n_0 n_2$ where λ is the wavelength and n_0 and n_2 characterize the intensity dependent index $n = n_0 + n_2 I$.

$$z_f = 0.367ka^2/\{[(P/P_{crit})^{1/2} - 0.852]^2 - 0.0219\}^{1/2} \qquad (1)$$

From this formula, we expect that for a given diffraction length ka^2 (k: the wave number; a: the radius at $1/e^2$ level of intensity of the beam), as the power P of the beam increases, z_f decreases. This was indeed true in the experiment. The position of the beginning of self-focussing (filamentation); i.e. z_f, moved towards the compressor as the peak power (energy) of the pulse was increased. According to eq. 1, the end of the filament should in principle be the position at which the peak power equals the critical power ($P/P_{crit} = 1$). We show in Fig. 5 the calculated z_f normalized to the diffraction length ka^2 (solid circles, right hand scale) of some equally spaced discrete slices of the front part of a Gaussian pulse (upper solid curve) as a function of the retarded (or local) time (normalized to the pulse width τ) of the pulse. The power distribution of the Gaussian pulse is normalized to the critical power. It can be seen that before the condition $P/P_{crit} = 1$ is reached, the distance between the foci of two adjacent slices starts to increase significantly starting from the position where $z_f / ka^2 = 1$. Starting from this position, the power of each slice decreases significantly so that the energy in the filament (self-focus) also decreases significantly. We expect that starting from roughly this position, the transmission through the pinhole will be too low to be detected within the limit of the detection sensitivity. This position would thus be roughly the end of the filament. This behaviour should be independent of the peak power of the main pulse. The peak power of the pulse serves only to move the beginning of the filament towards the compressor as discussed above.

The lower part of Fig.6 shows the experimental results (symbols) using 4 different pulse energies. The diameter of the diamond pinhole was 500 μm. This size was estimated to be the size of the self-focal region of pulses of a few GW (giving rise to an intensity of a few times10^{13} W/cm^2) at which significant multiphoton/tunnel ionization of air molecules[9] starts to balance the self-focussing act. The filament energy E_{fil} was defined as the near axis energy

passing through the 500μm diameter pinhole. The transmission is defined as $E_{fil}/\langle E_{tot}\rangle$ where $\langle E_{tot}\rangle$ is the local average total energy measured at the position of the pinhole.

The results (Fig. 6a) show first of all that as the distance z increases, the transmission goes from low to high and decreases again. As the energy (hence peak power) of the pulse increases, the beginning of the filament (peak position) moves towards shorter z; i.e. towards the compressor. The ends of the 4 filaments at 4 different input energies all converge to a common position which is around the diffraction length ka^2 . All these are what we expected in the above paragraph. What we did not expect was the occurrence of two maxima as the energy of the pulse increased. This is a new phenomenon of re-focussing and will be explained later on.

Another experiment was done that measured the cone angle of the various colors in the conical emission (CE). The experimental setup is shown in Fig. 7. At a position z_0, a 4mm-diameter aperture was centered on the beam axis. A razor blade blocked off half of the filament (hence half of the CE) at $z = z_0 + 2m$. This restricted the CE source to $z_0 < z < z_0 + 2m$. The conical emission was measured on a white screen placed at 20m after the aperture, a distance much longer than the source size. An interference filter with 10nm bandwidth was placed after the razor blade. The radii of the colored half rings were measured on the screen at the following wavelengths: 500, 550, 600, 650, 700, 750 nm. The last two ir rings were measured with the help of an ir viewer. No ring was observed at $\lambda > 800nm$ (the laser wavelength) which was what we expected in the above qualitative analysis. Measurements were performed at $z_0 = 40$, 50, 60m. The half angle θ_λ of the CE, being small, was defined as the ratio of radius r of the ring to the distance D from the middle of the CE source to the screen. Fig. 8 shows the experimental results (symbols) of the half-angle θ_λ of the CE vs wavelengths. The angles are given in both degrees and in relative units relative to the divergence angle of the input beam, $\theta_0 = \lambda_0/(2\pi a) = 0.0021^0$. The result shows that the cone angle is independent of z_0 which is again what we expected.

3b. Numerical simulation

We used the nonlinear Schroedinger equation under the slowly varying envelope approximation to simulate the propagation. MPI was included in the equation as the dominant process of electron generation. Group velocity dispersion is neglected since the dispersion length for a 250fs pulse used in the experiment in air is about 1km. The equation is:

$$2ik\{\partial/\partial z + (1/v_g)\,\partial/\partial t]\}E = \Delta_\perp E + (2k^2/n_0)\,\Delta nE - ik\alpha E, \qquad (2)$$

$$\Delta n = (\tfrac{1}{2})n_2|E|^2 - 2\pi e^2 N_e/m\omega^2 n_0 \qquad (3)$$

The intensity dependent electron density N_e is obtained at each space-time point by solving the rate equation $\partial N_e/\partial t = R(N_0 - N_e)$, where N_0 is the initial density of neutral molecules and R is the single MPI rate of oxygen and nitrogen molecules calculated according to the Szöke model[12]. We note that the Szöke model was the closest analytical model one could find at the time of our past investigation. It will be shown that it overestimated the rate of MPI as compared to direct experimental results of the MPI of oxygen using the same laser [9]. Nevertheless, the results are adequate to give us a basic understanding of the overall physical picture of the

propagation. Recently, our group (Larochelle et al[13]) discovered a better analytical formula for the MPI of atoms in the regime where the Keldysh parameter $\gamma \sim 1$. This is the regime where MPI/TI of oxygen and nitrogen molecules take place[9]. We believe this latter findings [9,13] should be used as the basis of MPI/TI of molecules in future calculations.

The input pulse in the simulation was $E(r, z = 0, \tau = t - z/v_g) = E_0 \exp(-r^2/2a^2 - \tau^2/2\tau_0^2)$ with $\tau_0 =$ 150fs (FWHM, 250fs) and $a = 170\mu m$. The latter was chosen to be smaller than that in the experiment so that both the initial and the contracted beam could be located on the same grid during the computation. The detail of the calculation technique was given in ref. (2, 7, 8). Some typical results of the simulation are presented in Fig.9. It shows both the spatio-temporal intensity distribution in the rest frame of the pulse at three different positions of propagation (Fig. 9a,c,e) and the corresponding spatio-spectral intensity distribution Fig. (9b,d,f). The latter was obtained through a spatio-temporal Fourier transform of the fields of the corresponding pulses. Fig. 9a and 9b shows the pair of temporal and spectral intensity distribution of the input pulse. Soon after propagation, time-dependent self-focussing started to develop with little ionization up to the position $z = 0.22z_d$ where the most powerful slice of the pulse ($\tau = 0$) forms a self-focus. At this point, self-focussing was stopped by the significant MPI that generated free electrons whose defocussing effect balanced the self-focussing effect. The pairs [Fig.(9c, 9d) and Fig.(9e, 9f)] show two examples of the consequences of the disturbance of the pulse due to the interaction with the free electrons further down stream. The positions of the self-focus (sharp peaks in Fig. 9c and 9e) move towards the front of the pulse as z increases. This indicates that successive slices of the front part of the pulse focus at different positions down stream; i.e. the moving focus model is valid. The trailing part of the pulse encounters the free electrons and is defocussed and completely deformed through its interaction with the plasma. The multiple ridges at the back of the pulse together with the sharp peak at the front form the basis of the visual model of the octopus looking pulse. They are the consequence of MPI/TI and the diffraction and SPM of the trailing part of the pulse in the plasma.

By inspection, one can see that the highly irregular temporal and spatial field distributions of the pulse shown in Fig. 9c and 9e should have strong phase modulations. Indeed, the result of their Fourier transforms given in Fig.8d and 8f shows a weak broadening in the Stokes side as expected in the qualitative analysis given above. At the anti-Stokes side, the broadening is much larger both along the propagation axis and along a cone (conical emission). Again, these have been expected qualitatively.

The solid lines (curves 1-3) at the bottom of Fig.8 show the cone angles at different colors plotted as a function of the wavelength at the three experimental positions along the propagation axis; i.e. at z = 40, 50 and 60m. Although they do not fit the experimental data, the quasi insensitivity of the results to the position of measurement is in qualitative agreement with the experimental results. The lack of better agreement with the experiment seemed to have arisen from the ionization model we used and the lack of the group velocity dispersion in the propagation model. Our experimental measurement of the MPI of rare gas atoms and oxygen molecules[9,13] showed that the Szöke model over estimated the ionization rate. We thus made a correction in accordance with the experimental result[9]. The result is shown by the solid curve 4 in Fig. 8 at which all three curves coincide with one another. It shows an excellent agreement with the experiment.

We also simulated the transmission experiment by calculating the normalized filament energy in the case of a $5P_{crit}$ peak power as a function of the propagation distance[7]. The filament energy E_{fil}^{sim} was defined as the energy contained in a circular aperture with diameter 167μm. The result is shown by the solid curve in Fig. 6b. It agrees with the experimental observation and the qualitative expectation that the transmission increases from a low through a high value and decreases again stopping at around the diffraction length. In particular, it reveals the unexpected phenonmenon of refocussing (double maxima) which we shall discuss in what follows.

3c. Re-focussing

Apart from the above mentioned agreement between experiment and simulation, the unexpected observation of re-focussing both experimentally and in the simulation reinforces our view that the fundamental physics we considered in the description of the propagation and in the simulation is correct. The re-focussing is manifested in Fig. 9 a,c and e. (Note the change of the vertical scale from a to c,e .) A significant increase in the near axial intensity of the trailing part of the pulse is seen in Fig. 9e as compared to the other two. Such an increase results in the second peak in Fig.6. The physical reason underlying this phenomenon is self-focusing of slices at the trailing part of the pulse, which were initially defocused and diffracted by the plasma. There is the following physical reason underlying this phenomenon. The power of a number of slices at the trailing part of the pulse, which were initially defocused and diffracted by the plasma, is larger than the critical power for self-focusing in air. Therefore, positive contribution to the refractive index produced by the rings at the back of the pulse is sufficient to cause self-focusing of these slices.

Indeed, the circular diffraction pattern of the field at 800nm around the central plasma column (filament) would induce a circular nonlinear index pattern. The nonlinear index change is negative in the central plasma region and is positive in the surrounding ring region because the circular intensity pattern interacts with the neutral Kerr medium surrounding the plasma column. Fig.10 shows sections of the intensity profile at the front and trailing parts of the pulse and the corresponding nonlinear index changes at the position $z = 0.34z_d$ corresponding to Fig. 9c. The front part of the pulse has a single peak (Fig. 10a) and the index change is positive (Fig. 10c) because the slices in the front part encounter always a neutral Kerr medium. The trailing part has a circular intensity distribution due to the diffraction by the plasma (Fig. 10b). The nonlinear index change at the center of the plasma column (filament) is negative (Fig. 10d). But if we look closer by zooming into Fig. 10d, we obtain Fig. 11. It shows indeed rings of positive nonlinear index change. Such rings of positive nonlinear index change contribute to the re-focussing of the trailing part of the pulse at certain moments of propagation. Recently, more rigorous calculation by the Arizona group shows also such re-focussing effect[14].

4. Condensed matter

The same phenomena of self-focussing, filamentation, supercontinuum and conical emission are also observed in all transparent condensed matter using femtosecond laser pulses. In those experiments, the filament is usually of the order of 1mm in length because the pulse is externally focused into the medium[15]. Indeed, the moving-focus model predicts that under external focussing the filament stops at the geometrical focus[11]. The corresponding experiment of free

propagation of an unfocussed pulse into a long path of condensed medium is usually impractical. However, it is expected that the fundamental physical process of the phenomena in condensed matter should be similar to that in air, since, after self-focussing, the rest of the phenomena is mostly the consequence of the interaction with free electrons which are universal. The question is the origin of the free electrons. After some systematic investigations using 140fs Ti-sapphire laser pulses , we come down to the conclusion that, unlike the case of air or gases, the free electrons are not generated through MPI/TI, but through multiphoton excitation from the valence band into the conduction band. In fact, a band gap threshold is found below which there is no continuum generation. This is the first report of a parameter predicting the width of the continuum in condensed media[16].

The 140fs Ti-sapphire laser pulses (796nm, 2.2mm in diameter at $1/e^2$ intensity level) was focussed by a 125 mm focal length lens into 15 types of transparent condensed matter (liquids and solids) and the spectra of the transmitted pulses were measured by a spectrograph equiped with a cryogenic 2D charge-coupled device (CCD) detector. Fig. 12 shows the anti-Stokes (blue) broadening, $\Delta\omega_+$, as a function of their band gap energy, E_{gap} (expressed in both eV, lower horizontal scale and photon energy, upper horizontal scale). They were taken under the condition $P = 1.1P_{th}$ where P is the input laser peak power and P_{th} the experimentally measured threshold input peak power for self-focussing in the material. The latter corresponds to the critical power for self-focussing[11].The experimental detail is given in ref. [16].

We choose to consider the anti-Stokes broadening because: (1) it is related to the SPM of the pulse in a free electrons 'gas' and is the principal part of the supercontinuum according to our analysis in the previous sections and (2) the Stokes broadening is much smaller and does not change much from one medium to another. Indeed, the dependence of the supercontinuum on the band gap is striking. There is a threshold band gap energy. The threshold value is about 4.7eV or 3 photon energy. Below this threshold, $\Delta\omega_+$ is negligibly small while above it, $\Delta\omega_+$ increases quickly with the band gap energy. Furthermore, we observed that P_{th}, (hence the critical power for self-focussing,) tends to increase with E_{gap}. Since the critical power is inversely proportional to the Kerr index[11], this implies that $\Delta\omega_+$ increases with decreasing nonlinearity. Yet, it is well known that the larger the nonlinear Kerr index is (such as CS_2), the easier self-focussing in a Kerr medium will be, whereas experimentally, CS_2 has produced a small $\Delta\omega_+$ (see Fig. 12). This apparent contradiction can be explained by the multiphoton excitation (MPE) of free electron from the valence band into the conduction band.

During self-focussing, an intensity spike corresponding to the self-focussing of a slice of the pulse develops[1,2,7,8,11,16, 17]. This generates a sufficiently high density of free electrons in the conduction band by MPE. Most of the MPE occurs at the very peak of the spike. Collisional ionization in the short duration of the peak is not important. The de-focussing effect of this electron 'gas' cancels the self-focussing effect thus limiting the diameter of the self-focal region. For low band gap material such as CS_2 (band gap energy = 3.3eV < 3hν where hν is the photon energy) even if it has a large nonlinear Kerr index to favor an easy self-focussing of the pulse, the relative ease of exciting free electrons into the conduction band via 3 photon excitation would produce a relatively large self-focal diameter. The intensity at the self-focus is clamped down to a relatively low value. At this value, the temporal and spatial slope of the pulse is so low that it generates a small gradient in the electron density. The effect of low electron density

gradient on the SPM of the pulse at low intensity results in a negligible $\Delta\omega_+$. Our results (Fig. 12) show that only when the band gap is larger than $3h\nu$ (i.e. 4 photon excitation or higher) will $\Delta\omega_+$ become significantly large and be qualified as supercontinuum.

5. White light laser

The supercontinuum has been used as a source for various type of applications. They range from being the seed pulse for further amplification in dye amplifiers and optical parametric amplifiers[18] to broadband absorption and excitation spectroscopy[19] characterising laser induced structural transition[20], etc. Because the supercontinuum can be a seed pulse for optical amplification, it is generally accepted that the supercontinuum is a coherent source. However, no one has yet identified that it is a white light laser simply because there seems to be no physical ground to say so. In what follows, we shall try to justify that the supercontinuum should indeed be called a white light laser.

As explained in sections 2 and 3, nonlinear propagation in a transparent optical medium turns a powerful ultrashort laser pulse from a football looking pulse to an elongated (chirped) octopus looking pulse. Before group velocity dispersion completely separates all the frequency components into separate individual waves in a very long optical medium, the octopus looking pulse is simply the original laser pulse which has been modified both spatially and temporally; hence spectrally. From this point of view, this is a spectrally broadened laser pulse whose spectral width is so broad that it should be called a white light laser. We try to justify it by the following experiment.

800nm, 170fs (FWHM) Ti-sapphire laser pulses were used (bandwidth : 7.18nm). They were focussed by a 10 cm lens into three different liquids, namely, water, methanol and CCl_4. Since multiple filaments are independent sources of SC[15], we chose to study the effect of one filament. The laser power was adjusted so that only one filament was created. The energy per pulse to generate one single filament in each liquid is 3μJ for water and 0.2μJ for both methanol and CCl_4. The maximum fluence in the filaments have been measured to be roughly 0.62, 0.54 and 0.44 J/cm^2 for water, methanol and CCl_4 respectively[16]. The intensity cannot be measured properly yet because the knowledge of the duration of the sharp intensity spike at the self-focus, hence, at the filament is not known. However, we have recently estimated them[16] to be of the order of 10^{12} W/cm^2 for water and 4×10^{11}W/cm^2 for both methanol and CCl_4. The SC output from the filament was then collimated by another 10cm focal length lens and was sent into in a Michelson interferometer followed by a spectrometer. The collimated beam illuminated the entrance slit of the spectrometer directly.

The output of the spectrometer showed spectral modulation[21]. (The details of the experiment will be published elsewhere[22].) Various wavelength regions across the whole SC and that of the laser line were chosen each with a constant width of 1nm. We define the coherence length as that path difference in the Michelson interferometer at which the spectral modulation disappears at that particular wavelength. These coherence lengths were compared with those of an incoherent white light source from an incandescent light bulb at the corresponding wavelengths under identical measuring conditions.

Fig. 13 shows the results of the comparison under the condition of a single filament in the liquids[22]. The vertical scale gives the ratios of the coherence lengths ($L_{coherent\ source}$) of the various wavelength components of the supercontinuum source to those of the incoherent source ($L_{incoherent\ source}$). The horizontal scale gives the wavelengths at which the coherence lengths were measured. The ratios are the same for all the three media whose band gap energies are[16] : 7.5eV (water), 6.2eV (methanol) and 4.8 eV (CCl_4); i.e. the ratios are independent of the material. This further supports the above idea that the generation of supercontinuum is a universal phenomenon.

In particular, in the range between 800nm and 500nm, the ratios are essentially all equal to the corresponding ratio of the Ti-sapphire laser line at 8oonm. Those at the longer and shorter wavelength sides (430nm and 900nm) are smaller since at these wavelengths, the supercontinuum signal decreases quickly in power by one order of magnitude or more. The influence of the unavoidable incoherent light coming from the plasma recombination in the self-focus and filament becomes important; i.e. the plasma contribution to the coherence length becomes important. This makes the ratios smaller.

We can thus conclude that the relative coherence lengths (with respect to an incoherent source) of all the wavelength components of the white light supercontinuum are essentially the same as that of the Ti-sapphire laser pulse. From the point of view of coherence length, since the 800nm pulse is a laser pulse, the other wavelength components in the supercontinuum should also be called laser pulses. This is not surprising if we remember the visualization of the elongated (chirped) octopus looking pulse representing the whole deformed laser pulse whose spectal width is braodened enormously through the interaction with the self-generated electrons.

The duration of the supercontinuum pulses at different wavelengths have recently been measured in the case of the supercontinuum generated from atmospheric pressure rare gases using 1.6TW, 120fs pulses of a Ti-sapphire laser[23]. It was found that at various wavelength regions of the supercontinuum, the pulses are chirped differently and the chirped durations range from 150 to 250fs. This reinforces the visulization of the elongated (chirped) octopus looking pulse. Consequently, we can say that the supercontinuum source is a continuum of chirped ultrashort laser pulses; or simply an ultrafast white light laser.

6. Short pulse vs long pulse

There is a general question as to why long laser pulses do not produce the same phenomena described above even if the peak power is as high as or higher than that of an ultrashort laser pulse. The reason is that there are essentially two physical processes competing with each other at the beginning of propagation. One is optical breakdown and the other is self-focussing. Optical breakdown is an accumulative process in time. It starts from the generation of a few free electrons in the medium through MPI or MPE depending on the material. It is followed by the acceleration of these electrons in the strong laser field (inverse Bremsstrahlung) and cascade ionization resulting in an avalanche and generating a strong plasma. This means that the longer the powerful laser pulse is, the lower the threshold of optical breakdown will be. On the other hand, self-focussing has a rather high threshold power. For long pulses, the threshold of optical breakdown is lower than that of self-focussing. Thus, optical breakdown occurs first and creates

a strong plasma that blocks the rest of the pulse through absorption, reflection and scattering before it could rise up to the self-focussing threshold. There is no significant SPM because the intensity is not high enough yet. Without self-focussing, the rest of the phenomena (filamentation and supercontinuum generation) would not occur. For short pulses, there isn't enough time for the generation of optical breakdown and the threshold of self-focussing is reached. This favors the domination of self-focussing that leads to the occurrence of the current phenomena.

7. Short focal length vs long focal length

In a similar manner, optical breakdown and self-focussing compete with each other in the case of focussing an ultrashort laser pulse into a transparent optical medium. One could use a tightly focussing geometry to favor optical breakdown and avoid or minimize self-focussing and filamentation. This is particularly true in condensed matter and high pressure gases in which the density is high and cascade ionization is relatively easy. If the external geometrical focussing is very tight, breakdown would occur first before self-focussing is reached. The reason is that self-focussing is a propagation effect; i.e. it takes some propagation distance to reach the self-focus while optical breakdown is a local effect. For a given short pulse length and focussing geometry, a high local intensity at a position before the geometrical focus could be reached such that optical breakdown would start before the self-focal position. The resulting strong plasma would stop the pulse from reaching the self-focal position, hence stopping the development into a filament and supercontinuum. This has been demonstrated experimentally by our group (Ilkov et al, [24]) in the case of high pressure CO_2 gas.

8. Conclusion and Looking ahead

We have presented the fundamental physical mechanism of the propagation of a powerful ultrashort laser pulse in a transparent optical medium which results in the universal phenomena of self-focussing, filamentation, supercontinuum generation and conical emission. It is the interplay between the Kerr self-focussing effect in the neutrals and the defocussing effect in the plasma (free electrons) generated at the self-focus that gives rise to the moving focus and the perception of a filament. The generation of free electrons takes the easiest (or most probable) route. In gases at normal pressures, multiphoton/tunnel ionization (MPI/TI) are responsible while in condensed matter, the transition from the valence to the conduction band dominates. The generation of the supercontinuum and conical emission is due to self-phase-modulation (SPM). The broad anti-Stokes part of the supercontinuum is due to temporal SPM of the self-focussed pulse in the self-created plasma. The narrow Stokes broadening is due to temporal SPM in the neutral which also contributes to a narrow part of the anti-Stokes side. The large angular divergence of anti-Stokes shifted radiation is due to spatial SPM in the self-created plasma.

The physical picture of the whole process is one in which the input powerful ultrashort laser pulse, through its interaction with the medium, self-transforms into a chirped (elongated) and highly deformed pulse both temporally and spatially. The manifestation of the latter deformation is spatio-temporal SPM, which results in supercontinuum generation and conical emission. Because the output of the propagation is still the same laser pulse except that it is severely deformed or re-shaped, one could consider the deformed pulse still as a laser pulse. Since the

spectral content of this deformed pulse spans from the near ir to the near uv, it could be called a white light laser pulse. More quantitatively, we have measured the coherent lengths of the various frequency components of the supercontinuum. We found that they are essentially all equal to that of the input 170 fs Ti-sapphire pulse when compared to those of the corresponding wavelengths of an incoherent light source. This justifies the claim that the output pulse with supercontinuum is indeed a chirped white light laser.

Such a white light laser pulse could find applications in various optical media. From the point of view of long distance propagation and filamentation in the atmosphere, atmospheric sounding[6], illumination and pollution measurement are some important applications. In the latter case, one relies on using the LIDAR technique to measure the finger print fluorescence pattern of the pollutant molecules which are ionized and fragmented in the strong field inside the filament. This technique does not depend so much on the wavelength of the laser. It depends principally on the intensity at the self-focus where MPI/TI and fragmentation take place.

The ionization of air molecules in the filament can be used as a long lightning rod to discharge thunder cloud. This idea of using the particularly long filament of the Ti-sapphire laser was first proposed informally by Mourou[25] and was later taken up and applied by other groups into real laboratory studies[26]. Recently, Chin and Miyazaki proposed an alternative but similar way to discharge thunder clouds[27]. It is to improve upon the current technique of lightning control in Japan that was proven successful (though with a low success rate) in real field tests by combining a CO_2 laser and a tall lightning tower[28]. The proposed femtosecond terawatt Ti-sapphire laser is to replace the CO_2 laser. The latter needs electron seeding to work while the former does not. Other applications that is related to the phenomena of self-focussing and filamentation are in the field of opto-electronics. Wave guides[29] and high density micron size dots[20] were successfully written in glasses using fs Ti-sapphire laser pulses. The former could find useful applications in integrated optics and optical communication while the latter holds great promises in high density 3D data storage.

Because of these interesting and potentially important applications, there are currently strong incentive (demand) to study the propagation dynamics in more detail so that quantitative agreement between experiment and theory is achieved. To do so theoretically, many of the appriximations used in our simulation should be relaxed. In particular, the group velocity dispersion should be included while the slowly varying envelope approximation should be relaxed even when considering pulses of the order of 100 fs (about 37 optical cycles for 800nm pulses). Even though the pulse duration is long enough to satisfy the slowly varying envelope approximation, the intensity spike at the self-focus is very sharp (order of a cycle of oscillation at 800nm; see Fig. 9). The slowly varying envelope approximation should breakdown with such short time scales. Furthermore, the instantaneous nonlinear response of the optical medium should also be relaxed. Such works are already started in other laboratories. For example, re-focussing can recur if the medium has a delayed Kerr response[14]. More detailed experimentations are also needed to study the detailed physical mechanism of all those promising applications. In fact, many laboratories have already embarked on such studies and the field is becoming more and more dynamic.

Acknowledgement

We gratefully acknowledge the partial supports of the Natural Sciences and Engineering Research Council of Canada, the Department of National Defense, Canada, le Fonds-FCAR of the Province of Quebec, NATO and the Army Research Office, USA. One of us (SLC) also thanks the partial support of the National Science Council during his short sabbatical visit (November –December, 1998) at the National Taiwan University, Taipei, Taiwan, Republic of China. We appreciate the technical help of S. Lagace, C-Y. Chien, J-P Giason , F. Borne and S. F. J. Larochelle. The useful discussions with K. Miyazaki, C. C. Yang, A. Talebpour, T. Walsh, F. Ilkov and N. B. Delone are highly appreciated.

REFERENCES

[1] N. Bloembergen, Opt. Commun., 8, 285(1973).

[2] O G Kosareva, V P Kandidov, A Brodeur and S L Chin, 'From filamentation in condensed media to filamentation in gases', *J Nonlinear Opt Phys.& Mat.*,6, 485-494 (1997).

[3] P. B. Corkum, C. Rolland and T. Srinavasan-Rao, Phys. Rev. Lett., 57, 2268(1986); P. B. Corkum and C. Rolland, IEEE J Quantum Electron. 25, 2634(1989).

[4] A. Braun, G. Korn, X. Liu, D. Du, J. Squier and G. Mourou, Opt. Lett., 20, 73(1995).

[5] E. T. Nibbering, P. F. Curley, G. Grillon, B. S. Prade, M. A. Franco, F. Salin and A. Mysyrowicz, Opt. Lett., 21, 62(1996).

[6] Recently, the Jena group in Germany demonstrated that the filament obtained using terawatt Ti-sapphire laser pulses can be used for atmosphere sounding at altitudes beyond 10 km. L. Worste, C. Wederkind, H. Wille, P. Rairoux, B. Stein, S. Nikolov, C. Werner, S. Niedermeier, F.Ronnerberger,H. Schillinger and R. Sauerbrey, Laser und Optoelektonik, 29(5), 51(1997).

[7] A Brodeur, C Y Chien, F A Ilkov, S L Chin, O G Kosareva & V P Kandidov, 'Moving focus in the propagation of powerful ultrashort laser pulses in air', *Opt Lett*, 22, 304-306(1997).

[8] O Kosareva,V Kandidov,A Brodeur,C Y Chien and S L Chin,'Conical emission due to laser plasma interactions in the filamentation of ultrashort laser pulses in air',*Opt. Lett.* 22,1332-1334,1997.

[9] A Talebpour, C Y Chien and S L Chin, 'The effect of dissociative recombination in multiphoton ionization of O_2', *J Phys B:At Mol Opt Phys*, 29, L677-L680 (1996). A. Talebpour, J. Yang and S. L. Chin, " Tunnel ionization of O_2 and N_2 by an intense femtosecond Ti-sapphire laser", in preparation(1998).

[10] V François, F A Ilkov & S L Chin, 'Experimental study of the supercontinuum spectral width evolution in CO_2 gas', *Opt Commun* 99, 241 (1993). S. L. Chin, J. Phys. B:At. Mol. Opt. Phys. 25, 2709(1992).

[11] J. H. Marburger, Prog. Quantum Electron. 4, 35 (1975).

[12] A. Szöke, in Atomic and MolecularProcesses with short intense laser pulses, A. D. Bandrauk ed. (Plenum, N.Y. 1987) p.207.

[13] S F J Larochelle, A Talebpour and S L Chin, 'Coulomb effect in multiphoton ionization of rare gas atoms', *J Phys B: At Mol Opt Phys*, 31, 1215-1224(1998).

[14] M. Mlejnek, E. M. Wright and J. V. Moloney, Opt. Lett. 23, 382(1998).

[15] See for example, A Brodeur, F A Ilkov & S L Chin, 'Beam filamentation and the white light continuum divergence', *Opt. Commun*, 129, 193-198(1996) and references therein

[16] A Brodeur and S L Chin, ' Band-gap dependence of the ultrasfast white-light continuum',

Phys.Rev. Lett. 80, 4406-4409(1998).
[17] D. Strickland and P. B. Corkum, Proc. SPIE, 1413, 54(1991); D. Strickland and P. B. Corkum,J. Opt. Soc. Am. B, 11, 492(1994).
[18] K. R. Wilson and V. V. Yakovlev, J. Opt. Soc. Am. B, 14, 444(1997).
[19] " The supercontinuum laser sources" edited by R. R. Alfano, Springer-Verlag, New York, 1989.
[20] E. N. Glezer, S. Siegal, L. Huang and E. Masur, Pyys. Rev. B, 51, 6959(1995).
[21] S. L. Chin, V. François, J. M. Watson and C. Delisle, Appl. Opt. 31, 3383(1992).
[22] S. L. Chin, S. Petit, F. Borne and K. Miyazaki, Jap. J. Appl. Phys., accepted (1998); S. Petit, F. Borne and S. L. Chin, " The white light supercontinuum is indeed an ultrafast white light laser", Submitted to CLEO 99.
[23] H. Nishioka, W. Odajima, Y. Sasaki and K. Ueda, OSA TOPS on Advanced Solid State Lasers, 1996, Vol. 1, Stephane A Payne and Clifford Pollock (eds.), Optical Society of America, 1996. also H. Nishioka, W. Odajima, K. Ueda and H. Takuma, Opt. Lett., 20, 2505 (1995).
[24] F A Ilkov, L Sh Ilkova & S L Chin, 'Supercontinuum generation vs optical breakdown', *Opt Lett*, 18, 681(1993).
[25] G. Mourou, private communication.
[26] X. M. Zhao, J. C. Diels, C. Y. Wang and J. M. Elizondo, 'Femtosecond ultraviolet laser pulse induced lightning discharges', IEEE J.Q.E. 31, 599(1995) and references given therein. So far as we know, real experimental and numerical tests of the feasibility of the idea of directly using the filament of an ultrashort laser pulse in the atmosphere is being carried out at least in the high voltage laboratory of Hydro Quebec, Varennes, Quebec, Canada.
[27] S. L. Chin and K. Miyazaki, "A comment on lightning control using a femtosecond laser", Jap. J. Appl. Phys., submitted(1998).
[28] T. Yamanaka, S. Uchida, Y. Shimada, H. Yasuda, S. Motokoshi, K. Tsubakimoto, Z. Kawasaki, Y. Ishikubo, M. Adachi and C. Yamanaka, " First observation of laser triggered lightning", Invited paper, SPIE Conference on High Power Laser Applications, Santa Fe, New Mexico, April, 1998; SPIE, vol. 3343, p. 281-288, 1998.
[29] K. M. Davis, K. Miura, N. Sugimoto and K. Hirao, Opt. Lett., 21, 1729(1996); K. Miura, J. Qui, H. Inouye, T. Mitsuyu and K. Hirao, Appl. Phys. Lett., 71, 3329(1997).

Figure captions

1a. Visualization of the ideal self-focussing of a sheet of light propagating in air.

1b. Visualization of the ideal transformation of a football looking pulse in air due to self-focussing. The initial football looking pulse (left) is transformed into a centrally squeezed ball (center) and then to a ball squeezed at both ends (right).

1c. Visualization of the transformation of the football looking pulse into an octopus looking pulse. The front end of the ball (pulse) always squeezes down slice by slice during propagation while the back end of the ball encounters the plasma left behind by the front part. Spatio-temporal SPM of the back part of the pulse leads to a complicated amplitude and phase change of the field; hence, an octopus looking structure qualitatively.

2. Schematic drawing of the realtionships between the various wave vectors of the pulse in air before (with subscript 0) and after SPM in the plasma giving rise to conical emission. The inset gives the mathematical relations of the wave vectors.

3. Burn pattern at an arbitrary position of the filament on a piece of Kodak linograph direct print paper showing the central darker spot surrounded by a larger weaker spot. The 800nm Ti-sapphire laser pulse duration was about 200fs and the energy in the pulse around 30mJ. The beam diameter was around 12mm which is the size of the larger burn pattern.

4. Experimental setup with pinholes along the propagation axis

5. Self-focal distance (solid circle) normalized to the diffraction length k a^2 for various slices of the front part of the pulse whose power distribution normalized to the critical power is given by the solid curve. The horizontal scale is the retarded time normalized to the pulse duration τ. No self-focussing should be expected at $P < P_{crit}$.

6a. Ratio of filament energy to average total energy versus distance of propagation.
6b. Simulation of the propagation giving the ratio of filament energy to average total energy versus distance of propagation normalized to the diffraction length.

7. Experimental setup: the conical emission emitted between the aperture and the razor blade is measured on the screen.

8. Conical emission angles as a function of the wavelengths: symbols, measured; curves, calculated. Triangle, z= 40m; circle, z=50m; squares, z=60m. In the simulation, the corresponding positions are $0.42z_d$ (curve 1), o.52 z_d (curve 2) and 0.62 z_d (curve 3). The vertical axis at the right hand side gives the absolute values of the measured CE angles in degrees. Curve 4 shows the simulated CE angles obtained after an effective correction for the real MPI rate.

9. (a), (c), (e) intensity $I(r,\tau)$ and (b), (d), (f) spatio-temporal spectrum $\log[|E(k_\perp, \omega)|^2/|E_{max}(k_\perp, \omega)|^2]$, where $|E_{max}(k_\perp, \omega)|^2$ is the maximum spectral intensity. (a), (b) z=0; (c), (d) $z=0.34z_d$; (e), (f), $z=0.42z_d$.

10. (a), (b) the sections of the laser beam and (c) , (d) the section of the nonlinear contribution to the refractive index Δn at $z = 0.34z_d$. (a), (c), at the front of the pulse: $\tau = -116$fs; (b), (d), at the center of the pulse: $\tau = 0$.

11. The magnified distribution of the nonlinear contribution to the refractive index Δn shown in Fig. 10(d).The negative minimum of the distribution cannot be seen on the plot.

12. Anti-Stokes broadening $\Delta\omega+$ vs band gap in 15 different condensed optical media. a, LiF; b, CaF_2; c, UV-grade fused silica; d, water; e, D_2O; f, 1-propanol; h, NaCl; I, 1,4-dioxane; j, chloroform; k, CCl_4; l, C_2HCl_3; m, benzene; n, CS_2; o, SF-11glass.

13. $L_{coherent\ source}$: the coherence length of a wavelength component of the supercontinuum light generated by 170 fs Ti-sapphire laser pulses in water, methanol and CCl_4 ; $L_{incoherent\ source}$: the coherence length of the same wavelength component of an incoherent light source measured under identical conditions. In the experiment, the laser pulse energy was adjusted so as to produce only one single filament in the medium. This plot gives the ratios of the coherence lengths $L_{coherent\ source}$ / $L_{incoherent}$ as a function of the wavelengths at which the coherence lengths are measured. The insets give the experimental conditions of the spectrometer and the energy per pulse.

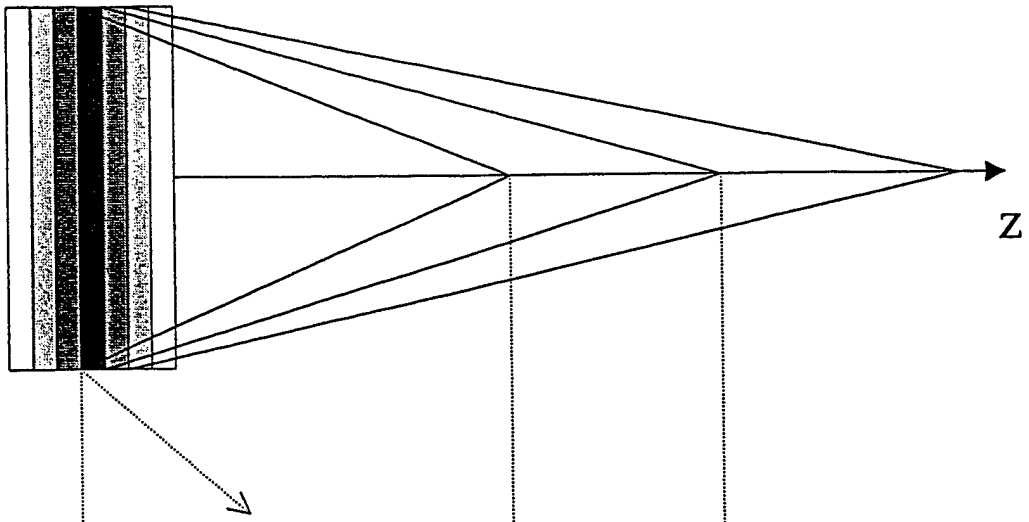

Strongest slice

(1a)

(1b)

(Fig.1c)

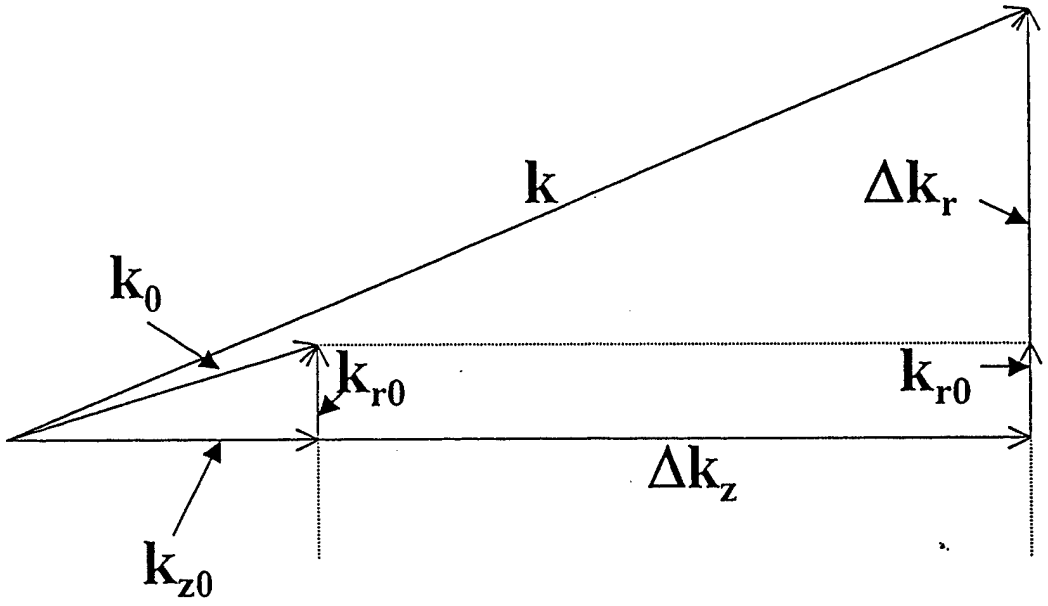

$$k_z = k_{z0} + \Delta k_z$$

$$k_r = k_{r0} + \Delta k_r$$

$$k = k_z + k_r$$

$$\theta_0 = k_{r0} / k_{z0}$$

$$\theta = k_r / k_z = k_{r0} / k_z + \Delta k_r / k_z \cong \theta_0 + \Delta k_r / k_z$$

Fig. 2

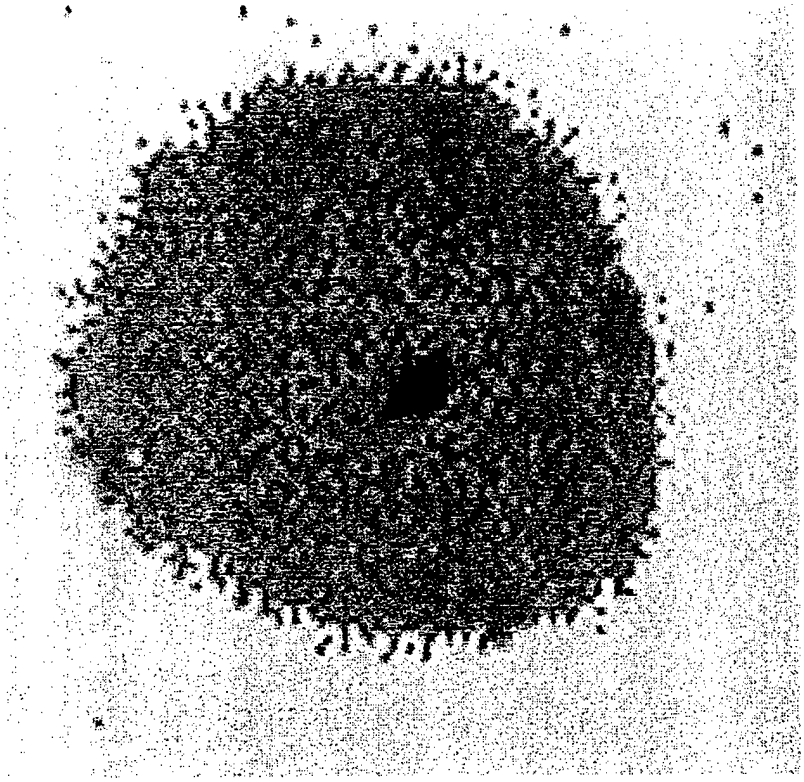

(Fig. 3)

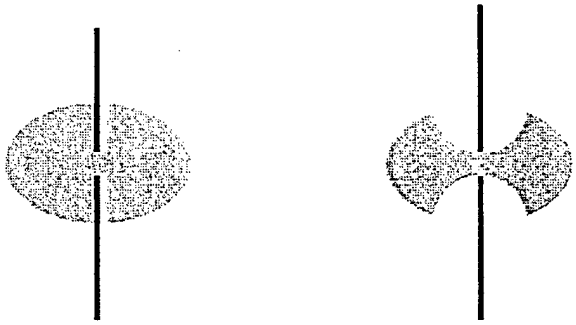

(Fig. 4)

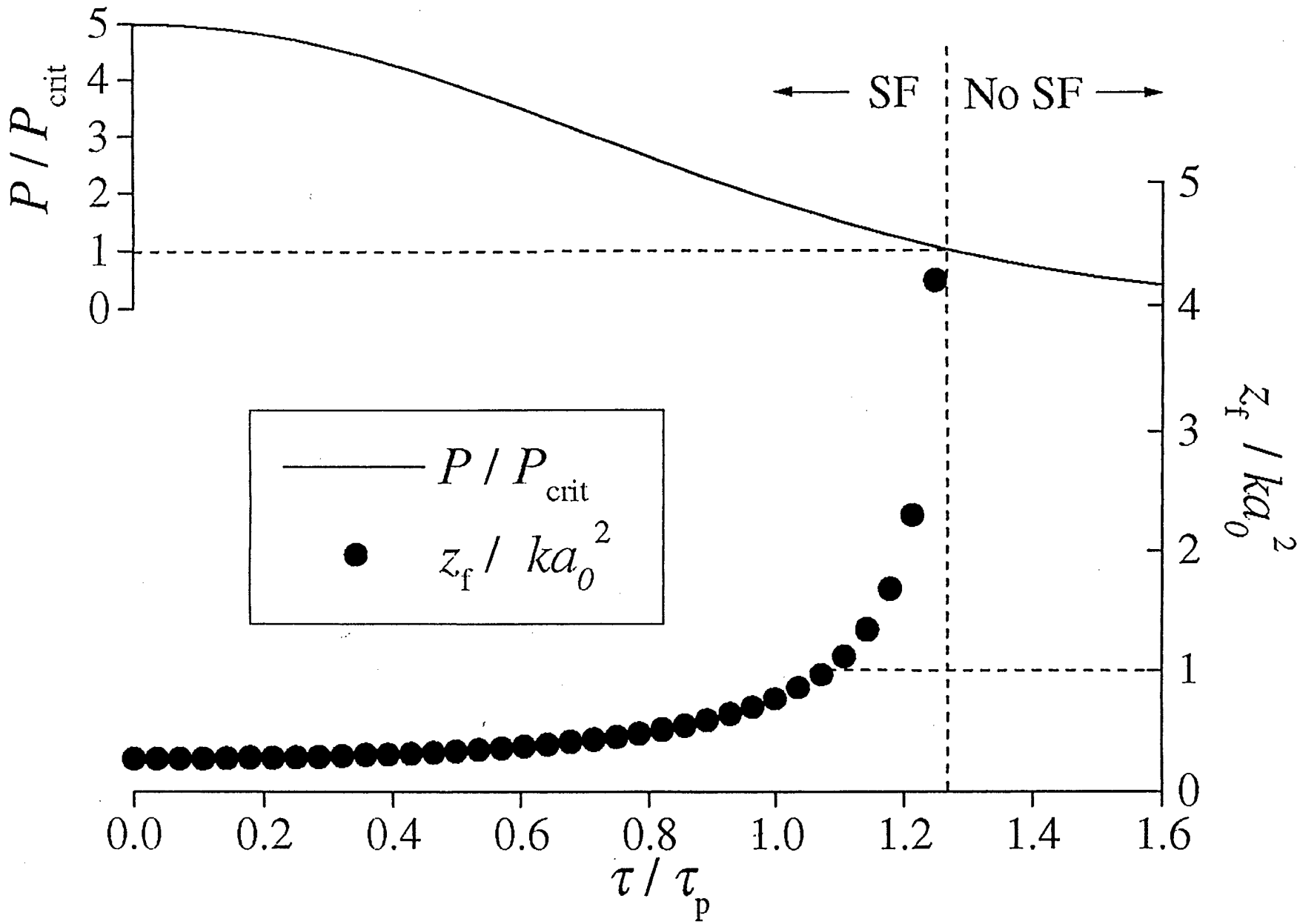
SF
No SF
P / P_{crit}
z_f / ka_0^2
P / P_{crit}
z_f / ka_0^2
τ / τ_p
0.0
0.2
0.4
0.6
0.8
1.0
1.2
1.4
1.6
0
1
2
3
4
5

figs.

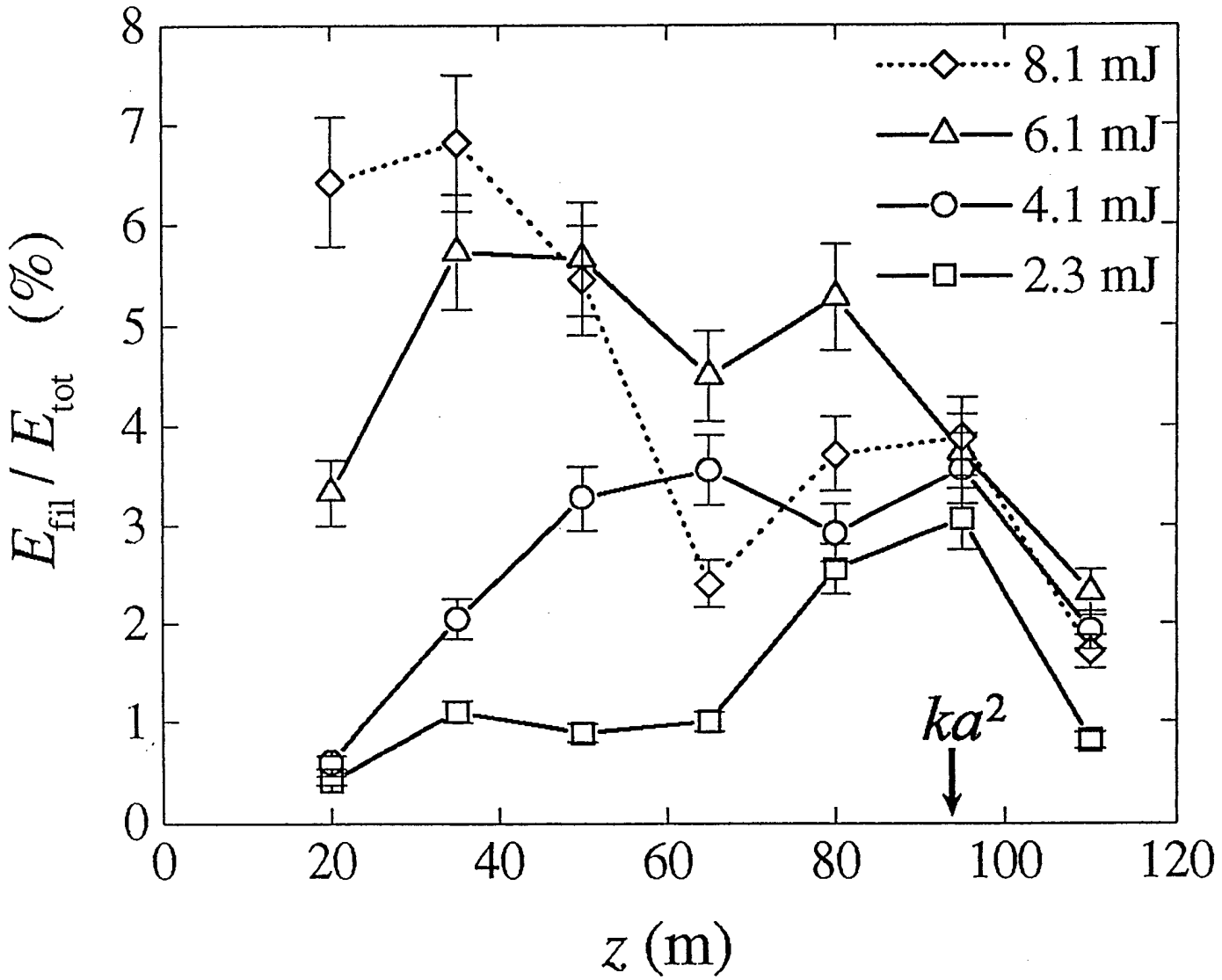
8.1 mJ
6.1 mJ
4.1 mJ
2.3 mJ
E_{fil} / E_{tot} (%)
z (m)
ka^2
0
1
2
3
4
5
6
7
8
0
20
40
60
80
100
120

Fig. 6a

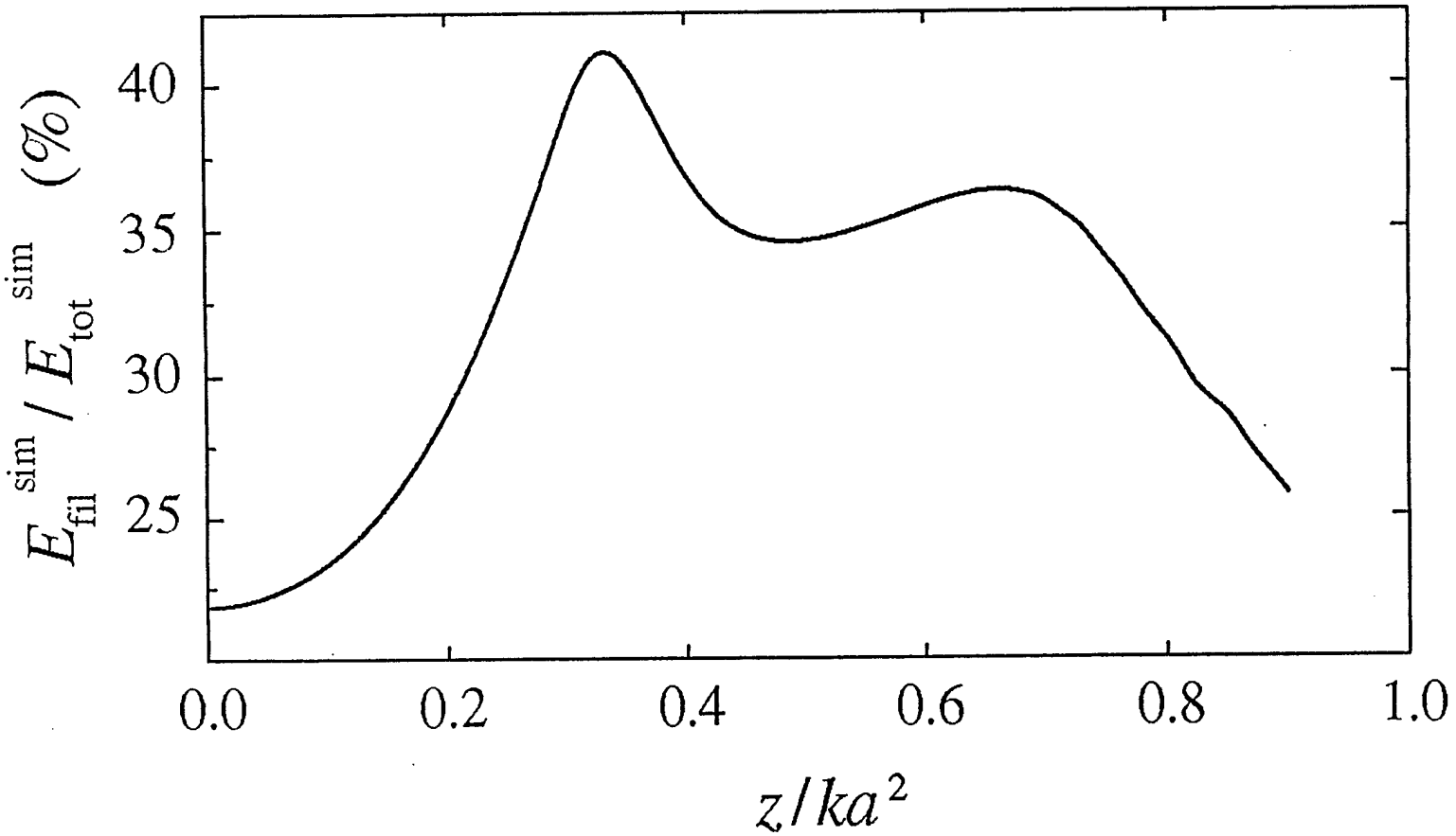

Fig. 6b

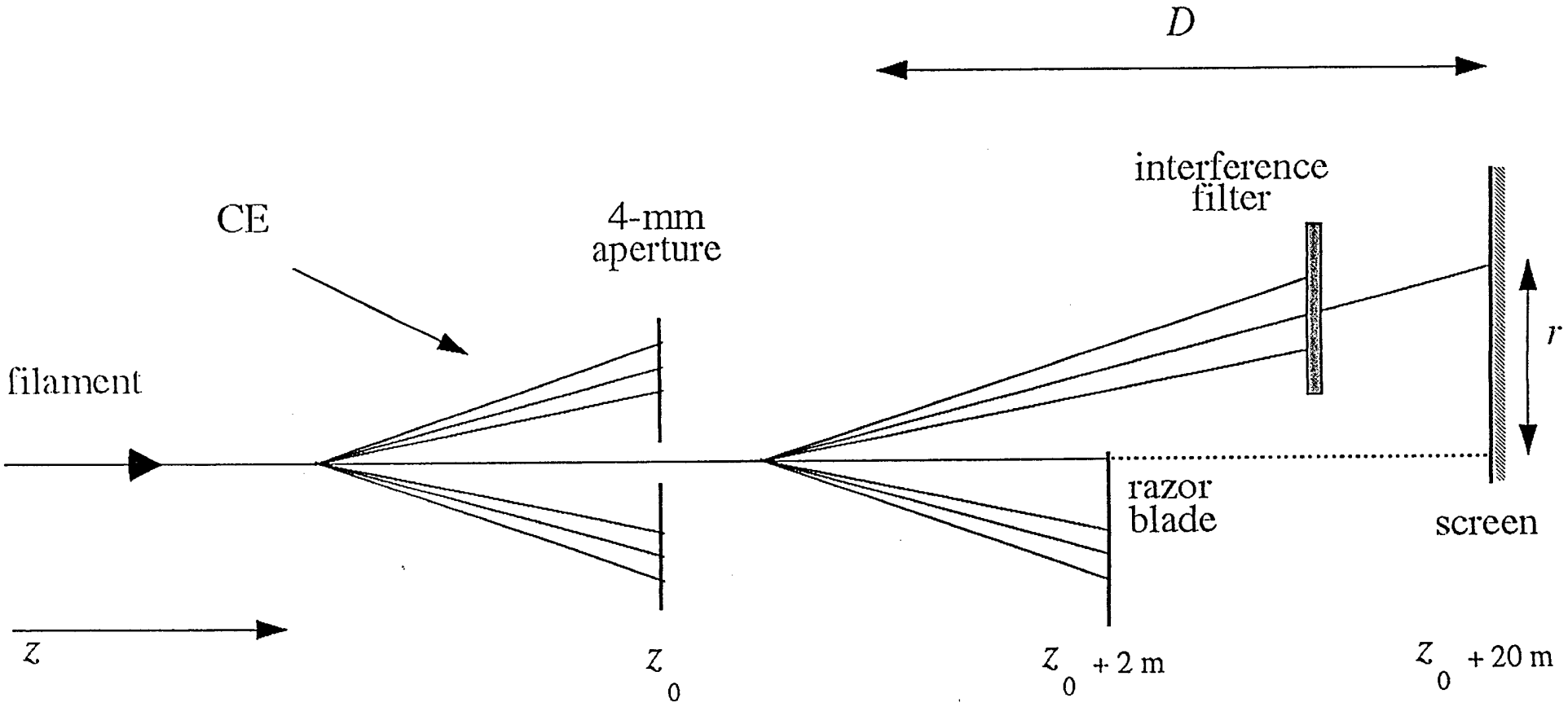
D
interference
filter
CE
4-mm
aperture
filament
r
razor
blade
screen
z
z 0
z 0 + 2 m
z 0 + 20 m

Fig 7

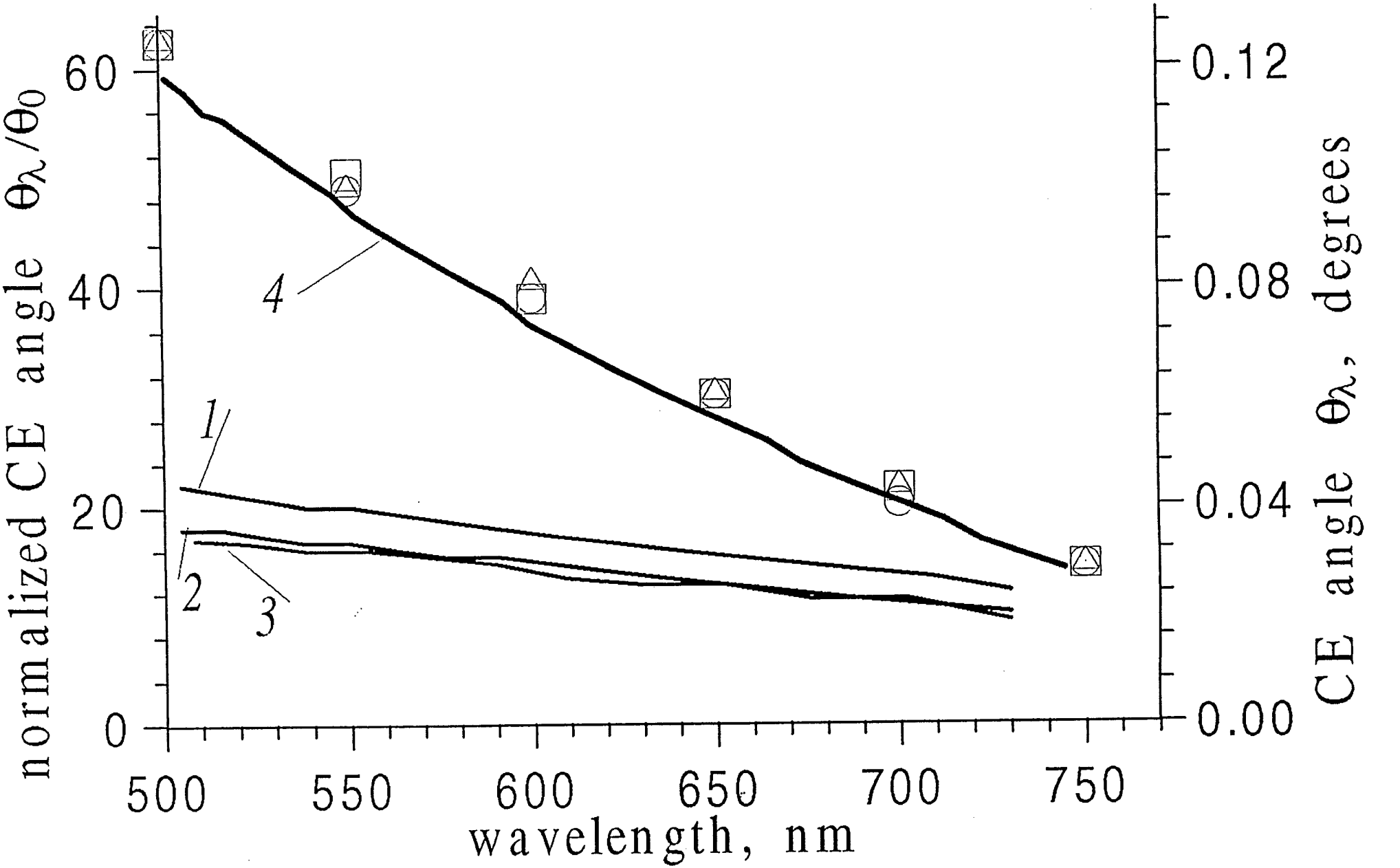
normalized CE angle θλ/θ0
60
40
20
0
0.12
0.08
0.04
0.00
CE angle θλ, degrees
1
2
3
4
500
550
600
650
700
750
wavelength, nm

Fig 8.

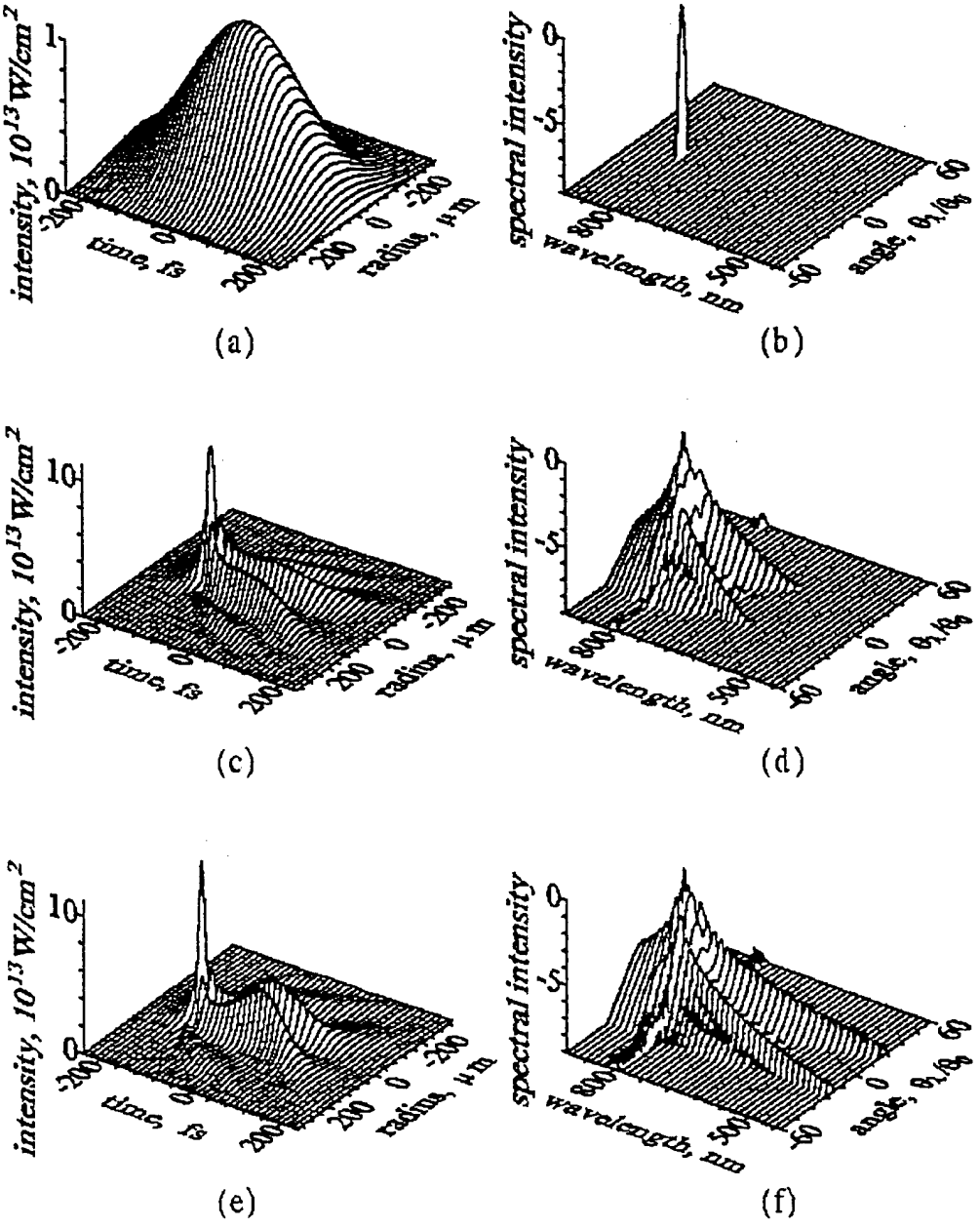
intensity, 10^{13} W/cm^2
1
0
-200
0
200
time, fs
200
0
-200
radius, μm
(a)
spectral intensity
0
800
500
wavelength, nm
-60
0
60
angle, θ, deg
(b)
intensity, 10^{13} W/cm^2
10
0
(c)
spectral intensity
(d)
intensity, 10^{13} W/cm^2
10
0
(e)
spectral intensity
(f)

Fig. 9

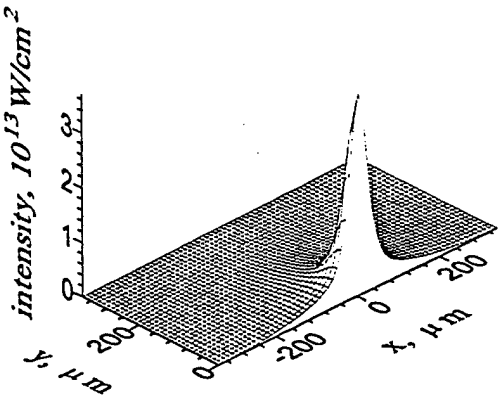
intensity, 10^{13} W/cm^2
0
1
2
3
y, μm
200
0
x, μm
-200
0
200

(a)

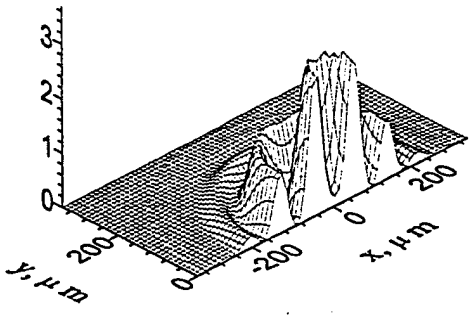
0
1
2
3
y, μm
200
0
x, μm
-200
0
200

(b)

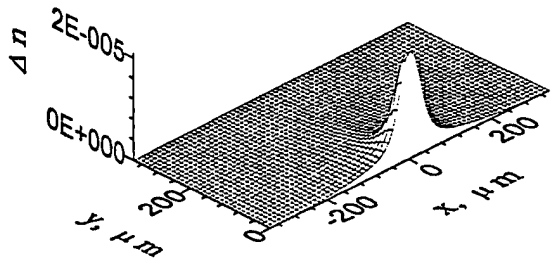
Δ n
2E-005
0E+000
y, μm
200
0
x, μm
-200
0
200

(c)

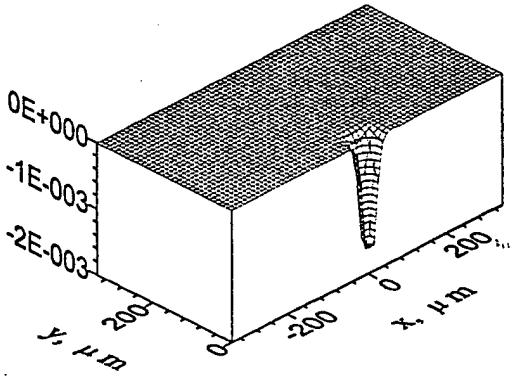
0E+000
-1E-003
-2E-003
y, μm
200
0
x, μm
-200
0
200

(d)

Fig. 10

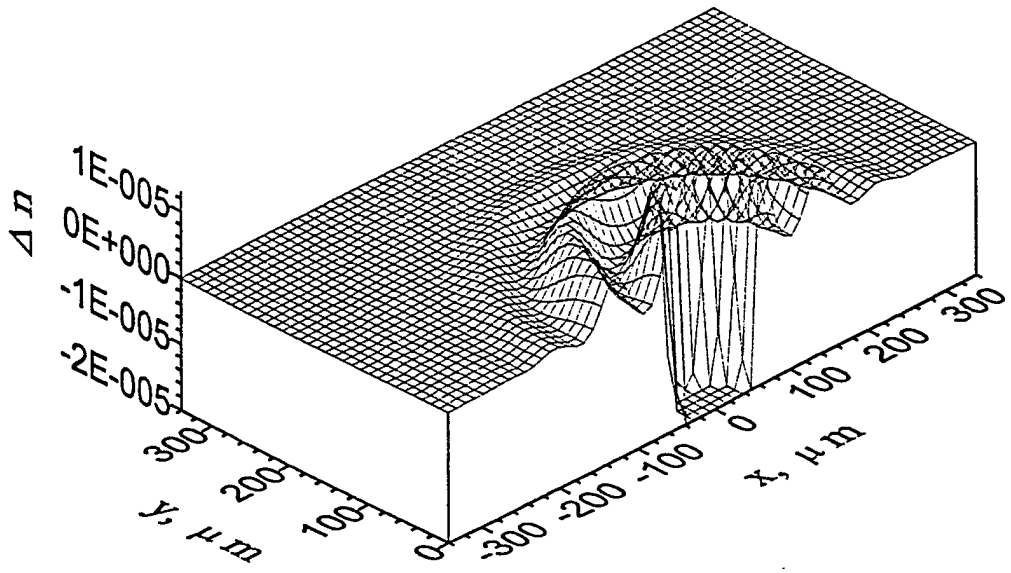
Δn
1E-005
0E+000
-1E-005
-2E-005
300
200
100
0
y, μm
-300
-200
-100
0
100
200
300
x, μm

Fig.11

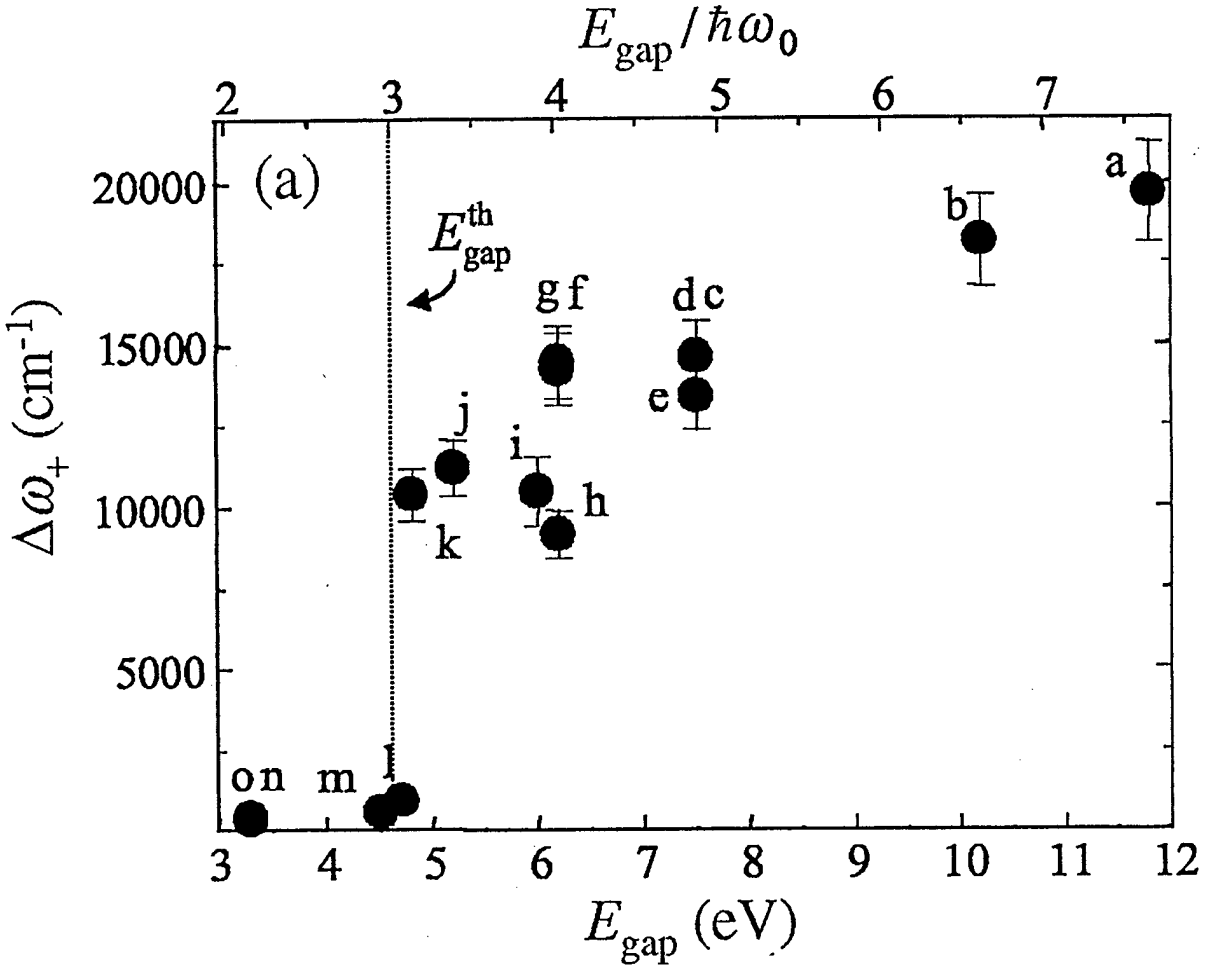
$E_{gap}/\hbar\omega_0$
2
3
4
5
6
7
(a)
E_{gap}^{th}
20000
15000
10000
5000
$\Delta\omega_+$ (cm^{-1})
a
b
c
d
e
f
g
h
i
j
k
l
m
n
o
3
4
5
6
7
8
9
10
11
12
E_{gap} (eV)

Fig.12

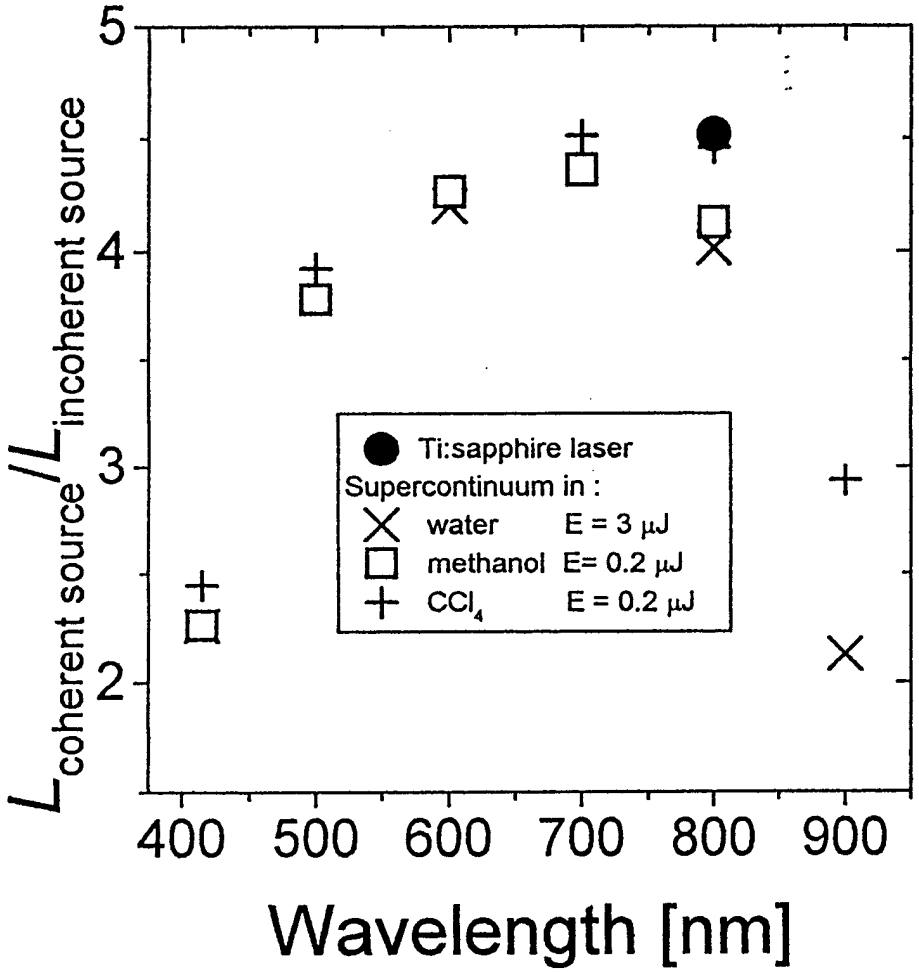
5
4
3
2
400
500
600
700
800
900
$L_{coherent\ source}/L_{incoherent\ source}$
Wavelength [nm]
Ti:sapphire laser
Supercontinuum in :
water E = 3 μJ
methanol E= 0.2 μJ
CCl_4 E = 0.2 μJ

Fig. 13

Appendix 2

The White Light Supercontinuum Is Indeed an Ultrafast White Light Laser

See Leang CHIN[1,2], Stéphane PETIT[1], Frédéric BORNE[1] and Kenzo MIYAZAKI[2]

1 Center for Optics, Photonics and Laser, and Department of Physics, Laval University, Quebec, Qc. G1K 7P4, Canada
2 Institute of Advanced Energy, Kyoto University, Uji, Kyoto 611-0011, Japan

(Received November 2, 1998; accepted for publication Dec. 14, 1998.)

Abstract

We identify the white light supercontinuum generated by femtosecond Ti-sapphire laser pulses as an ultrafast white light laser because the relative coherence lengths of all the wavelength components of the supercontinuum are essentially the same as that of the laser pulse when compared to an incoherent white light source.

KEYWORDS: femtosecond, supercontinuum, white light laser

The white light supercontinuum source has been known for a long time. It is usually generated by focussing powerful ultrashort laser pulses into transparent optical media. The output becomes a broadband source ranging from the near infrared to the ultraviolet.1-15) Recent development of very powerful femtosecond lasers such as the Ti-sapphire laser even allows the generation of such a supercontinuum without using a focussing lens.16-20) In all these cases, the laser pulse self-focuses first, becoming a filament (according to the moving focus model16-18)) whose length ranges from around a mm in condensed media15) to 100 m16-20) or even km.21) White light is emitted from all positions of the filament in the forward direction.16-18) This supercontinuum has a divergence as good as that of the input laser pulse.6,7,9,10)

The application of this white light source is widespread, ranging from a seed pulse for further amplification in dye amplifiers and optical parametric amplifiers22) to broadband absorption and excitation spectroscopy,2) and the characterisation of laser-induced structural transition.23)

In spite of the widespread usage of this light source and its long history, it is only recently that the fundamental physical mechanism responsible for the self-focussing, filamentation and supercontinuum generation has become better understood.16-18,24) Very briefly, it is the balance between the Kerr self-focussing effect in the neutrals and the defocussing effect in the plasma (free electrons) generated at the self-focus that gives rise to the moving focus and the filament.

The generation of the supercontinuum (SC) is a universal phenomenon in all transparent optical media and is due to self-phase modulation (SPM). The generation of the broad anti-Stokes part of the SC is due to SPM of the self-focussed pulse in the self-created plasma. The narrow Stokes broadening is due to SPM in the neutral Kerr medium which also contributes to a narrow part of the anti-Stokes side.

Because the SC can be a seed pulse for optical amplification, it is generally accepted that the SC is a coherent source. However, no one has yet identified that it is a white light laser simply because there seems to be no physical grounds for saying so. In this short letter, we try to justify that the SC should indeed be called a white light laser.

In the present experiment, 800 nm (7.18 nm bandwidth), 170 fs (FWHM) Ti-sapphire laser pulses were used. They were focussed by a 10-cm-focal-length lens into three different liquids, namely, water, methanol and CCl4. Since multiple filaments are independent sources of SC,15) we chose to study the effect of one filament. The laser power was adjusted so that only one filament was created. The energy per pulse required to generate one single filament in each liquid is 3 mJ for water

and 0.2 mJ for both methanol and CCl4. The maximum fluence in the filaments has been measured to be roughly 0.62, 0.54 and 0.44 J/cm2 for water, methanol and CCl4, respectively.24) The intensity cannot be measured properly yet because the duration of the sharp intensity spike at the self-focus, hence, at the filament, is not known. However, we have recently estimated them24) to be on the order of 1012 W/cm2 for water and 4 x 1011 W/cm2 for both methanol and CCl4. The SC output from the filament was then collimated by another 10-cm-focal-length lens and was sent into in a Michelson interferometer followed by a spectrometer. (The details of the experiment will be published elsewhere.25))

The output of the spectrometer showed spectral modulation.26) Six wavelengths across the whole SC and that of the laser line were chosen, each having a constant width of 1 nm. We define the coherence length as the path difference in the Michelson interferometer at which the spectral modulation disappears for that particular wavelength. These coherence lengths were compared with those of an incoherent white light source from an incandescent light bulb at the corresponding wavelengths under identical measuring conditions.

Figure 1 shows the results of the comparison under the condition of a single filament in the liquids. The vertical scale gives the ratios of the coherence lengths (Lcoherent source) of the various wavelength components of the SC source to those of the incoherent source (Lincoherent source). The horizontal scale gives the wavelengths at which the coherence lengths were measured.

We note two aspects. 1) The ratios are independent of the materials whose bandgap energies24) are 7.5 eV (water), 6.2 eV (methanol) and 4.8 eV (CCl4). This supports the idea that the generation of SC is a universal phenomenon. 2) In the range between 800 nm and 500 nm, all ratios are essentially equal to the corresponding ratio of the Ti-sapphire laser pulse at 800 nm. Those at the longer and shorter wavelength sides (430 nm and 900 nm) are smaller, since at these wavelengths, the SC signal power decreases quickly by one order of magnitude or more. The influence of the unavoidable incoherent light originating from plasma recombination in the self-focus and filament becomes important, i.e., the plasma contribution to the reduction of the coherence length becomes important. This makes the ratios smaller.

We can thus conclude that the relative coherence lengths (with respect to an incoherent source) of all the wavelength components of the white light SC are essentially the same as that of the Ti-sapphire laser pulse. From the point of view of coherence length, since the 800 nm pulse a laser pulse, the other wavelength components in the SC should also be called laser pulses. In fact, the duration of the SC pulses at different wavelengths has recently been measured in the case of SC generated from rare gases at atmospheric pressure, using 1.6 TW, 120 fs pulses of a Ti-sapphire laser.6,7) It was found that at various wavelength regions of the SC, the pulses are chirped differently, with the chirped durations ranging from 150 to 250 fs. Consequently, the SC source is a continuum of chirped ultrashort laser pulses, or simply an ultrafast white light laser.

From the point of view of practical application, it is desirable to increase the spectral intensity of such sources. Our current understanding of the fundamental physical processes underlying the generation of the SC allows us to predict and design some schemes to increase the intensity.

Since SC generation is due to SPM, which is proportional to the temporal gradient of the intensity profile, the spectral intensity of the SC is proportional to the maximum peak intensity that can be reached in the self-focus. The latter is determined by the threshold intensity for the generation of a plasma at the self-focus. In principle, one can envisage two ways of increasing the spectral intensity.

1. For a single filament, one should select a material with a high resistance to the generation of a plasma. In condensed matter, it is related to a large bandgap24); in gases, this is related to a high ionization potential.

2. After the selection of the material, one could further increase the spectral intensity by increasing the laser power to generate multiple filaments. Since multiple filamentation is a consequence of the spatial power fluctuation, each filament can be considered to be an independent source of a white light laser. Together, they constitute a bundle of lasers all having the same characteristics. The total spectral intensity will be proportional to the number of filaments one can produce in the optical medium. In water, one can easily generate hundreds of them.15) That is why the white light generated from water was extremely bright when the full power (1 mJ/100 fs) of a kHz Ti-sapphire laser beam was focussed into it.

In the work of the Electro-Communication University group,6,7) apparently without knowing our physical argument, they did exactly the same experiment as suggested above by selecting high-ionization-potential gases (rare gases) and using the highest peak power to generate multiple filaments. (The original objective was to extend the white light spectrum into the ultraviolet range.) The spectral intensity obtained by them is very significant, in the range of 100-1000 MW/nm.

One can also select different wavelength components of the white light laser and amplify them. The standard known amplifying medium is a dye amplifier. From the point of view of making an all-solid-state laser system, one can use the technique of optical parametric amplification (OPA) in a crystal. In fact, this technique is already being used in commercial products.27)

In conclusion, the white light SC generated by ultrashort laser pulses has been identified as an ultrafast white light laser from the point of view of its coherence length. Various schemes for increasing the spectral intensity of the white light laser can be envisaged. Most of these schemes have already been put into practice by many laboratories "unknowingly".

Acknowledgements

The experimental work is supported partially by the Natural Sciences and Engineering Research Council of Canada, le Fonds-FCAR, the Department of National Defence of Canada and the US Army Research Office. One of us (SLC) acknowledges the support of the Institute of Advanced Energy, Kyoto University during his sabbatical visit (July - October, 1998).

References

1) R R.Alfano and S.L.Shapiro: Phys. Rev. Lett. 24 (1970) 584.
2) The supercontinuum laser sources, ed. R.R.Alfano (Springer-Verlag, New York, 1989).
3) N.Bloembergen: Opt. Commun. 8 (1973) 285.
4) W.L.Smith, P.Liu and N.Bloembergen: Phys. Rev. A 15 (1977) 2396.
5) R.L.Fork, C.V.Shank, C.Hirlimann, R.Yen and W.J.Tomlinson: Opt. Lett. 8 (1983) 1.
6) H.Nishioka, W.Odajima, Y.Sasaki and K.Ueda: OSA TOPS on Advanced Solid State Lasers, eds. S.A.Payne and C.Pollock (OSA, Washington DC, 1996) Vol. 1.
7) H.Nishioka, W.Odajima, K.Ueda and H.Takuma: Opt. Lett. 20 (1995) 2505.
8) G.Y.Yang and Y.R.Shen: Opt. Lett. 9 (1984) 510.
9) P.B.Corkum, C.Rolland and T.Srinivasan-Rao: Phys. Rev. Lett. 57 (1986) 2268.
10) P.B.Corkum and C.Rolland: IEEE J. Quantum Electron. 25 (1989) 2634.
11) F.A.Ilkov, L.Sh.Ilkova and S.L.Chin: Opt. Lett. 18 (1993) 681.
12) V.Francois, F.A.Ilkov and S.L.Chin: Opt. Commun. 99 (1993) 241.
13) V.Francois, F.A.Ilkov and S.L.Chin: J. Phys. B 25 (1992) 2709.
14) G.S.He, G.C.Xu, Y.Cui and P.Prasad: Appl. Opt. 32 (1993) 4507.
15) A.Brodeur, F.A.Ilkov and S.L.Chin: Opt. Commun. 129 (1996) 193.
16) O.G.Kosareva, V.P.Kandidov, A.Brodeur, C.Y.Chien and S.L.Chin: Opt. Lett. 22 (1997) 1332.
17) A.Brodeur, O.G.Kosareva, C.Y.Chien, F.A.Ilkov, V.P.Kandidov and S.L.Chin: Opt. Lett. 22 (1997) 304.
18) O.G.Kosareva, V.P.Kandidov, A.Brodeur and S.L.Chin: J. Nonlinear Opt. Phys. & Mat. 6 (1997) 485.
19) A.Braun, G.Korn, X.Liu, D.Du, J.Squier and G.Mourou: Opt. Lett. 20 (1995) 73.
20) E.T.Nibbering, P.E.Curley, G.Grillon, B.S.Prade, M.A.Franco, F.Salin and A.Mysyrowicz: Opt. Lett. 21 (1996) 62.
21) L.Worste, C.Wederkind, H.Wille, P.Rairoux, B.Stein, S.Nikolov, C.Werner, S.Niedermeier, F.Ronnerberger, H.Schillinger and R.Sauerbrey: Laser und Optoelektronik 29 (5) (1997) 51.
22) K.R.Wilson and V.V.Yakovlev: J. Opt. Soc. Am. B 14 (1997) 444.
23) E.N.Glezer, S.Siegal, L.Huang and E.Masur: Phys. Rev. B 51 (1995) 6959.
24) A.Brodeur and S.L.Chin: Phys. Rev. Lett. 80 (1998) 4406.
25) S.Petit, F.Borne and S.L.Chin: in preparation for submission to Appl. Opt.
26) S.L.Chin, V.Fran□$B9P□(Jis, J. M.Watson and C.Delisle: Appl. Opt. 31 (1992) 33 83.
27) M.K.Reed, M.K.Steiner-Shepard and D.Negus: Opt. Lett. 19 (1994) 1855.

Figure caption:

Fig.1. Ratios of the coherence lengths Lcoherent source/ Lincoherent source as a function of the wavelength at which the coherence lengths are measured. Lcoherent source, the coherence length of a wavelength component (width = 1 nm) of the supercontinuum light generated by 170 fs Ti-sapphire laser pulses in water, methanol and CCl4; Lincoherent source, the coherence length of the same wavelength component of an incoherent light source measured under identical conditions. In the experiment, the laser pulse energy E was adjusted so as to produce only one single filament in the medium. The insets give the experimental conditions of the spectrometer and the energy E per pulse.

Appendix 3

The photo-emission spectra of N_2 interacting with a femtosecond Ti:Sapphire laser pulse

A Talebpour† †, A D Bandrauk‡ and S L Chin†

† Centre d'Optique, Photonique, et Laser (COPL) and Dépt. de Physique, Université Laval, Québec, Qc, Canada, G1K 7P4 Fax : 418-656-2623. Tel : 418-656-2131 ext. 4482

‡ Laboratoire de Chimie théorique, Faculté des Sciences, Université de Sherbrooke, Sherbrooke, Qc. Canada J1K 2R1

Abstract. The photoemission spectra of N_2 molecule interacting with a strong Ti:Sapphire laser pulse was studied. A detailed analysis of the spectra revealed evidences suggesting that photo-emission in the first negative band of N_2^+ molecular ion is due to the re-scattering of the ionized electrons to their parent ion.

PACS number: 32.80F

Short title: The photo-emission spectra of N_2 interacting with a femtosecond Ti:Sapphire laser pulse

January 22, 1999

† E-mail address: talebpou@phy.ulaval.ca

1. Introduction

In recent years, the physics of the interaction of diatomic molecules with femtosecond strong laser pulses has been studied extensively. In all the experimental studies the ion signal, and to a lesser extent, the electron signal have been used to probe the mechanisms involved in the phenomenon (Codling and Frasinski 1993). These signals, though useful in their own right, are not sufficient to provide all the information necessary for a complete description of the phenomenon. For example, it is expected that during interaction with strong laser pulses, the neutral molecules or molecular ions will be excited to some higher excited states. Detection of such an event is very difficult using ion or electron signal. In these cases the photons emitted by the excited molecules might be used as a complementary tool. However, to our knowledge there has been only few reports on utilizing photon signal to probe the interaction of the strong laser field with diatomic molecules (Liang *et al* 1995). Our goal in the present article is to show the usefulness of photon signals in studying the interaction of N_2 molecule with a Ti:Sapphire laser pulse. In this case, the photo-emission not only is used to indicate the creation of the excited molecular ion, but also it provides enough information about the mechanism responsible for the phenomenon. The merits of choosing N_2 is threefold. Firstly, the N_2^+ molecular ion in the excited state is very stable and does not undergo easily the fragmentation process. Secondly, the knowledge on the interaction of this molecule with strong femto-second laser pulses is useful in modeling the propagation of the laser pulses in the atmosphere which has recently attracted a lot of attention (Brodeur *et al* 1997, Kosareva *et al* 1997, Mlejnek *et al* 1998) . Finally, there is an extensive literature on the band spectra and the related parameters of the molecule (Lofthus and Krupenie 1977).

2. Experimental set-up and results

The schematics of our experimental setup is presented in fig. 1. A beam of Ti:Sapphire laser pulses is focused using a 100 cm focal length lens into a chamber containing N_2 gas with a variable pressure of 5-1000 Torr. Our laser system consists of a Ti:Sapphire oscillator followed by a regenerative and two multiple pass Ti:Sapphire amplifiers that can deliver pulses with energies of up to 200 mJ. The transform limited pulse duration is 200 fs (FWHM) and the central wavelength is 800 nm. The beam is focused to a spot with diameter of 98 μm (at $1/e^2$). To measure the spot size, the beam was attenuated by successive reflections from high-quality glass plates. The beam was then focused by the 100 cm focal length lens and the image of the focused area was analyzed by a microscopic objective associated to a CCD camera. As a result of interaction with the laser at the focal region a faint filament with a length of about 10 cm is visually

observed spanning the focal region. The central part of the filament is imaged onto the opening of a spectrometer with a resolution of 3 A°. The spectrometer is calibrated for the wavelength and the spectral response.

In figures 2 we present the resulting spectra for the case when the pressure in the tube is 5 Torr. The laser intensity is estimated to be $1\times\ 10^{15}$ W/cm^2 (the estimation of the intensity is based on the measured laser parameters; pulse duration, pulse energy and the spot size at focal region). From 470 nm up to 800 nm there is no signal, therefore this part is not presented in the figure. Below 300 nm and beyond 800 nm the detection efficiency of our spectrometer is very low. Thus we did not measure the spectrum in these regions.

The observed violet degraded lines are assigned to two band systems; the second positive system of N_2 ($C^3\Pi_u - B^3\Pi_g$ transition) and the first negative system of $N_2{}^+$ ($B^2\Sigma_u^+ - X^2\Sigma_g^+$ transition) respectively. The details of assignment and the strength of lines is summarized in table 1. In this table by I and II we mean the first negative system of $N_2{}^+$ and the second positive system of N_2 respectively.

3. Discussion

As already mentioned, the emission spectra of fig. 2 is assigned to the second positive system of N_2 molecule and the first negative system of $N_2{}^+$ molecular ion respectively. For the purpose of the present article we will be mainly concerned with the first negative system and the discussion of the second positive system will be postponed to a future publication.

The first negative system of $N_2{}^+$ ion results from transitions from different vibrational levels of the second excited potential surface of the ion, $B^2\Sigma_u^+$, to different vibrational levels of its ground potential surface, $X^2\Sigma_g^+$ (fig. 3). In what follows, different possible excitation mechanisms are considered. However, before proceeding further we discuss the way in which the molecular ion is prepared through multiphoton ionization (MPI).

As we have recently reported (Talebpour *et al* 1998) the rate of MPI of diatomic molecules is very well predicted by the PPT (Prelemov *et al* 1965) model by assuming that the electron tunnels through a barrier given by Z_{eff}/r instead of the pure Coulomb barrier $1/r$ which is used in the calculation of the MPI of atoms. Here, Z_{eff} is a fitting parameter to simulate the effective Coulomb potential felt by the electron that tunnels out. This parameter depends principally on the random orientation of the ground state neutral molecule. The importance of this finding is in its practicality; the only parameter needed for predicting the MPI rate of a diatomic molecule is a single parameter, Z_{eff} . By experimentally measuring the probability of MPI of N_2 and comparing with theory Z_{eff} is found to be 0.9 for this molecule (for details of comparison

Table 1. The wavelength (in nm), measured strengths (in arbitrary units) and the assignments of band heads of fig. 2. 'I' and 'II' pertains to the fist negative system of N_2^+ and the second positive system of N_2 respectively. v' and v'' are the vibrational index of the upper and lower level respectively.

Measured Wavelength (nm)	Strength (arb. unit)	Expected Wavelength II (nm)	Transition II (v', v'')	Expected Wavelength I (nm)	Transition I (v', v'')
353.44	15.25			353.26	(5-4)
353.85	8.73	353.67	(1-2)		
354.96	5.42			354.89	(3-2)
356.59	12.19			356.29	(2-1)
357.70	11.63	357.69	(0-1)		
358.31	9.43			358.21	(1-0)
371.1	1.49	371.05	(2-4)		
375.37	3.91	375.54	(1-3)		
380.44	5.59	380.49	(0-2)		
388.56	8.75			388.43	(1-1)
391.4	71.45			391.44	(0-0)
394.26	1.2	394.3	(2-5)		
399.94	1.49	399.84	(1-4)		
406.13	1.05	405.94	(0-3)		
412.22	2.02			412.13	(5-6)
414.14	1.14	414.18	(3-7)	414.05	(4-5)
416.78	0.79			416.68	(3-4)
419.93	2.99	420.05	(2-6)	419.91	(2-3)
423.78	4.8			423.65	(1-2)
426.93	3.07	426.97	(1-5)		
427.74	12.94			427.81	(0-1)
446.63	0.91			446.66	(6-8)
448.66	1.64	449.02	(2-7)	449.03	(5-7)
451.61	1.15			451.59	(4-6)
455.36	0.55			455.41	(3-5)
459.93	0.75			459.97	(2-4)
465.4	1.04			465.18	(1-3)
470.99	1.39			470.92	(0-2)

between experiment and theory see Larochelle *et al* 1998a). In figure 4 we present the experimentally measured ion vs intensity curve of N_2^+ along with the theoretical curve calculated from the PPT model with $Z_{eff} = 0.9$. In this figure the ion vs intensity curve in the case of circularly polarized laser pulses is also presented for later discussion.

Equipped with an analytical model for the rate of MPI, we can calculate the population of different electronic-vibrational levels of the molecular ion following MPI. Depending on the shell from which the electron is ionized, the molecular ion might be produced in the vibrational levels of different potential surfaces. The electronic configuration of ground state N_2 is $KK(\sigma_g 2s)^2(\sigma_u 2s)^2(\pi_u 2p)^2(\sigma_g 2p)^2$ (Herzberg 1950). The MPI of an electron from $(\sigma_g 2p)^2$, $(\pi_u 2p)^2$ or $(\sigma_u 2s)^2$ configurations leaves the ion in the vibrational levels of $X^2\Sigma_g^+$, $A^2\Pi_u^+$ and $B^2\Sigma_u^+$ respectively. W_{nv}, the rate of MPI to level v of the potential surface n with ionization potential E_{nv} and oscillator strength f_{nv} with respect to the ground state of N_2 is given by

$$W_{nv} = f_{nv} W_{PPT}(E_{nv}) \tag{1}$$

where W_{PPT} is the MPI rate given by the PPT model. Using eq. 1 the number of ions in the state nv, N_{nv}, is calculated from the following relation

$$N_{nv} \propto \int_V dV \left(1 - exp\left(-\int_{-\infty}^{\infty} dt W_{nv}\left(I(\mathbf{r},t)\right)\right)\right) \tag{2}$$

where $I(\mathbf{r},t)$ is the time dependent intensity of the pulse at point $\mathbf{r}$ which is assumed to be given spatially and temporally by a Guassian function and V is the interaction region. Using eq. 2 we have calculated the number of ions in different states and summarized the results in table 2. The f_{nv} values are taken from Jain and Sahni (1968). All the values are normalized to the value of $N_0(X^2\Sigma_g^+)$ which is the number of the molecular ions created into the ground vibrational level of the $(X^2\Sigma_g^+)$ potential surface.

Table 2. The number of ions created in different electronic-vibrational states following the MPI of N_2

v	$N_v(X^2\Sigma_g^+)$	$N_v(A^2\Pi_u^+)$	$N_v(B^2\Sigma_u^+)$
0	1.000	5.359E-2	7.144E-3
1	7.007E-2	4.543E-2	4.835E-4
2	3.009E-2	1.999E-2	7.262E-6
3	1.153E-3	7.675E-3	2.257E-8
4	5.104E-6	2.356E-3	8.931E-9
5	3.033E-7	6.772E-4	4.306E-11

A quick inspection of table 2 indicates that if post-ionization processes are not taken into account, the observed spectra of fig. 2 cannot be explained solely by considering the population through the MPI of the inner shell electrons. If this were the case, the

transitions $v' - v''$ (hear v' and v'' denote the vibrational levels of $B^2\Sigma_u^+$ and $X^2\Sigma_g^+$ respectively) with $v' \geq 2$ would be too weak to be observed because the population in $B^2\Sigma_u^+$ ($v' \geq 2$) is too small. Observation of 5-6 transition (note: from table 2, the population of $B^2\Sigma_u^+$ ($v' = 5$) is very low, $\sim 10^{-11}$) at wavelength 412.13 nm (see table 1 and fig. 2) with appreciable intensity strongly suggests that some post-ionization processes must have contribution in further populating the different vibrational levels of $B^2\Sigma_u^+$ potential surface.

Pumping up the population to the upper state ($B^2\Sigma_u^+$) either by three photon coupling from the $X^2\Sigma_g^+$ potential surface (similar to the three photon coupling as in the case of H_2^+ discussed by Bandrauk 1994) or by two photon coupling from $A^2\Pi_u^+$ cannot be a good candidate either. In the former case, since a three photon transition from the $v'' = 0$ (the most populated) level of $X^2\Sigma_g^+$ is in quasi resonance with the $v' = 5$ level of $B^2\Sigma_u^+$, most probably this level will be populated. In the latter case a two photon resonance will populate the levels $v' \geq 3$ of $B^2\Sigma_u^+$. However, from table 1 it is observed that the strongest band are those which originate from $v' = 0$. This indicates that even though up-pumping through two or three photon couplings from the lower potential surface is a possibility, it can have insignificant contribution in populating the $B^2\Sigma_u^+$ potential surface.

As another possibility, it could be argued that as a result of the re-scattering of the ionized electron to its parent ion (Kuchiev 1987, Corkum 1993), it could make an inelastic collision with the ion and excite it to higher states. The recent experimental and theoretical results on the non-sequential multiple ionization of atoms (Larochelle *et al* 1998b, Becker and Faisal 1996) makes this scenario very appealing. Despite the fact that calculating the predicted spectra from this hypothesis at present is very difficult, still we might offer strong arguments in its favor. We should recall that from the point of view of the energy the process is possible. At our working intensity, 1×10^{15} W/cm^2, the pondromotive energy, U_p, amounts to 60 eV and the maximum energy of the electrons may reach up to $12U_p$ in the case of molecules (Bandrauk and Yu 1999). Thus, many of the re-scattered electrons (which is half of the total number of the electrons produced through the MPI) have energies higher than the threshold energy of exciting the electron from the vibrational levels of $X^2\Sigma_g^+$ and $A^2\Pi_u^+$ to the vibrational levels of $B^2\Sigma_u^+$.

There are two important evidences in favor of dominance of the electron re-scattering in populating the excited levels. The first one comes from comparison of the laser intensity dependence of the strength of the band heads and the ion signal (number of the N_2^+ ions). In fig. 5 we present the laser intensity dependence of the strength of the strongest band head (391.4 nm). Also in the figure we have included the theoretically calculated ion vs intensity curve of fig. 4. The strength of the band head is scaled vertically in a way that its value is equal to the value of the ion at their corresponding saturation intensities. It is observed that the strength of the band head is proportional

to the number of ions in the focal volume, hence, proportional to the probability of MPI of N_2 to N_2^+. This observation is reminiscent of a similar observation in the studies on the non-sequential multiple ionization of atoms. There it has been shown that the probability of non-sequential double ionization of atoms near the saturation intensity of the first charge is proportional to the probability of MPI to the singly charged ion (Talebpour *et al* 1998, Larochelle *et al* 1998b). This was shown to be the consequence of re-scattering of electrons. This similarity suggests that the underlying physics might be the same, i.e., the current phenomena results from the re-scattering of electrons.

The second evidence is provided from the polarization dependency of the intensity of the band heads. From a classical picture of the electron re-scattering theory it is well established that using circularly polarized pulses the ionized electron will not return back to its parent ion. If the process of populating the levels of $B^2\Sigma_u^+$ is really achieved through the collision of the re-scattered electron with the parent ion, then using a circularly polarized light the population of the excited states and consequently the strength of the band heads of the first negative system would be suppressed. This is in fact observed experimentally. In fig. 6 the dependence of the strength of the band head at 391.44 nm is presented as a function of angle between the polarization axis of the laser beam and the axis of a quarter wave-plate which is used to transform the linearly polarized light to an elliptically polarized light. When the angle is zero the beam is linearly polarized, and for an ideal wave-plate it is expected that at an angle 45 degrees the beam must be circularly polarized. However, at high intensities the wave-plate is not perfect and at 45 degrees the polarization of the beam is elliptical with an ellipticity 0.9. As it is observed from fig. 6, even at this level of ellipticity the intensity of the band head has dropped by a factor of 11. The same observation holds for all other band heads of the first negative system. Note that the decrease of the strength of the band heads cannot be attributed to the decrease in the probability of MPI as a result of changing the polarization of the laser from linear to circular. As it can be noticed from fig. 4, at our working intensity (1×10^{15} W/cm^2) the ion signal in the casse of circular polarization is only by a factor of 0.63 lower than that in the case of linear polarization. Thus, the observed decrease in the srength of the lines can be attributed to the electron re-scattering.

4. Conclusion

The photo-emission spectra from the N_2 molecule interacting with a Ti:Sapphire laser pulse was measured. The spectrum in the visible region consists of two well known systems; the second positive band system of N_2 and the first negative band system of N_2^+. In the present article only the latter band system was considered. A detailed discussion along with a comparison with the phenomenon of non-sequential double

ionization enabled us to attribute the observation of the first negative band system of N_2^+ to the re-scattering of electrons created through the MPI to their parent ion. The inelastic collision of these electron can excite the molecular ion to its excited states which later relax and radiate the bands of the first negative system.

Acknowledgments

It is our pleasure to acknowledge the technical assistance of S. Lagace and fruitful discussions with T. T. Nguyen-Dang and S. Larochelle. This work was supported in part by NSERC, le Fonds FCAR, US Army Research office and the Department of National Defence of Canada.

References

Bandrauk A D 1994 Editor *Molecules in Laser Fields*, Marcel Dekker Inc. New York.
Bandrauk A D and Yu H 1999 *Phys. Rev. A*, **59** 539
Brodeur A, Kosareva O G, Chien C-Y, Ilkov F A, Kandidov V P and Chin S L 1997 *Opt. Lett.* **22** 304
Codling K and Frasinski L J 1993 *J. Phys. B: At. Mol. Opt. Phys.* **26** 783.
Corkum P B *Phys. Rev. Lett.* **71** 1994
Becker A and Faisal F H M 1996 *J. Phys. B: At. Mol. Opt. Phys.* **29** L197
Gilmore F R 1965 *J. Quant. Spectrosc. Radiat. Transfer* **5** 369
Herzberg G 1950 *Molecular spectra and molecular structure* Vol. I, Van Nostrand Reinhold
Jain D C and Sahni R C 1968 *Int. J. Quantum Chem.* **2** 325
Kosareva O G, Kandidov V P, Brodeur A, Chien C Y and Chin S L 1997 *Opt. Lett.* **22** 1332
Kuchiev M Yu 1987 *Sov. Phys.-JETP Lett.* **45** 404
Larochelle S F J, Talebpour A and Chin S L 1998a *J. Phys. B: At. Mol. Opt. Phys.* **31** 1215
Larochelle S F J, Talebpour A and Chin S L 1998a *J. Phys. B: At. Mol. Opt. Phys.* **31** 1201
Liang Y, Augst S, Beaudoin Y, Chaker M, Yu H, Bandrauk A D and Chin S L 1995 *J. Phys. B: At. Mol. Opt. Phys.* **28** 3661
Lofthus A and Krupenie P H 1997 *J. Phys. Chem. Ref. Data* **6** 113
Mlejnek M, Wright E M and Moloney J V 1998 *Opt. Lett.* **23** 182
Perelemov A M, Popov V S and Terent'ev M V 1966 *Sov. Phys.-JETP* **23** 924
Talebpour A, Larochelle S and Chin S L 1997c *J. Phys. B: At. Mol. Opt. Phys.* **30** L245
Talebpour A, Larochelle S and Chin S L 1998 *J. Phys. B: At. Mol. Opt. Phys.* **31** L49

Figure captions

Figure 1. Experimental set-up

Figure 2. Spectrum of N_2 at a pressure of 5 Torr. The lines marked by arrows are assigned to the first negative band of N_2^+. In the inset of the lower graph, signal in the range between 440 to 472 nm is multiplied by three to enhance the visibility of the peaks.

Figure 3. The first three potential energy curves (potential surfaces) of N_2^+ molecule (Gilmore 1965)

Figure 4. Multiphoton ionization of N_2 using linearly and circularly polarized laser pulses from a Ti:sapphire laser. The theoretical ion yield is calculated from the PPT model with $Z_{eff} = 0.9$.

Figure 5. The intensity dependence of the strength of the band head at 391.4 nm. The points present sigle shot data. The solid curve is the theoretical curve of fig. 4.

Figure 6. The dependence of the strength of the band head at 391.4 nm on the angle between the polarization of the laser beam and the axis of a quarter wave-plate. Each point is an average over 100 shots. The "error" bars giving the maximum scattering of the data points are presented at two different angles. Note that the ellipticity of the beam achieves to 0.9 at 45 degrees.

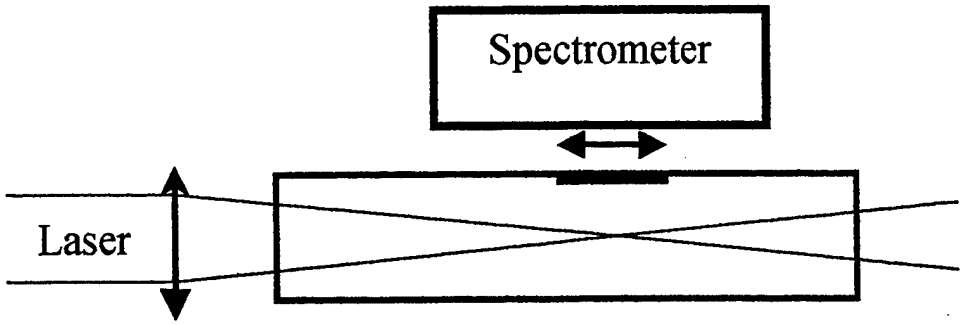
Spectrometer
Laser

Fig. 1

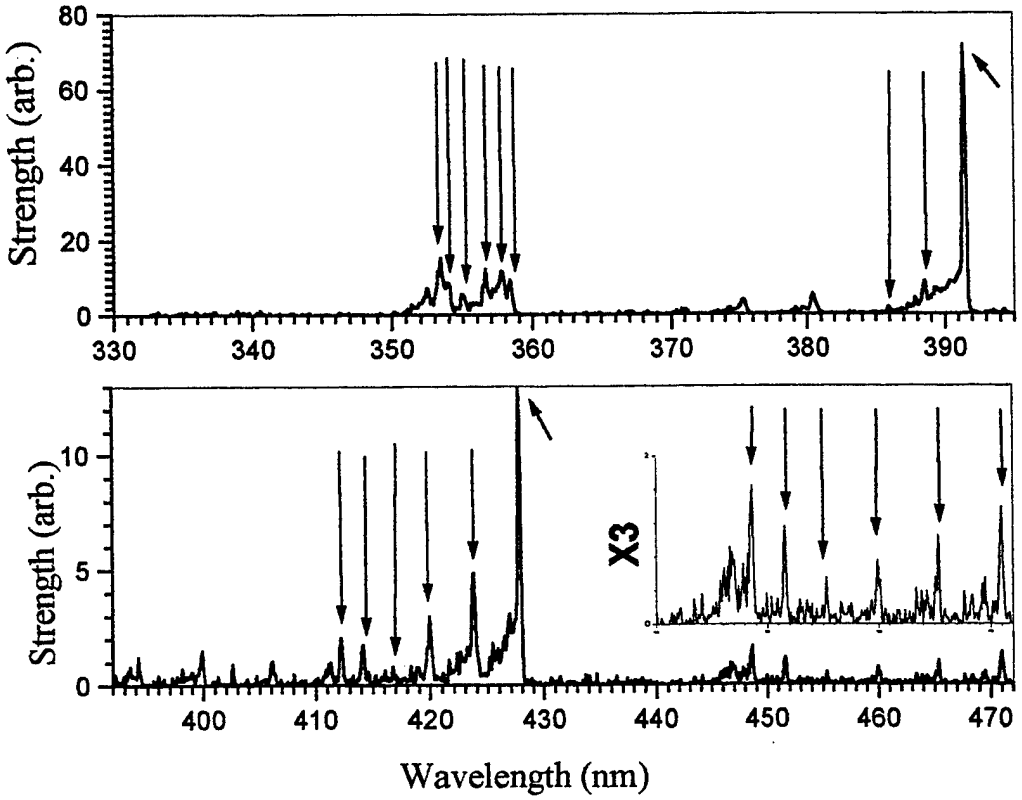
Strength (arb.)
80
60
40
20
0
330
340
350
360
370
380
390
Strength (arb.)
10
5
0
X3
400
410
420
430
440
450
460
470
Wavelength (nm)

Fig. 2

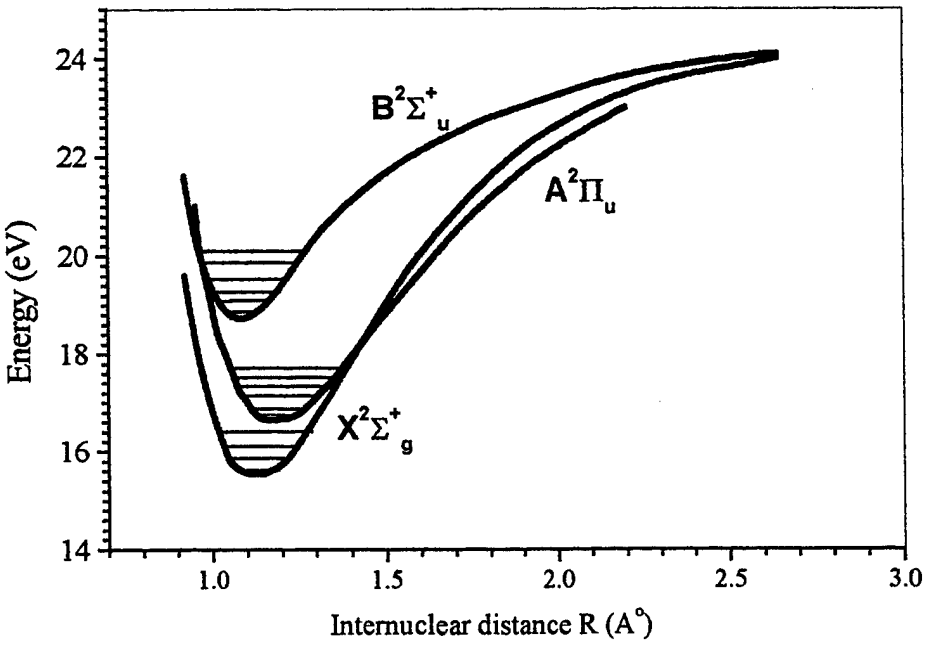
24
22
20
18
16
14
Energy (eV)
$B^2\Sigma^+_u$
$A^2\Pi_u$
$X^2\Sigma^+_g$
1.0
1.5
2.0
2.5
3.0
Internuclear distance R (A°)

Fig. 3

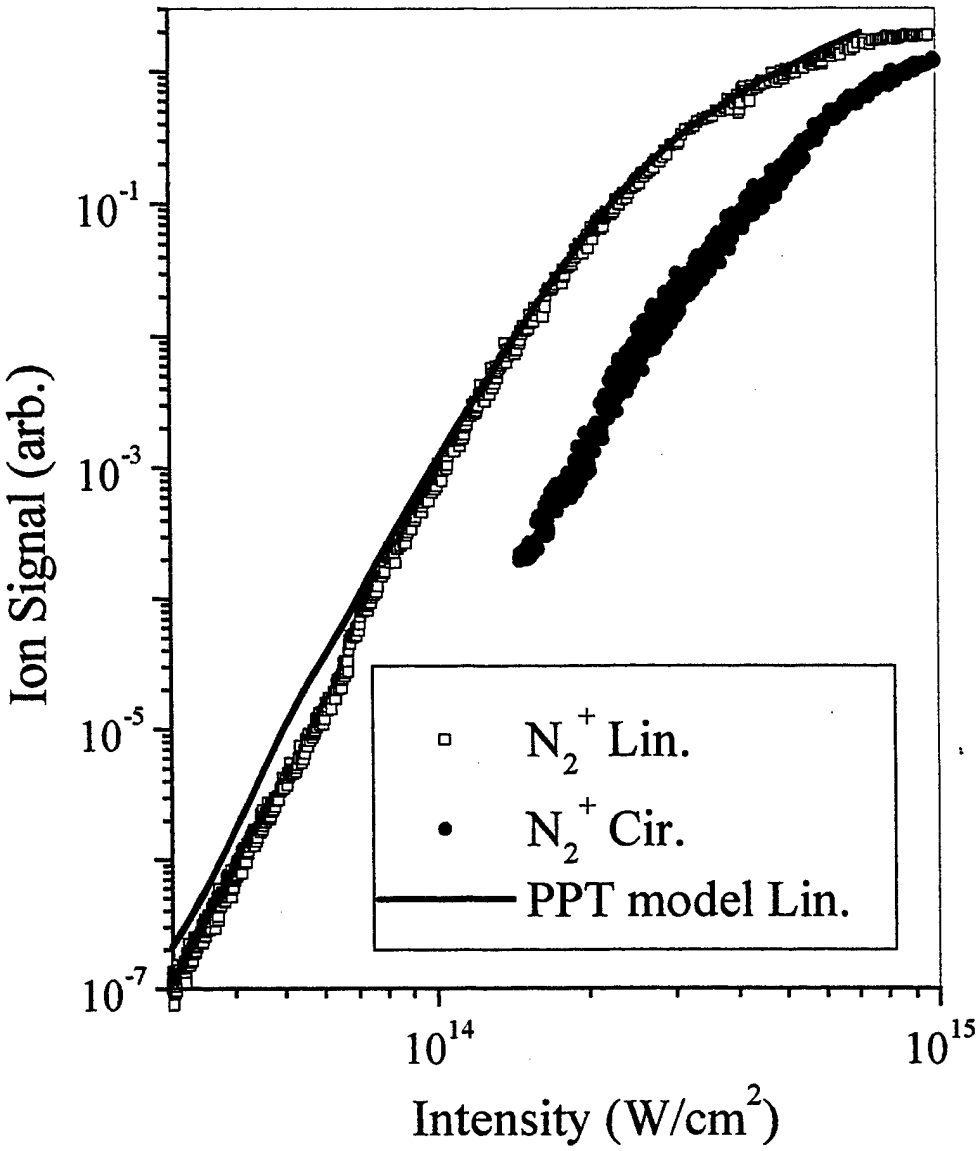
Ion Signal (arb.)
10^{-1}
10^{-3}
10^{-5}
10^{-7}
10^{14}
10^{15}
Intensity (W/cm^2)
N_2^+ Lin.
N_2^+ Cir.
PPT model Lin.

Fig. 4

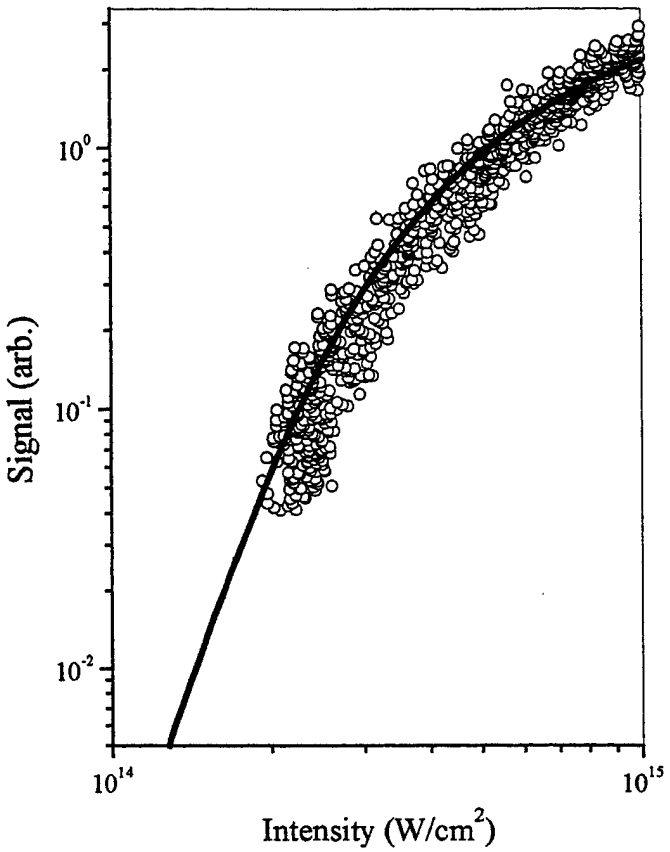

Fig. 5

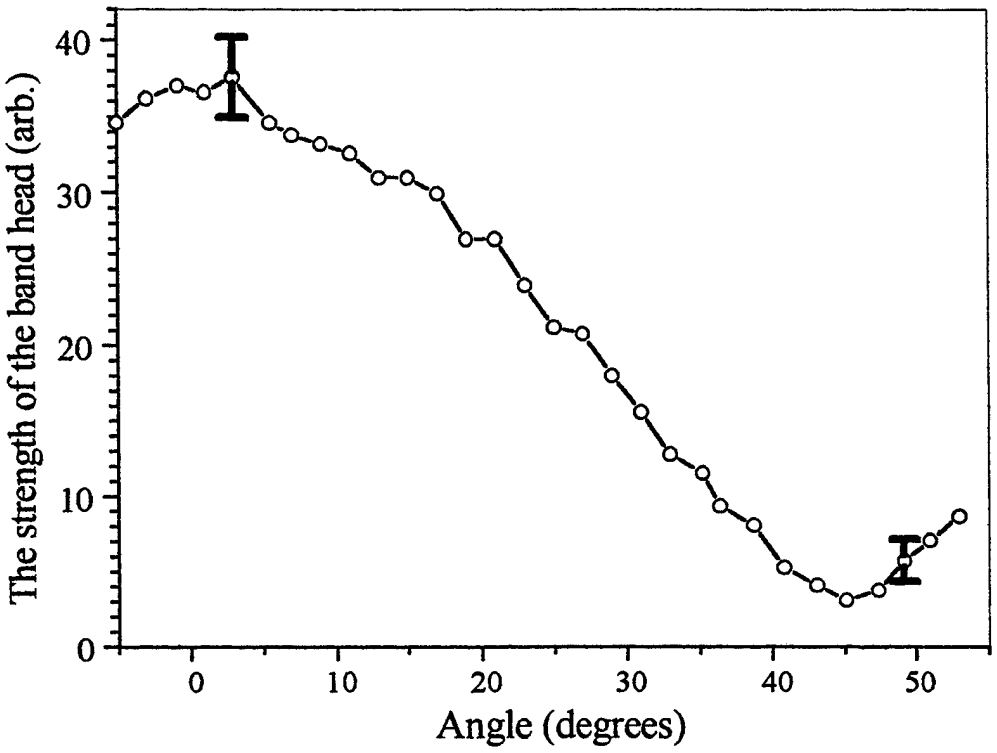
The strength of the band head (arb.)
40
30
20
10
0
0
10
20
30
40
50
Angle (degrees)

Fig. 6

Appendix 4

Re-focusing during the propagation of a focused fs Ti:Sapphire laser pulse in air

A. Talebpour, S. Petit and S. L. Chin

Centre d'Optique, Photonique, et Laser (COPL) and Dépt. de Physique. Université Laval, Québec, Qc, Canada, G1K 7P4

Abstract

The dependence of the intensity of a focused Ti:Sapphire laser pulse in air on the propagation distance was studied by measuring the photo-emission spectrum of N_2 and N_2^+. Refocusing was observed directly that agrees with the predictions put forward by Mlejnek et al, Opt. Lett. 23 382 (1998).

In recent years the phenomenon of the propagation of strong ultrafast laser pulses in the atmosphere that leads to self-focusing, filamentation, supercontinuum generation and conical emission, has been studied both experimentally and theoretically [1-5]. As a result a qualitative picture has emerged which is able to explain the fundamental physical mechanisms of the phenomenon [2-4]. However, more rigorous models of recent years predicted some new phenomena such as re-focusing, etc which need more careful measurement of intensity distribution in the filament for a quantitative comparison. Due to the high intensity in the filament, incorporating measurement systems directly into the beam is nearly impossible; therefore the intensity distribution should be determined from measurement of some quantities outside the filament. In the present letter we offer the results of our measurement that reflects the gross intensity in the filament as a result of the propagation of a focused femtosecond laser pulse in air. These results confirm the phenomenon of refocusing of the laser pulses after the geometrical focus [5]. The setup of experiment is presented schematically in fig.1. A Ti:Sapphire laser pulse with a duration of 220 fs is focused through 1.5 m lens creating a filament in air. The filament is visible to the naked eyes in a range of 20 cm spanning the focal region. The radiation from the filament was analyzed spectrally. The central part of the filament was imaged onto the entrance slit of a spectrometer which is calibrated for the spectral response. A sample spectrum of the radiation is presented in figure 2. As it is observed, there is no detectable continuum radiation, characteristic of collisional ionization, in the spectrum. The observed violet degraded lines are assigned to two band systems: the second positive system of N_2 ($C^3\Pi_u - B^3\Pi_g$ transition) and the first negative system of N_2^+ ($B^2\Sigma_u^+ - X^2\Sigma_g^+$ transition) respectively.We have studied these spectra through detailed experiments and the results concerning their physical origin will be analyzed in a separate paper. Later in this paper, we will discuss the significance of the signal detected by the photomultiplier in fig. 1, and it will be shown that it is a monotonically increasing function of the gross intensity in that region of the filament beneath the detector.

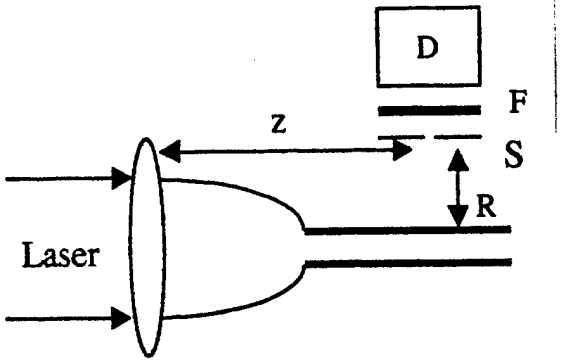

Fig. 1. Experimental set-up

The total intensity of the radiation from a restricted part of the filament (restricted by a slit. S, with an opening of 0.2 mm, situated at R=1 cm above the filament) at a distance z from the lens in a frequency range of $330 < \lambda < 460$ nm (filtered by F) is detected by a photomultiplier (D). The amplitude of the output of the detector is taken as the measured signal. In fig. 3, the results of our measurement using two different beam sizes (11 mm and 4 mm) is presented. When using the 11 mm diameter beam (fig. 3a) the peaks of the plots occur at a position before the geometrical focus indicating self-focusing. The distance of the focusing point from the geometrical focus increases with the energy of the pulse. This is consistent with the prediction of the moving focus model [6]. After focusing, the beam rapidly converges as indicated by the decrease of the signal. If the energy of the pulse is sufficient, the beam divergence stops along some distance before it starts to diverge again. This is clearly seen from the first shoulder of the curves after the geometrical focus. At higher energies of the pulse, more than one shoulder could be observed. Thus, the detailed behavior of the beam strongly depends on the pulse energy. When using the 4 mm diameter beam (fig. 3b), again the peak (self-focus) moves towards the lens, though with an amount more appreciable than the case of larger beam diameter. This is well anticipated noting that in this case, the input power is about 7.6 times (=the ratio of the cross sections of the two beams) higher than the case of a larger beam with the same energy and pulse duration. After self-focusing a more interesting situation arises; the signal level increases clearly through

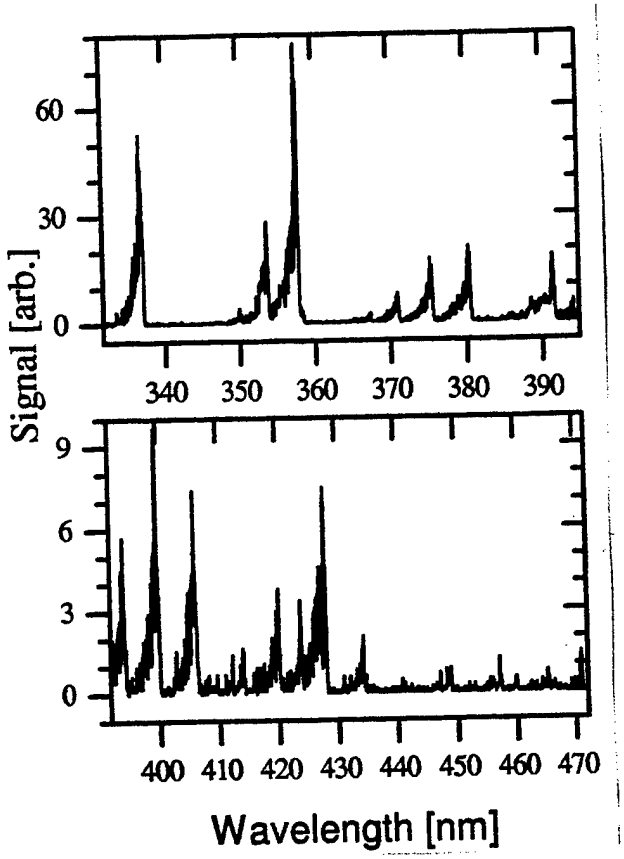

Fig. 2. Spectrum of air interacting with a 220 fs laser pulse.

a second peak indicating that the beam after a slight divergence focuses again. This is a clear demonstration of the phenomena of re-focusing [2-5]. In particular, the prediction of re-focusing in ref. 5 in the case of a focusing geometry is clearly observed here. Unfortunately, in the case of small beam we are not able to increase the energy of the pulse more than 10 mJ to verify clearly the multiple focusing predicted by the simulations of ref. 5. However, by analogy the shoulders of fig. 3a might be considered as indicating the re-focusing. If so, the appearance of multiple shoulders in the case of high-energy pulses could be considered as the occurrence of multiple refocusing.

As it was noticed by comparing the two figures 3.a and 3.b, for a given energy of the pulse the manifestations of the nonlinear propagation effects (early focusing, refocusing and slow divergence after focusing meaning filamentation or a streak of moving foci) is weaker in the case of the beam with larger diameter, or more precisely shorter Rayleigh range. This enables us to study the significance of the signal. We thus performed a separate experiment by increasing the diameter of the beam to 2 cm. It was focused using a 1 m focal lens in air using a set-up similar to fig. 1. In this case due to the short

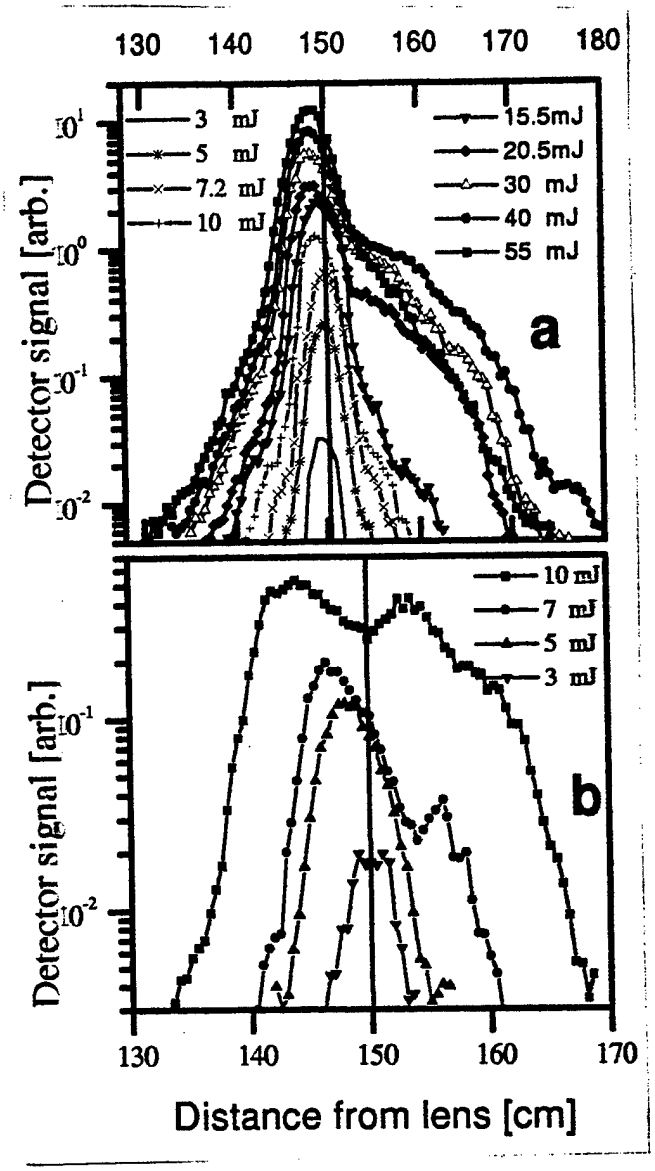

Fig 3. The signal of the PMT detector versus, z, the distance of the lens and the slit(S) in fig. 1 with the energy of pulse as parameter. Each point is average over 100 shots. The upper and lower graphs correspond to the beams with diameters of 1.1 and 0.4 cm respectively.

Rayleigh range ($\simeq$ 20 mm) as compared to the case of fig. 3 the effect of self focusing before the geometrical focus is negligible, such that the distribution of intensity at the focal region does not deviate strongly from the one expected in vacuum. This fact is readily observed in the inset of fig. 4, which represents the detector signal at a distance from the lens. Even at the appreciably large value of the pulse energy, 20 mJ, the curve is symmetric and focusing practically occurs at the geometrical focus. We measured the laser pulse energy dependence of the signal with the detector placed above the focal point (z=100 cm). The result is shown as open circles in fig.4.

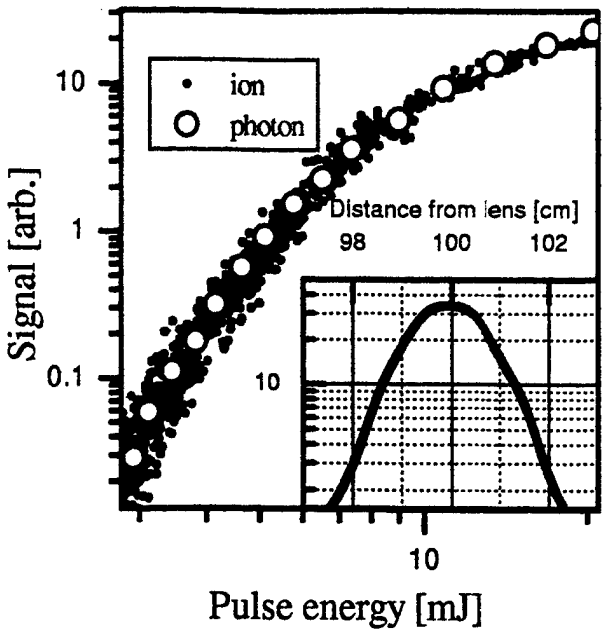

Fig. 4. The signal of the PMT (photon) and the ion number (ion) as a function of pulse energy for the case of a beam with a diameter of 2 cm and a focusing lens with focal length of 1 m. The measurement is done at the focus of the lens. The energy in the case of photon signal is multiplied by a factor of 2. In the inset the dependence of the photon signal on the propagation distance is presented.

Then, in a vacuum chamber the intensity dependence of the total number of N_2^+ ions was measured (for the details of the experiment see [6]), and the result is shown as dots in fig. 4. The photon signal has been shifted vertically such that the turning point coincides with the saturation point of the ion curve and horizontally by a factor of two towards higher pulse energy. The complete overlap of the two curves indicates two aspects. Firstly, the photon signal reflects the gross intensity in the filament and is a monotonically increasing function of the pulse energy. Secondly, the probability of photon emission scales in the same way as the probability of multiphoton ionization to N_2^+ molecular ion at a pulse energy twice lower. We can thus take advantage of this observation to propose the following for theorists to test the validity of their propagation model. We could say that the photon signal generated at a theoretically calculated intensity $I(\mathbf{r},t)$ in the filament is proportional to the ion signal generated at intensity $I(\mathbf{r},t)/2$ in the vacuum chamber. We can calculate the ion number , $N(I/2)$, in this case precisely by the following formula

$$N(I/2) \propto \int_V dV \left(1 - e^{\left(-\int_{-\infty}^{\infty} dt W(I(\mathbf{r},t)/2)\right)}\right) \quad (1)$$

where W is the rate of multiphoton ionization of N_2 molecule. Recently, we have measured the rate of the MPI of this molecule and concluded that it is very well predicted by the PPT model [8] with $Z_{eff} = 0.9$ (for the significance of Z_{eff} and relevant discussions see [9]). As we have concluded earlier, $N(I/2)$ thus obtained must be proportional to the signal we measure in fig. 3. Thus, the calculated ion signal as a function of z should fit those curves in fig. 3 if the model were correct.

In conclusion, we have measured the radiation emitted by the N_2 molecules and N_2^+ molecular ions interacting with the laser pulse in the filament. The result of the measurement gives the gross intensity in the filament as a function of the propagation distance showing a multiple refocusing which agrees qualitatively with the results of the simulations of ref. 5.

It is our pleasure to acknowledge the technical assistance of S. Lagace and M. Abdel Fattah and fruitful discussions with C.M. Bowden and N. Akozbek. This work was supported in part by NSERC, le Fonds FCAR, US Army Research Office and the Department of National defence of Canada.

1. H. R. Lange, G. Grillon, J. F. Ripoche, M. A. Franco, B. Lamouroux, B. S. Prade, A. Mysyrowicz, Opt. Lett. **23**,120 (1998); A. Braun, G. Korn, X. Liu, D. Du, J. Squier, G. Mourou, Opt. Lett. **20**, 73 (1995); X. M. Zhao, J. C. Diels, C. Y. Wang, J. M. Elizondo, IEEE J. Quantum Electron. **31**, 599 (1995); E. T. J. Nibbering, P. F. Curley, G. Grillon, B. S. Prade, M. A. Franco, F. Salin, A. Mysyrowicz, Opt. Lett. **21**, 62 (1996).
2. A. Brodeur, C. Y. Chien, F. A. Ilkov, S. L. Chin, O. G. Kosareva and V. P. Kandidov, Opt. Lett. **22**, 304 (1997).
3. O. G. Kosareva, V. P. Kandidov, A. Brodeur, C. Y. Chien and S. L. Chin, Opt. Lett. **22**, 1332 (1997).
4. O. G. Kosareva, V. P. Kandidov, A. Brodeur and S. L. Chin, IJNLOM **6**, 485 (1997).
5. M. Mlejnek, E. M. Wright and J. V. Moloney, Opt. Lett. **23**, 382 (1998).
6. A. Talebpour, S. Larochelle and S. L. Chin, , J. Phys. B. **30**, 1927 (1997).
7. J. H. Marburger, Prog. Quant. Electron. **4**, 35 (1975).
8. A. M. Perelomov, V. S. Popov and M. V. Terent'ev, Soviet Phys. JETP **23**, 924 (1966)
9. A. Talebpour, S. Larochelle and S. L. Chin, J. Phys. B. **31**, L49 (1998).

Appendix 5

Semi-empirical model for the rate of tunnel ionization of N_2 and O_2 molecule in an intense Ti:Sapphire laser pulse

A Talebpour†, J Yang and S.L.Chin

Centre d'Optique, Photonique,et Laser (COPL) and Département de Physique,

Université Laval Quebec, Qc. G1K 7P4 Canada

Abstract: A semi-empirical model capable of predicting the rate of tunnel ionization of N_2 and O_2 molecules interacting with strong Ti:Sapphire laser pulses is derived.

1. Introduction

The interaction of two major ingredients of the atmosphere, N_2 and O_2, with a strong femtosecond laser pulse determines the dynamics of its propagation in the atmosphere. Owing to the nonlinear index, the laser pulse self-focuses first. The contribution of the plasma generated from tunnel ionization (TI) counteracts self-focussing. The competition between these two processes results in filaments according to the moving focus model [1]. Therefore, any meaningful simulation of the propagation needs a predictive model for the rate of TI of the atmospheric gases. For this purpose, in the past, different analytical models such as ADK model [2, 3], above barrel suppression ionization model [4], Szoke's model [5] or a simple I^N model [6] have been used in various types of application, such as propagation [1, 7], plasma interaction [8] etc.. The recent findings of Larochelle *et al* [9] showed that none of these model is capable of providing a satisfactory result for the rate of TI of species as simple as rare gas atoms. Instead,

they verified that two equivalent models, Perelemov A.M, Popov. V. S and Trent'ev's model (PPT model) [10] and Krainov's model [11], correctly predicted the TI rate of atoms. Based on this work, Talebpour *et al* [12] were able to model the TI rate of D_2 molecule. The remarkable finding of this work is that instead of a pure Coloumb barrier $\frac{1}{r}$ which is used in the calculation of the TI rate of atoms, the rate of TI of diatomic molecule can be calculated using the PPT model by assuming that the electron tunnels through a barrier given by $\frac{Z_{eff}}{r}$ ($Z_{eff}<1$, Z_{eff} is an effective charge defined to a fictitious atom with the same ionization potential as the molecule in such a way that the tunneling rate of this atom is the same as the tunneling rate from the barrier created by the molecule). This finding is translated to a simple recipe; to calculate the rate of TI of a diatomic molecule one has to find a single parameter Z_{eff}, and use this parameter in the PPT model. To find Z_{eff} from calculation is not simple for molecules other than H_2, but this is barely needed. For practical uses Z_{eff} can be found from experimental results. In this article, we attempt to find Z_{eff} for N_2 and O_2 by comparing the experimentally measured ion versus intensity curves with the theoretical curves obtained by integrating over the pulse duration and the interaction volume of the TI rate using the PPT model with different values of Z_{eff}. The result is immediately applicable in the modeling of the propagation and filamentation of intense femtosecond laser pulses in the atmosphere for different application such as LIDAR. Appendix (I) gives the formula of the PPT model.

2. Experimental results and discussion

The experimental ion vs intensity curves of N_2 and O_2 (presented in figures 1 and 2 respectively) have been obtained using a Ti:Sapphire laser, with a pulse duration of 200 fs and wavelength of 800 nm. A detailed description of the experimental technique can be found in Talebpour *et al* [13]. In figure 1 the ion vs intensity curve of Xe (IP=12.130 eV [14] ,which is similar to that of O_2,12.063 eV [14]) and in figure 2 the ion vs intensity curve of Ar (IP=15.759eV [14], which is similar to that of N_2, 15.576 eV [14]) are included for comparison. As it is noted the probability of TI of a molecule is suppressed compared to that of an atom with a similar ionization potential. The suppression might be explained to result from the random orientation of the neutral molecules with respect to the polarization of the laser [9] which is manifested in a value of $Z_{eff}<1$.

In both figures we have included the ion vs intensity curves predicted by Szoke's model, SFA model [15] and the ADK model. None of these models, contrary to their widespread use in simulations of the pulse propagation, is capable of offering a satisfactory fit with the experimental results. None of these models could be forced to fit the experimental results by varying the Z_{eff} either [9]. The SFA completely neglect the Coulomb potential and the Szoke's model considers the Coulomb potential, in the final state, as a constant, thus both these two models do not depend on Z_{eff}. The ADK model depends on Z_{eff} theoretically, but the predicted slope by this model, regardless the amount of Z_{eff}, always underestimates the experimental value. This is because the ADK model is valid in the region of intensity where Keldysh's parameter [16] γ is less than 0.5 [3]. In the current experiment, γ is of the order of 1. We have not included the curves predicted by the BS model [17] Because of its false construction of on-off ionization process, this model predicts a curve with very large slope (theoretically infinite) on a log-log graph and therefore is very far from the reality.

Contrary to the other models, the PPT model and equivalently the Krainov's model fit the experimental results on the TI of atoms due to their correct handling of the effects of the Coloumb potential [9]. As it is observed the PPT model is capable of predicting the rate of the TI of both of the molecules satisfactorily. In the case of O_2 we have used a value of 12.55 eV for the ionization potential. The reason is that the ionization rate of any molecule is a weighted average (the weighting factors being the Frank-Condon coefficients) of the ionization rate to different vibrational levels of the ground potential surface of the molecular ion. Without performing a detailed calculation from the potential energy curves of N_2 and O_2 [18] we might argue that while N_2 molecule will most probably ionize to the first vibrational level of its ion, O_2 molecule can ionize to many possible vibrational levels of its ground potential surfaces. In fact from the photo-ionization results of Samson and Gardner [19] it is noticed that the Frank-Condon factors for thansition to the five first vibrational levels of O_2^+ is nearly similar. Without going into the details of calculation we might argue that the weighted average of MPI probability to all these levels should be nearly the same as transition probability to the second vibrational level of O_2^+ with ionization potential of 12.55 eV.

3. Conclusion

In the light of the theoretical analysis of the TI of D_2 molecule, we have been able to offer a semi-emperical analytical model capable of correctly predicting the rate of TI of O_2 and N_2.

4 Acknowledgments

It is our pleasure to acknowledge the technical assistance of S Lagace. This work is supported in part by NSERC, Le fonds-FCAR and US Army Research Office.(Grant number:

Appendix

The PPT model, as used in the present calculation, is adopted from references [8] and [9]. In this model the rate of the TI from an state of an atom with ionization potential E_i, quantum numbers l and m and effective charge Z_{eff} in a laser field with frequency ω and peak electric field F, in atomic units is given by

$$W_{PPT} = |C_{nl}|^2 f_{lm} E_i \left(\frac{2(2E_i)^{3/2}}{F}\right)^{2n^*-|m|-3/2} \times \left(1+\gamma^2\right)^{|m|/2+3/4} A_m(\omega,\gamma) \times e^{-\left(\frac{2(2E_i)^{3/2}}{3F} g(\gamma)\right)} \quad (1)$$

where

$$n^* = \sqrt{2E_i}\,/\,Z^2$$

$$\gamma = \frac{\omega F}{\sqrt{2E_i}} \quad (2)$$

$l^* \approx n^* - 1$, and

$$f_{lm} = \frac{(2l+1)(l+|m|)!}{2^{|m|}|m|!(l-m)!} \quad (3)$$

$$g(\gamma) = \frac{3}{2\gamma}\left[\left(1+\frac{1}{2\gamma^2}\right)\sinh^{-1}(\gamma) - \frac{\sqrt{1+\gamma^2}}{2\gamma}\right] |C_{lm}|^2 \frac{2^{2n^*}}{n^*\Gamma(n^*+l^*+1)\Gamma(n^*l^*)}$$

The coefficient $A_m(\omega,\gamma)$ is given by

$$A_m(\omega,\gamma) = \frac{4}{\sqrt{3\pi}}\frac{1}{|m|!}\frac{\gamma^2}{1+\gamma^2} \times \sum_{n>\upsilon}^{\infty} w_m\left(\sqrt{\frac{2\gamma}{1+\gamma^2}}(n-\upsilon)\right)e^{-(n-\upsilon)\alpha(\gamma)}$$ where

$$w_n(x) = e^{-x^2}\int_0^x \left(x^2-y^2\right)^{|m|} e^{y^2} dy$$

$$\alpha(\gamma) = 2\left(\sinh^{-1}(\gamma) - \frac{\gamma}{\sqrt{1+\gamma^2}}\right)$$

$$\nu = \frac{E_i}{\omega}\left(1+\frac{1}{2\gamma^2}\right)$$

References

[1] O.G. Kosareva, V.P.Kandidov, A.Brodeur, C.Y.Chien and S.L.Chin, *Opt.Lett.***22**(1997), 1332; A.Brodeur, O.G.Kosareva, C.Y.Chien, F.A.Ilkov,V.P.Kandidov and S.L.Chin, *Opt.Lett.***22,** 304(1997); O.G.Kosareva,V.P.Kandidov,A.Brodeur and S.L.Chin, *J.Nonlinear Opt.Phy.&Mat.*,**6,** 485(1997).

[2] Ammosov M V, Delone N B, and Krainov V P *Sov. Phy.-JETP* **64**(1986) 1191;

[3] Ilkov F, Decker J E and Chin S L *J.Phys. B:At Mol. Opt. Phys.* **25**(1992) 4005

[4] Augst S, Talebpour A, Chin S L,Beaudoin Y and Chaker M *Phy. Rev. A* **52**(1995) R917

[5] Perry M D, Szoke A, Landen O L and Campbel E M *Phy.Rev. Lett.* **60**(1988) 1270

[6] Chin S L, Peter Lambropoulos, *Multiphoton ionization of atoms* Academic Press(1984)

[7] M. Mlejnek, E. M. Wright, and J. V. Moloney *Phys.Rev.E* **58**(1998), 4903

[8] Fedosejevs R, Wang X F and Tsakiris G D *Phys. Rev. E* **56** (1997)4615.

[9] Larochelle S F J, Talebpour A, and Chin S L *J. Phys. B At. Mol.Opt. Phys* **31**(1998) 1215

[10] Perelemov A M, Popov V S and Terent'ev M V *Soviet Phys. JETP*, **23**(1966) 924 ; Perelemov A M and Popov V S *Soviet Phys. JETP*, **25**(1967) 336; Perelemov A M, Popov V S and Kuznetsov *Soviet Phys. JETP*, **27**(1968) 451

[11] Krainov V P *JOSA B* **14**(1997) 425

[12] Talebpour A., Larochelle S and Chin S L , *J. Phys. B: At Mol. Opt. Phys.* **31** (1998) L49

[13] Talebpour A, Larochelle S, and Chin S L *J.Phys .B: At. Mol. Opt. Phys.***30** (1997) 1927

[14] Robert C. Weast, David R. Lide, Melvin J.Astle, and William H. Beyer *CRC Handbook of Chemistry and Physics(70 edition)* CRC Press, Inc. Boca Raton, Florida(1990)

[15] Reiss H R Phys. Rev. A 22(1980) 1786

[16] Keldysh L V *Soviet Phys. JETP* **23** (1965) 54

[17] Augst S, Meyerhofer D D, Strickland D and Chin S L *JOSA B* **8**(1991)858

[18] Glimore F R *J. Quant. Spectrosc. Radiat. Transfer.* **5** (1965) 369

[19] Samson J A R and Gardner J L *Can. J. Phys.* **53** (1975) 1948

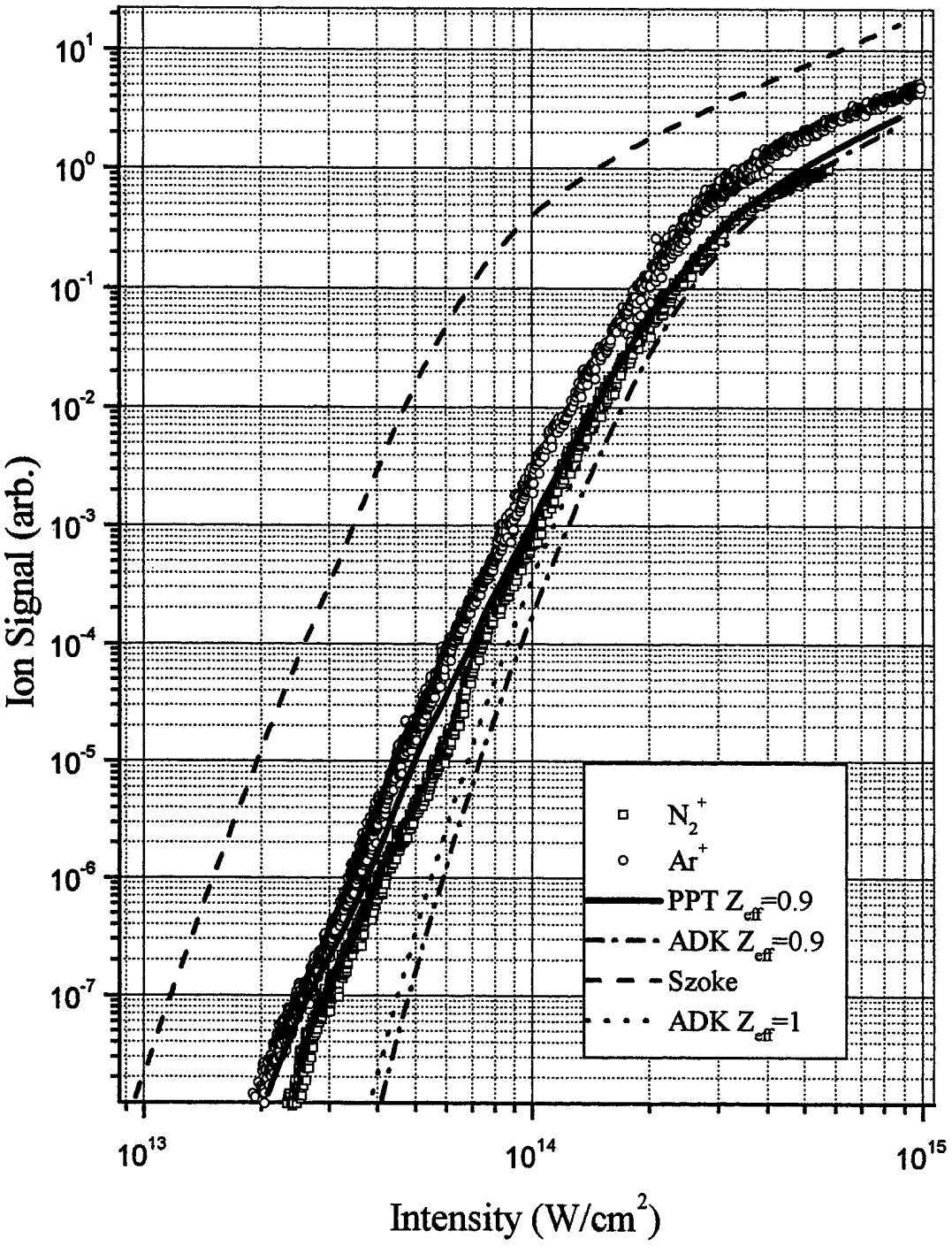
Ion Signal (arb.)
Intensity (W/cm^2)
10^{1}
10^{0}
10^{-1}
10^{-2}
10^{-3}
10^{-4}
10^{-5}
10^{-6}
10^{-7}
10^{13}
10^{14}
10^{15}
N_2^+
Ar^+
PPT Z_{eff}=0.9
ADK Z_{eff}=0.9
Szoke
ADK Z_{eff}=1

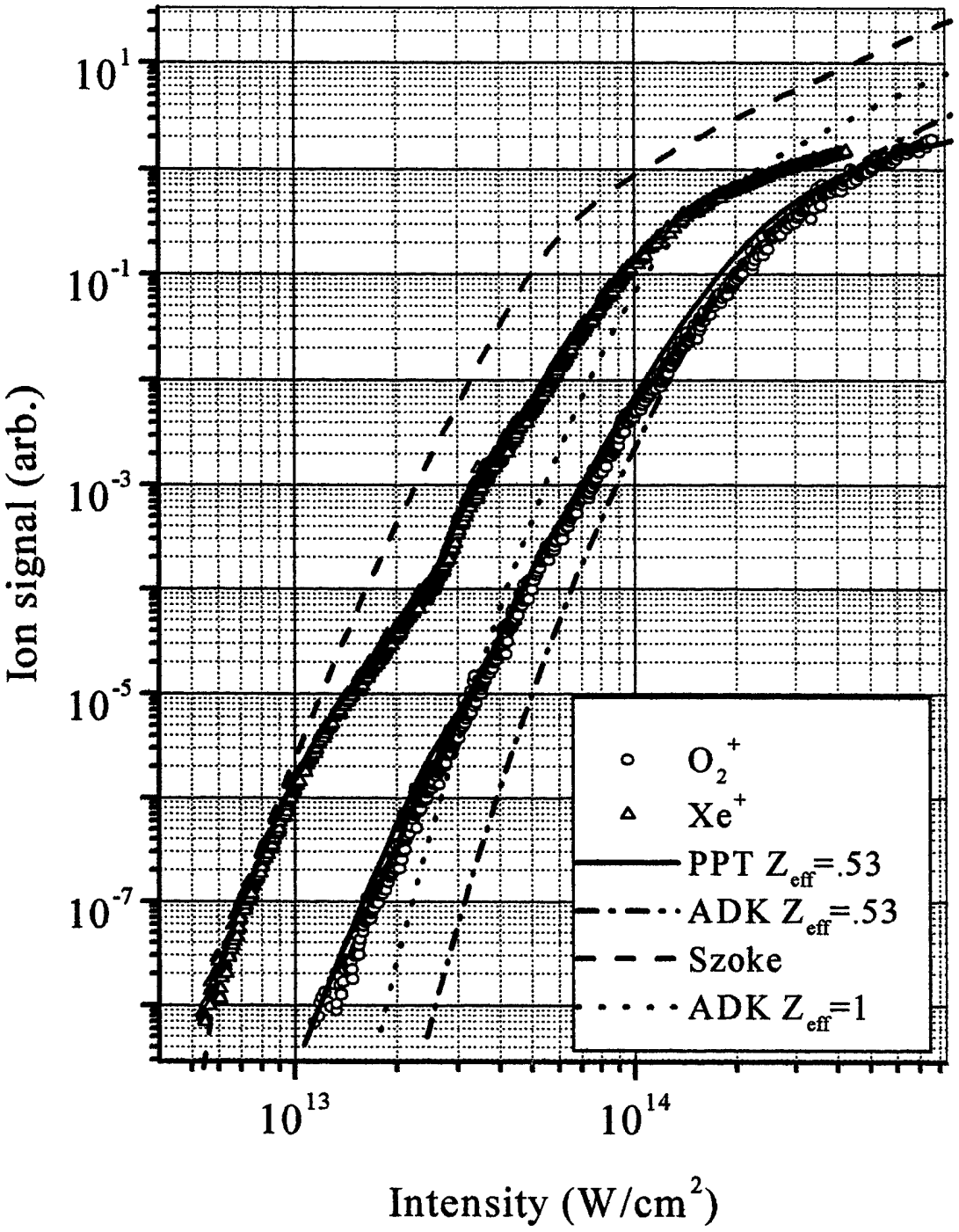
Ion signal (arb.)
10^{1}
10^{-1}
10^{-3}
10^{-5}
10^{-7}
10^{13}
10^{14}
Intensity (W/cm^2)
O_2^+
Xe^+
PPT Z_{eff}=.53
ADK Z_{eff}=.53
Szoke
ADK Z_{eff}=1

Figure Captions:

Fig. 1. Tunnel Ionization of N_2 using stable linearly polarized laser pulses from a Ti:sapphire laser(800nm). The theoretical ion yield (from left to right) are calculated from Szoke's model, ADK theory with Z_{eff} =1,PPT model with Z_{eff}=0.9 and ADK theory model with Z_{eff}=0.9 respectively.

Fig. 2. The same as figure 1 for O_2 (Z_{eff}=0.53)